

# **Assessing Built-up Areas in Flood zones of the Teesta Basin in the Sikkim Himalaya**

A Dissertation Submitted

To

**Sikkim University**



In Partial Fulfilment of the Requirement for the

**Degree of Master of Philosophy**

By

**Dakshina Tamang**

Department of Geography

School of Human Sciences.

**December, 2022**

***Dedicated to my Beloved***

***Aama (mom)***

***Late Rohita Tamang***

इल, सामदुर, तादोंग - 737102  
क, सिक्किम, भारत  
03592-251212, 251415, 251656  
फैक्स - 251067  
ईट - [www.cus.ac.in](http://www.cus.ac.in)



6th Mile, Samdur, Tadong-737102  
Gangtok, Sikkim, India  
Ph. 03592-251212, 251415, 251656  
Telefax : 251067  
Website : [www.cus.ac.in](http://www.cus.ac.in)

## सिक्किम विश्वविद्यालय SIKKIM UNIVERSITY

(भारत के संसद के अधिनियम द्वारा वर्ष 2007 में स्थापित और नैक (एनएएसी) द्वारा वर्ष 2015 में प्रत्यापित केंद्रीय विश्वविद्यालय)  
(A central university established by an Act of Parliament of India in 2007 and accredited by NAAC in 2015)

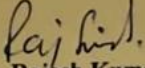
Date: 27/12/2022

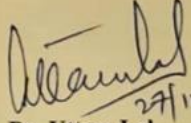
### Certificate

This is to certify that the dissertation titled “Assessing Built-up Areas in Flood Zones of the Teesta Basin in the Sikkim Himalaya” submitted to Sikkim University for the partial fulfillment of the degree of **Master of Philosophy** in the Department of Geography, embodies the result of bonafide research work carried out by **Dakshina Tamang** under my guidance and supervision. No part of the dissertation has been submitted for any other degree, diploma, associateship and fellowship.

All the assistance and the help received during the course of investigation have been duly acknowledge by her

We recommend this dissertation to be placed before the examiners for evaluation.

  
**Dr. Rajesh Kumar**  
(Supervisor)  
Assistant Professor  
Department of Geography  
School of Human Sciences

  
**Dr. Uttam Lal**  
(In-Charge)  
Assistant Professor  
Department of Geography  
School of Human Sciences

इल, सामदुर, तादोंग - 737102  
क, सिक्किम, भारत  
03592-251212, 251415, 251656  
फैक्स - 251067  
वेबसाइट - [www.cus.ac.in](http://www.cus.ac.in)



6th Mile, Samdur, Tadong-737102  
Gangtok, Sikkim, India  
Ph. 03592-251212, 251415, 251656  
Telefax : 251067  
Website : [www.cus.ac.in](http://www.cus.ac.in)

## सिक्किम विश्वविद्यालय SIKKIM UNIVERSITY

(भारत के संसद के अधिनियम द्वारा वर्ष 2007 में स्थापित और नैक (एनएएसी) द्वारा वर्ष 2015 में प्रत्यापित केंद्रीय विश्वविद्यालय)  
(A central university established by an Act of Parliament of India in 2007 and accredited by NAAC in 2015)

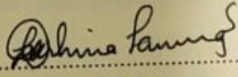
Date: 22/12/2022

### PLAGIARISM CHECK REPORT

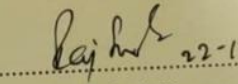
This is to certify that the plagiarism check has been carried out for the following M.Phil. Dissertation with the help of **URKUND SOFTWARE** and the result is 0% which is within the permissible limit (below 10% tolerance rate) as per the norms of Sikkim University.

**“Assessing Built-up Areas in Flood Zones of the Teesta Basin in the Sikkim Himalaya”**

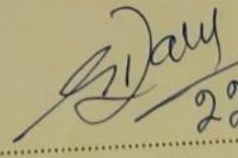
Submitted by **Dakshina Tamang** under the supervision of **Dr. Rajesh Kumar**, Assistant Professor, Department of Geography, School of Human Sciences, Sikkim University.

 22/12/22

Dakshina Tamang  
Signature of Scholar

 22-12-2022

Dr. Rajesh Kumar  
Signature of Supervisor

 22/12/2022

पुस्तकालयाध्यक्ष  
Librarian  
केन्द्रीय पुस्तकालय Central Libr  
सिक्किम विश्वविद्यालय  
Sikkim University

## **CONTENTS**

Declaration  
Certificate  
Plagiarism checked certificate  
Acknowledgements  
Contents  
List of Tables  
List of Figures

### **Chapter I**

<i>Sl no.</i>	<i>Contents</i>	<i>Page no.</i>
<i>1.1</i>	<i>Introduction</i>	<i>1-3</i>
<i>1.2</i>	<i>Statement of Problem</i>	<i>3</i>
<i>1.3</i>	<i>Overview of Literatures</i>	<i>4-21</i>
<i>1.4</i>	<i>Study area</i>	<i>21-22</i>
<i>1.5</i>	<i>Research Questions</i>	<i>22</i>
<i>1.6</i>	<i>Objectives</i>	<i>22</i>
<i>1.7</i>	<i>Database and Methods</i>	<i>23-25</i>
<i>1.8</i>	<i>Chapterisation Scheme</i>	<i>25-26</i>
<i>1.9</i>	<i>Scope of the Study</i>	<i>26</i>
<i>1.10</i>	<i>Limitations of the study</i>	<i>26-27</i>

### **Chapter II**

#### *Assessment of Spatio-Temporal Variation of Channel Morphology*

<i>Sl no.</i>	<i>Contents</i>	<i>Page no.</i>
<i>2.1</i>	<i>Introduction</i>	<i>28-30</i>
<i>2.2</i>	<i>Methods</i>	<i>31-32</i>
<i>2.3</i>	<i>Valley and Channel Morphology</i>	<i>32-41</i>
<i>2.4</i>	<i>Geological settings of the study area</i>	<i>42-43</i>
<i>2.5</i>	<i>Variation of Sinuosity Index in the Selected Reaches</i>	<i>43-45</i>
<i>2.6</i>	<i>Aggradation and Degradation</i>	<i>46-48</i>
<i>2.7</i>	<i>Conclusions</i>	<i>48-49</i>

## CHAPTER III

### *Demarcation of Flood Zones at 25, 50 and 100-Year Return Period Discharge*

<i>Sl no.</i>	<i>Contents</i>	<i>Page no .</i>
<i>3.1</i>	<i>Introduction</i>	<i>50</i>
<i>3.1.1</i>	<i>Concept of Floodplain Zoning and Return Period</i>	<i>51-52</i>
<i>3.1.2</i>	<i>Significance of Empirical Equation in Discharge Estimation</i>	<i>52</i>
<i>3.2</i>	<i>Methods</i>	<i>53-54</i>
<i>3.2.1</i>	<i>Accuracy Assessment of DEMs</i>	<i>53-54</i>
<i>3.2.2</i>	<i>Empirical Equations for Peak Flood Estimation</i>	<i>55</i>
<i>3.2.3</i>	<i>Site Selection for Computation of Physiographic and Meteorological Parameters</i>	<i>56-58</i>
<i>3.2.4</i>	<i>One-Dimensional Steady Flow modelling</i>	<i>58-63</i>
<i>3.3</i>	<i>Output of One-Dimensional Steady Flow Modelling</i>	<i>63-64</i>
<i>3.3.1</i>	<i>Inundated Areas in Flood Zones</i>	<i>64-71</i>
<i>3.4</i>	<i>Validation of One-Dimensional Steady Flow Modelling Output</i>	<i>72-75</i>
<i>3.5</i>	<i>Conclusions</i>	<i>76</i>

## CHAPTER IV

### *Assessment of Flood Zone-Wise Built-up Areas*

<i>Sl no.</i>	<i>Contents</i>	<i>Page no.</i>
<i>4.1</i>	<i>Introduction</i>	<i>77-78</i>
<i>4.2</i>	<i>Methods</i>	<i>79</i>
<i>4.3</i>	<i>Flood Zone wise Built-up Area (2006-2021)</i>	<i>79-91</i>
<i>4.4</i>	<i>Conclusions</i>	<i>91-92</i>

## CHAPTER V

<i>Conclusions</i>	<i>93-95</i>
<i>References</i>	<i>96-107</i>
<i>Appendices</i>	<i>108-110</i>

## ***LIST OF TABLES***

<b>Table no.</b>	<b>Titles</b>	<b>Page no.</b>
1	Primary and secondary data sets	<b>23-24</b>
2.1	Selected Sampled Reaches	<b>30</b>
2.2	Variation of Sinuosity Index	<b>44</b>
2.3	Channel Belt and Bar Area (2006 to 2021)	<b>45</b>
2.4	Ratio of the Total Bar Area to the Total Channel Belt	<b>45</b>
3.1	Catchment-wise computation of physiography and meteorological parameters	<b>57</b>
3.2	LULC-wise Manning's n values	<b>59</b>
3.3	Computed discharges at specified sites of the Teesta,	<b>62</b>
3.4	Flood zone-wise flooded area in hectare	<b>64</b>
4.1	Built-up area (in hectare) and percentage change in the flood zones of the Ranikhola from 2006 to	<b>81</b>
4.2	Built-up area (in hectare) and percentage change in the flood zones of the Teesta river from 2006 to 2021	<b>85</b>
4.3	Built-up area (in hectare) and percentage change in the flood zones of the Ranpochu from 2006 to 2021	<b>87</b>
4.4	Built-up area (in hectare) and percentage change in selected stretch of the Rangit river from 2006 to 2021	<b>91</b>

## *LIST OF FIGURES*

<b>Figure no.</b>	<b>Titles</b>	<b>Page no.</b>
<b>1</b>	<b>Location map of the study area</b>	<b>21</b>
<b>2.1</b>	<b>Selected section of six reaches from the Teesta and the Rangit river for the analysis of dynamism of the channel morphology</b>	<b>30</b>
<b>2.2</b>	<b>Flow chart of methodology</b>	<b>32</b>
<b>2.3</b>	Change of terrace morphology and change of channel margin in reach 1 of the Rangit river between 2006 and 2021	<b>33</b>
<b>2.4</b>	Change of terrace morphology and change of channel margin in reach 2 of the Rangit river between 2006 and 2021	<b>35</b>
<b>2.5</b>	Bank failure in the Rangit at Legship area	<b>36</b>
<b>2.6</b>	Erosion of Mid-level terrace in the Rangit at Legship area	<b>36</b>
<b>2.7</b>	Erosion of lower terrace downstream of Jorethang Loop HEP in the Rangit at Rothak area	<b>37</b>
<b>2.8</b>	Change terrace morphology and change of channel margin of selected stretches of the Teesta and the ranikhola between 2010 and 2017	<b>38</b>
<b>2.9</b>	Change of terrace morphology and change of channel margin of the selected stretch of the Rangpochu between 2006 to 2021	<b>39</b>
<b>2.10</b>	Change in terrace morphology and change in channel margin of the Teesta River stretched in between Singtam and Rangpo between 2006 to 2021	<b>40</b>
<b>2.11</b>	Slope failure at the selected stretch of the Rangpochu due to landslides , Lateral Shift of lower terrace at the Rangpochu due to erosion	<b>41</b>
<b>2.12</b>	Teesta IV dam upstream of Singtam causing diversion of river channel	<b>41</b>



<b>2.13</b>	Geology of the selected study sites in the Teesta,the Ranikhola , the Rangpochu	<b>42</b>
<b>2.14</b>	Geology of the selected study sites in the Rangit	<b>42</b>
<b>2.15</b>	Source of sediment supply in the study sites	<b>47</b>
<b>3.1</b>	Planform map of the selected reference points	<b>54</b>
<b>3.2</b>	Location of points where discharge have been calculated	<b>57</b>
<b>3.3</b>	Rainfall (mm) at 25-year, 50 and Return period using empirical formula	<b>58</b>
<b>3.4</b>	LULC map of the selected reaches of Teesta, Ranikhola and Rangpochu (2021)	<b>60</b>
<b>3.5</b>	LULC map of the selected reach of the Rangit river (2021)	<b>61</b>
<b>3.6</b>	Flow chart of methods	<b>63</b>
<b>3.7 (A)</b>	Flood zone of 25 year return period flood in the selected stretches of the Teesta, Ranikhola and Rangpochu	<b>65</b>
<b>3.7 (B)</b>	Flood zone of 50 year return period flood in the selected stretches of the Teesta, Ranikhola and Rangpochu	<b>66</b>
<b>3.7 (C)</b>	Flood zone of 100 year return period flood in the selected stretches of the Teesta, Ranikhola and Rangpochu	<b>66</b>
<b>3.8</b>	Flood zones of 25,50 and100 year return period in selected stretches of the Teesta, Ranikhola and Rangpochu	<b>67</b>
<b>3.9</b>	Elevation range of flood zones of 25, 50 and100 year return period 73 flood in the selected stretches of the Teesta, Ranikhola and Rangpochu	<b>67</b>
<b>3.10(A)</b>	Flood zone of 25-year return period flood along the Rangit river	<b>68</b>
<b>3.10 (B)</b>	Flood zone of 50-year return period flood along the Rangit river.	<b>69</b>
<b>3.10 (C)</b>	Flood zone of 100-year return period flood along the Rangit river	<b>70</b>

<b>3.11</b>	Flood zones of 25,50 and 100-year return period at selected stretches of the Rangit river	<b>71</b>
<b>3.12</b>	Elevation range of flood zones of 25, 50 and 100 year return period along the Rangit river	<b>71</b>
<b>3.13</b>	<i>Portion of mapped lower and mid-level terraces likely to get inundated in case of simulated flood scenarios along the selected stretches of the Rangit river</i>	<b>73</b>
<b>3.14</b>	Portion of mapped lower and mid-level terraces likely to get inundated in case of simulated flood scenarios along the selected stretches of the Teesta, Ranikhola and Rangpochu	<b>74</b>
<b>3.15</b>	Simulated flood zone of 25, 50 and 100-year return period flood at Singtam bazar and observed maximum flood zone at Singtam in October, 1968.	<b>74</b>
<b>3.16</b>	Simulated flood zone of 25, 50 and 100-year return period flood at Legship Bazar area and observed maximum flood zone at Legship bazar area (1975 to 2021).	<b>75</b>
<b>4.1</b>	Built-up area in (Grid 6) along the Teesta and the Ranikhola	<b>81</b>
<b>4.2</b>	Built -up areas within the flood zones of 25, 50 and 100year return period In stretches of the Teesta, the Ranikhola and the Rangpochu in the year 2006	<b>82</b>
<b>4.3</b>	. Built -up areas within the flood zones of 25, 50 and 100 year return period in the selected stretches of the Teesta, the Ranikhola and the Rangpochu in the year 2021	<b>83</b>
<b>4.4</b>	<i>Water level overflowing embankments at A: Adarsh gaon(27.23N 88.49E); B: Lalbazar side (27.231 N, 88.492 E); C: Lalbazar side (22.23 N 88.49 E); D: confluence point of Teesta and the Ranikhola (27.23 N, 88.498 E)</i>	<b>85</b>
<b>4.5</b>	Built-up area in (Grid 23) along the Teesta and the Rangpochu	<b>86</b>

<b>4.6</b>	Built -up areas within the flood zones of 25, 50 and 100-year return period in the selected stretches of the Rangit river in the year 200	<b>88</b>
<b>4.7</b>	Built -up areas within the flood zones of 25, 50 and 100-year return period in the selected stretches of the Rangit river in the year 202	<b>89</b>

Date:27/12/22

## **DECLARATION**

I, **Dakshina Tamang**, hereby declare that the research work embodied in the dissertation titled “**Assessing Built-up Areas in Flood Zones of the Teesta Basin in the Sikkim Himalaya**” submitted to Sikkim University for the award of the **Degree of Master of Philosophy**, is my original work. The dissertation has not been submitted for any other degree of this University or any other University.

**Dakshina Tamang**

**Roll Number: 20MPGP01**

**Registration Number: 20/M.Phil/GOG/01**

**Name of the Department: Geography**

**Name of the School: Human Sciences**

## ACKNOWLEDGEMENT

I dedicate this work to my beloved mother. She has been my invisible source of inspiration who pushed me in every phase of this work. I am thankful to my supervisor Dr. Rajesh kumar for guiding me to accomplish this work by consistently reviewing my work, assisting me in technical portions and adding his valuable comments. I thank to my Research Advisory Committee members Dr. Uttam Lal and Dr. Ishwarjit E. Singh for giving valuable suggestions which helped me lot to improve my work. Especial thank to faculty members Dr. Abdul Hannan, Mr. Biswanath Shah, and Professor Sohel Firdos.

I extend my gratitude to Tulshi Sir and Satyajeet Sir for always maintaining cordial décor and always being ready to assist in GIS lab where I could work efficiently. I thank to god for making me to come across genuine friends and seniors like Khemraj Aley, DixchenGolay, Ninchen Tamang, Kessang Choden Sherpa, Bijay Chettri, Mohan Sharma, Rana Roy who never step back to encourage me whenever I used to be low and always ready to give ideas and suggestions whenever I used to be clueless.

I thank to my family for beleieving in me and always encouraging me to pursue this path especially my beloved sister , dad , grandmother and Subhash agu.

Dakshina Tamang

## ***CHAPTER I***

### **1.1. Introduction**

In the 21<sup>st</sup> century, hazard both natural and man-made causing loss and destruction to people is one of the critical problems in the earth system (Smith & Petley, 2009). Hazard is of two types –natural hazard and man-made hazard. Natural hazards can be categorized into a hydrological hazard (e.g., flooding), geological (e.g., earthquake), meteorological (cyclones), and climatological (drought) and human-induced are war, terrorism, epidemics, etc., (Barnes et al., 2019). According to the Centre for Research on Epidemiology of Disasters (CRED, 2015) 218 million people were affected by natural disasters annually across the world between 1994 and 2013. Through the bibliometric analysis technique, Barnes et al. (2019) found flood to be the most common natural hazard affecting 55% of the world population followed by drought (25%). Flooding is the most ruinous natural hazard amongst all in the world (Sanyal & Lu, 2004).

The analysis of the state-wise flood-induced damaged data from 1953 to 2017 issued by the Central Water Commission, India, 2021 reflects that the Indian Himalayan states both the Western and the Eastern Himalayas have been left over by the bruises of various flood-induced damage claiming about 7371 human lives from 2001 to 2007 overall the Indian Himalayan states. The Himalayan sites are prone to flood, the historical analysis of flood events in the Indian Himalaya following the examination of paleo flood deposits through the OSL and 14 C-AMS (Accelerator Mass Spectrometry) dating techniques of some selected sites of the Indian Himalaya region, i.e., the Alakananda- Mandakini river system of the Garhwal Himalaya, Indus river flowing through Ladakh, NW Himalaya, and the Brahmaputra river, NE Himalaya reflected that

these sites are subject to flood since the history (Srivastava et al., 2017). The Indian Himalayan states are being drained by three major rivers viz., the Ganga, the Indus, and the Brahmaputra. As Per the National Disaster Management Authority (2008), India can be broadly divided into four flood-prone regions viz., the Brahmaputra River Region, the Ganga River Region, the North – West River Region, Central India, and the Deccan Region. The Brahmaputra River basin covering the states of Assam, Nagaland, Sikkim, Meghalaya and Arunachal Pradesh is in the prior zone of flooding (Mohapatra and Singh, 2003). Assessing the vulnerability atlas of the flood zone in India, issued by the CWC, Indo-Ganga- Brahmaputra plain and eastern and western coastal plains hold higher vulnerability due to floods (Tripathi, 2016). The Brahmaputra River region consists of the rivers Brahmaputra and Barak and their tributaries covering the states of Assam, Arunachal Pradesh, Meghalaya, Mizoram, Manipur, Tripura, Nagaland, Sikkim, and northern parts of West Bengal and during the month of May to September, the catchments of these rivers vary from 110 cm to 635 cm for which severe flood occurs more or less frequently. Moreover, the hills where these rivers originate are fragile and susceptible to erosion leading to excessive silt discharge in rivers and also earthquake and landslides are triggering catchment instability.

Among the floods, flash floods are the deadliest responsible for higher casualties (Jonkman, 2005). Flash flooding is sudden and leads to more death than other types of floods because the latter are much predictable than the former (Opolot, 2013). According to the National Institute of Disaster Management (NIDM), during flash flood flow of small volume and high discharge rises very fast and suddenly causes extreme damage and is common mainly in a hilly region where heavy rainfall and cloudbursts are common.

Within the Brahmaputra River basin, the Teesta River mainly the upper basin covering Sikkim state is at risk of future flash floods and Glacial Lake Outburst flood (GLOF) as per the research conducted in the past and present. The hydrological system of the Teesta River is not simple. Besides rainwater, melting glaciers, snow, and also groundwater fulfill the Teesta River (Wiejaczka et al., 2014; Mandal and Chakrabarty, 2016). Many scholars have started to bring Sikkim's flood issue into the limelight through their works and have tried to zoom in flood risk in Sikkim from different aspects eliciting the present and future flood problem and risk in Sikkim mainly assessing GLOF risk (Aggarwal et al., 2017; Kumar et al., 2020; Islam & Patel, 2021) and climate change trends (Sharma and Goyal, 2020) but currently, the most alarming problem of the Upper Teesta basin is the problem of accelerating water level rise increasing risk to the settlements (commercial, residential) along the river channel for which there is a need of zooming in this issue.

## **1.2. Statement of Problem**

Due to hilly topography, the upper Teesta basin is hit by orographic rainfall, and the stream is fed by the ice meltwater and in case of flash flood occurrence, life and property are at critical risk (Mandal & Chakrabarty, 2016).

As per the analysis of the Central Water Commission report (2019) on state-wise flood-induced damage on nine parameters from (1953- 2017) there is an increase in flood-induced damage in the State of Sikkim.

Mandal and Chakraborty (2016) made flood risk assessment, one of the vital non-structural measures along the Upper Teesta River basin covering the entire state of Sikkim and part of Darjeeling district of West Bengal using Hydrologic Modelling System (HEC-HMS) simulation modelling. In consideration to the computed



hydrograph based on rainfall data obtained from the India Meteorological Department (IMD) at each point of the river channel and as per the analysis of peak discharge volume and time, Singtam, Rongpo, Meli, Chungthang, and Jorthang are under high flash flood risk whereas Teesta Bazar, Yumthang, Dambung, and Thangu Valley are under moderate zones.

However, at present, the most alarming problem of the Upper Teesta basin is the problem of accelerating water level rise increasing the risk to the settlements (commercial, residential) along the river channel of getting inundated. As per the CWC report (2021), the water discharge level at three flood forecasting sites of the upper Teesta basin viz., Mali Bazar, Jorethang, Singtam is recorded to be above 225.25 m, 353.20 m and 379.17 m, respectively. The main reason for the exacerbation of damages and loss incurred by the 2013 Kedarnath flash flood is believed to be mainly due to a higher rate of urbanisation causing encroachment of buildings, hotels, etc even at lower terraces of the river channel and also due to narrowing of Mandakini River (Uniyal, 2013). So, realising the increasing future risk of inundation of encroached built-up areas, this study aims to assess the occupation of built-up areas in flood zones of the Teesta River and its selected tributaries and the problem of water rise over the period and a chance of future inundation.

### **1.3. Overview of Literature**

The literature has been categorized into two sections, one focusing on concepts and another on relevant methods and these two sections have been further categorized into different sub-sections which are as follows:

### **1.3.1 Conceptual literature**

#### **1.3.1.a. Flood Zones**

Flood zones are the land area that has the chance of being covered by flood water. FEMA has put more than 20000 communities in the United States under the category of flood zones (Flood Partners, 2022).

According to the CWC Model Bill for Flood Plain Zoning, 1975 (International Environmental Law Research Centre, 2021), every Indian state were given the authority to work on imposing limits on human activities along and adjacent to the river channel and to keep certain distance limits or thresholds as per the requirements found after proper surveys and no person shall undertake any activity within the prohibited area without the prior permissions of Flood Zoning Authority. The Bill was recirculated in 1996 due to a cold response from the State governments. However, till date Manipur (1978), Rajasthan and Uttarakhand (December 16, 2012) viz., the Uttarakhand Flood Plain Zoning Act (2012) are some of the states that have enacted or passed these bills through the acts but other states have failed to pay heed to this bill.

In February 2016, the Ministry of Environment Forests and Climate change (MOEF &CC) put forth the draft notification for River Regulation Zones through which it was proposed to prohibit the developmental activities on riverfronts and flood plains and circulated to all the states and UTs. One of the key proposals of the said draft is related to the issue of demarcation of River Regulation Zones to curb any kind of developmental and industrial activities upto 5 km from the river banks with flood plain and also for mountain/hill rivers. The river stretches and their tributaries have been classified into three categories viz., flood plain rivers, seasonal rivers and mountain rivers/hill streams. The river regulation zones have been divided into three section

depending on the permission granted to carry out developmental activities and they are the Prohibited activities zones (upto 500 m from the highest flood level in the past 50 years), Restricted activities zones (outer limit of the prohibited zone to 1 km), and Regulated activities zones (outer limit of the restricted zone to 3 km) and the activities permitted in the regulated zone are grazing animals, fishing and organic farming, discharge of treated domestic wastewater, withdrawal of groundwater using hand pump, etc., whereas dumping of solid wastes, construction of new embankments, withdrawing water for commercial purposes other than hydropower and irrigation projects, bunding are prohibited (Ministry of Housing and Urban affairs, GOI, 2021).

#### **1.3.1.b. Problem of Encroachment along the River Channel**

Rao et al. (2014) made investigations on the post-flood causes and impact of the 2013 flash floods along the Kedarnath valley. In this study, as per the analysis through the satellite imageries and simulation study through the hydrological and hydraulic model using Hydrologic Engineering Center- Hydrologic Modeling System (HEC-HMS) and Hydrologic Engineering Centre-River Analysis System (HEC-RAS) software respectively, the authors found that the peak discharge of more than  $2800 \text{ m}^3\text{s}^{-1}$  on the Mandakini at Rudraprayag during the flash flood period caused many villages situated along its course to get washed away, 64 and 47 buildings got washed away and damaged respectively with many more intense structural damages.

The transformation of precipitation to runoff is controlled by factors viz., land use, soil type, evaporation and storage (Rhoads, 2020) Change in land use and land cover (LULC), urbanization, human-induced climate change, etc., are some of the vital anthropogenic factors indirectly impacting river system unlike dam construction, river channelization, mining of river sediment which have direct control on river system

Alteration in Land Use and Land Cover pattern rooted to urbanisation fosters negative consequences over the hydrological processes in the basin disturbing infiltration and increasing runoff that in turn affects flood peak, volume (Suriya & Mudgal, 2012).

Thus, the above literatures reflect the significance of pre-flood analysis of LULC pattern mainly along the river channel to curb hazard turning into a disaster.

### **1.3.1.c. Channel Width and Siltation/Sedimentation**

As per the Central Water Commission report (2009), frequent river course alteration, beheading, heavy shoal formation causing diversion of the main current, heavy river bed aggradation which causes high flood levels resulting in overtopping of banks/embankments, riverbank erosion by hill streams due to flash floods, erratic behaviour of braided rivers, etc are the basic natural problems of river whereas impacts of urbanization, river bed cultivation and construction, constriction of river width due to barrage/ bridge construction, extraction of sand and boulders from the river beds and banks etc are some of the anthropogenic problems of the fluvial system. Water and sediment are the basic inputs that control river dynamics which in turn brings changes in the river system (Rhoads, 2020).

As Per the Ministry of Water Resources, River Development and Ganga Rejuvenation (MoWR, RD & GR), Government of India, Siltation implies the phenomenon when suspended silt particles settle down in the river water whereas when the same phenomenon takes place in the reservoir, it is called sedimentation. The sedimentation or siltation regime is characterized by two processes viz., aggradation and degradation. Excessive sedimentation or aggradation in rivers poses a problem of high flood levels besides the problem of navigation whereas degradation of river beds results in indirect impacts such as bank erosion, downward cutting and channel widening lowering of

water surface elevations close to the river. Siltation in rivers may or may not be accumulative but the sedimentation in reservoirs is usually accumulative in nature. Siltation is the function of both physical and hydrological characters of the catchment viz., slope, LULC, erosion intensity (sheet, rill, gully and stream channel erosion), quality, quantity and concentration of the sediment brought down by the river and also the size, shape and length of river and reservoir.

As per the National Institute of Disaster Management report (2008), one of the major factors leading to increasing chance of flooding is an inadequacy of the rivers in the context of its capacity to hold water brought down from the upper catchments during heavy rainfall and sometimes due to uncertainties in rainfall pattern and amount, areas that are not prone to floods over the historical age also experience severe inundation. Thus, some vital factors viz., riverbed siltation, fall in carrying and holding capacities of river channels, beds and banks erosion causing changes in river courses, flow obstructions due to landslides, synchronised floods in the main and tributary rivers which mainly affect the confluence point.

Lauer et al. (2017) made change detection of the channel width of the Minnesota river and its major tributaries through the analysis of aerial photographs over the period of 1938 to 2018 and as per the findings, the channel width of both main stream and major tributaries was found to increase.

Dar et al. (2019) analysed the influence of geomorphic and anthropogenic activities on channel morphology of river Jhelum in Kashmir valley and found that one of the causes of overbank water flow over a certain stretch of Jhelum River was due to narrowing of the river channel, the anthropogenic causes were found to lead for siltation and narrowing of channel width. Mitra et al. (2020) worked on the assessment of the

evolution of channel system of the Balason and the Mahananda River with one of the objectives of analysing the anthropogenic impact on the Balason and the Mahananda River through geospatial technique, field survey and found that for 29 and 31 years certain channel sections of both rivers have undergone narrowing mainly due to mushrooming of built-up areas increasing impervious surface along the river channel over the period. Some point and channel bars were found to be occupied by built-up land.

Yin and Li (2001) studied the role of human activities in fostering flood disaster in Mid-Yangtze River basin, China and one of the findings was because of siltation, during 1940-2001 with an annual average siltation rate of 0.1 billion m<sup>3</sup>, the size of Tongting lake reduced from 4350 km<sup>2</sup> to 2000 km<sup>2</sup> with a fall in water storage capacity from 29 m<sup>3</sup> to 17.4 billion m<sup>3</sup>. Charlton (2008) has elicited in his book that an adequate amount of river bedload which usually comes from the upper catchment area and also from bank erosion is required for bar formation and sedimentation which results in a reduction of river depth and also channel bar formation. The channel form greatly influences the mode of water and sediment movement, the narrow channel experiences highly concentrated flow with high potential for erosion. Buckingham and Whitney (2007) have worked on change detection of the morphology of Las Buckingham Vegas Wash, one of the tributaries of the Colorado river using GIS technique especially through the comparative analysis of aerial photographs of the varying time period. The aerial photographs of two comparing years were overlapped or superimposed to examine the nature of temporal changes in channel mainly in terms of channel erosion. The eroded points were identified through superimposed photos. Gazi et al. (2020) assessed the morpho-dynamics of channel and bars of the Gorai-Madhumati River, Bangladesh and in context of river channel assessment of change in channel width using

GIS and RS technique, the used datasets seven satellite imageries and was seen that out of major and minor river sections segmented by the authors for the study purpose, channel width was found to both widened and narrowed. The bank line was extracted using Normalised Difference Water Index (NDWI) and Modified Normalised Difference Water Index (MNDWI). Bank line acted as the boundary of a water body and the area within bankline represents river channel and sand bars. Hassan & Mahmud-ul-Islam, 2016 worked on the assessment of change in land use, erosion and bar deposition in Chowhali Upazila region of Bangladesh which is drained by the Jamuna River using 30 m satellite imageries of two periods 1989 (TM) and 2015 (Landsat 8) and superimposed to assess the eroded and deposited area and as per the assessment and finding, over the period of 26 years an average area of 1340 hectares got eroded whereas 630 hectares got deposited in the form of channel bar. The accuracy rate of classification was assessed through the Kappa index and 98% was the accuracy rate of erosion rate and bank deposition. Usually, channel bars develop due to heavy siltation which usually results in alteration in river flowing direction (Hassan & Mahmud-ul-Islam, 2016)

### **1.3.2. Literature on Methods**

#### **1.3.2.a. Flood Management Approach and Its Paradigm Shift**

Flood management strategies can be divided into three sections viz., pre-flood, during a flood, and post-flood (Opolot, 2013). Flood management can be categorized into four phases and they are prediction, preparation, prevention, and mitigation, and damage assessment (Konadu & Fosu, 2007). Pre-flood measures, forecasting of flooding, and post-flood measures are the three flood management strategies (Kourgialas & Karatzas, 2011). Thus, different scholars have different views on flood management aspects. However, in the context of management measures, Knight and Shamseldin (2006) in

their book asserted that there are two types of flood management techniques viz., structural and non-structural, the authors have encouraged sustainable non-structural measures mainly through Modelling (rainfall-runoff models, Dam break modeling, Climate change modeling, sediment debris modeling), Management (flood plain, river, basin or catchment), forecasting & warning (flood, precipitation, river flow), DSS (Decision Support System), etc., because the engineering or structural measures (embankments, etc.) disturb various aspects like runoff pattern, vegetation along the catchment area. Likewise, Grabs et al. (2007) put forth the need for a paradigm shift in flood management approach from defensive (structural) to pro-active (non-structural) for the sustainability of the basin-like an assessment of flood vulnerability and risk, involvement of stakeholders participation, etc without disturbing the ecological aspects of the basin embracing an integrated approach which entails the integration of land and water resources development in a river basin without disturbing either factor and focusses on human security and sustainable development. Sayers et al. (2013) elicited in their book the paradigm shifts in flood risk management from traditional engineering standard-based approach aimed at reducing the probability of flood occurrence through the engineering structures like the construction of dykes, levees, dams, channel diversion, etc to the strategic approach aimed at reducing not only the probability but also the consequences of flooding (like assessing exposure, vulnerability, resilience, adaptability to flood, etc.) to maintain sustainability across the entire catchment area without disturbing any mechanisms. As per the authors, from the 1960s to 1980s, flood mitigation measures were confined to engineering structures but now non-structural techniques seemed to be crucial for flood risk management and these includes well-planned developments in flood-prone areas, warning and evacuation, flash flood forecast, flood -specific building codes, insurance, the role of governance,



communities, individuals, etc. The structural measures are costly, unsustainable and also brings inequality among social-group in the context of protection from flood due to high cost. Since both measures sometimes might fail so building resilience and adaptive capacities among the social groups is also inevitable.

Shah (2013) also emphasized a shift in flood management approaches from structural to non-structural techniques considering the economic and ecological aspects because the former is expensive as well as unsustainable. The author has discussed how the Twelfth Five Year Plan shifted from a structural management approach supporting the construction of embankments and dams to a non-structural or “room for the river” approach such as efficient management of flood plains, flood plain zonation, disaster preparedness, flood forecasting, and warning, reliefs and flood insurance.

#### **1.3.2.b. Use of Geographical Information System (GIS) and Remote Sensing (RS) for Non-structural Flood Management**

Remote sensing and GIS techniques are vital in all three stages of flood management underpinned by the reasons that the RS technique is economically viable and also holds the feasibility of capturing data even from inaccessible sites. On the other hand, GIS facilitates the hydrological model in data collection, analysis, querying, and representation of information in a simplified manner (Opolot, 2013). GIS plays a crucial role in managing natural hazards because of the multi-dimensionality and spatiality of these hazards (Sanyal & Lu, 2004). GIS technique is apt for flood management in real-time monitoring, early warning, post-flood and RS technique provides a wider view of the flood situation and the integrated approach ease up flood management through flood inundation mapping, flood plain zoning, river morphological analysis and others (CWC, 2005). There has been technical evolution and advancement in GIS and RS

technique which has upgraded the standard of flood management starting from the availability and use of poor dataset Landsat MSS, 80m subsequently followed by Landsat TM band 4, 30m from around 1980s which seemed to be effective for distinguishing water and dry land, Landsat band 7 in assessing flood inundation, SPOT multispectral imageries, AVHRR imageries which though suffered from the problem of the bad resolution and cloud coverage, it seemed to be effective in capturing real-time data, flood depth from a tonal variation of floodwater. Later radar imageries were brought into use to tackle the problem of cloud coverage and the author that time i.e. 2004, concluded SAR (Synthetic Aperture Radar) imageries seemed to be the most commonly used dataset to that date (Sanyal & Lu, 2004).

However, the accuracy of DEM (Digital Elevation Model) is vital in determining flood depth in flat land (Sanyal & Lu, 2004). Accessing high-cost, high-resolution imageries for good result are the main challenges in GIS and RS techniques (Opolot, 2013).

### **1.3.2.c. Significance of Accuracy of Topographic Datasets**

Cook et al. (2009) have discussed their paper about the major findings of how the difference in topographic datasets, geometric data and modelling affects the properties of flood inundation mapping. According to the authors, out of the four topographic datasets analysed in their study viz., ASTER DEM (30m), SRTM DEM (90m), LIDAR (1m), cartography map, LIDAR DEM seemed to be the most appropriate for making topographic and geometric analysis for running modelling and ASTER DEM holding the least position.

To remove the problem of overestimation or an underestimation of elevations, it is vital to assess the accuracy of a DEM. There are two kinds of error related to DEM vertical error and horizontal error. Vertical error is in terms of height or elevation (Uuemaa et

al., 2020) whereas horizontal error is related to the actual/true positioning of objects on the land surface (Hawwa et al., 2011). Common means of assessing the accuracy of DEM is to compare its point value with the actual GPS point value (Uuemaa et al., 2020).

However, the DEM accuracy mainly in the context of consideration of river channel for modelling flood could be enhanced through ground survey data taking GPS points and also in the case of modelling of a river with frequent flood, high-resolution DEM is required otherwise the problem of overestimation and underestimation of flood extent and depth may occur.

#### **1.3.2.d. Accuracy Assessment of ASTER, SRTM, ALOS PALSAR and CARTOSAT-1 DEMs**

Elkhrachy (2018) assessed the vertical accuracy of ASTER and the updated SRTM Version 3 for Najran city, Saudi Arabia. Firstly, the downloaded DEM was projected to Universal Transverse Model (UTM), The elevation value for the reference dataset which was extracted from the toposheet and also the satellite imageries with georeferenced ground points were also changed into the same coordinate system. Then the Root Mean- Square -Error (RMSE) was calculated to assess the vertical accuracy. Digital Elevation Model (DEM) is highly influenced by the slope (Uuemaa et al., 2020). The RMSE is one of the significant and standard statistical tools for the analysis of DEM accuracy (Shawky et al., 2019). According to Apeh et al. (2019) closer the value of RMSE towards zero more accurate is DEM height.

Elkhrachy (2018) states that the most vital thing during the extraction of reference ground point for assessing DEMS accuracy is the consideration of only bare surface avoiding natural vegetation, buildings coverage. Shawky et al. (2019) worked on

horizontal and vertical accuracy of SRTM (Global) GL1 DEM V003 (28.5m), ALOS DSM 28.5 (m) and PALSAR DEMs of (12.5m) and (28.5m) resolution of the place called San Luis Obispo country, along the western coast of California, USA. The authors used LIDAR DSMs and DTM as reference data set. The horizontal accuracy was assessed through the extraction of channel networks and Strahler stream orders from all the considered DEMs as well as reference DEM i.e. LIDAR DEM which was further validated by the visual interpretation and comparison with Google earth imageries and found that the extracted channel networks and stream orders matched well with that of Google earth imageries whereas, vertical accuracy was assessed through comparing the pixel-based elevation of all three DEM with that of reference data set and computed the RMSE. For the assessment of horizontal accuracy, there is a need to consideration of well and large structures and features rather than definite small points (Hawwa et al., 2011).

Gesch et al. (2016) assessed the absolute vertical accuracy of ASTER GDEMv3 Conterminous USA by comparing the reference elevation value obtained from geodetic survey ground control points and at each point the GPS benchmark (GCP obtained from the geodetic survey) was subtracted from GDEM v3 to find the errors. The calculated Root Mean Square Error (RMSE) for ASTER GDEM v 3 was 8.52m. The RMSE is calculated considering three elements viz., reference elevation at the considered point, DEM elevation at the same considered point and the number of ground checkpoints.

Apeh et al. (2019) assessed the accuracy rate of three DEMs viz., ALOS W3D30, SRTM 30 and ASTER GDEM 2 for Nigeria comparing 65 GPS points collected from the Office of Surveyor General Federation (OSGoF), Nigeria and the calculated RMSE values were 5.40m, 7.47m and 20.03m respectively. Santillan and Makinano (2016)

assessed vertical accuracy rate of 30m resolution ALOS world -3D-30 m (ALOS W3D30), ASTER Global DEM Version 2 (ASTER GDEM 2) and SRTM -30m for the North eastern Mindano, Philippines through the means of calculated RMSE and Mean Error. The DEMs elevation values were calculated with the reference elevation in the form of transects consisting 274 ground control points (GCPs) rather than spatially-distributed points and the considered elevation range was from 1.76m to 61.14m. The vertical control points were collected by the Philippines National Mapping and Resource Information Authority (NAMRIA). Control points were selected from the spots which are considered to be unchanged and stable for a long time. The DEM elevation at each point was extracted with the help of ArcGIS 9.3 software, then the elevation error was calculated the GCP value from the DEM value. The calculated Mean Error and RMSE values for ALOS W3D30 were 4.36 and 5.68 respectively, for ASTER GDEM 2 it was 8.37 and 11.98 m respectively and SRTM -30m were 6.91 and 8.28m. Santillan and Makinano (2016) calculated mean error and RMSE for three DEMS even in the context of land cover and found that ALOS W3D30 performed better.

Moreover, SRTM DEMs (30m and 90m spatial resolution) suffer from missing data for instance radar shadow that toughens flood modelling.

#### **1.3.2.e. Modelling Techniques**

The ontology- approach is one of the significant approaches in flood management which entails linkage between the environmental models (here it implies geospatial processing, algorithms, and calculations) and disaster-related data in the Flood Disaster Management System (FDMS). Environmental Information System plays a vital role in

all phases of flood disaster management either by atmospheric or hydrological models for forecasting, early warning and flood simulation (Du et al., 2018).

Hydrological Engineering Centre (HEC-RAS), MIKE 11, and FLO 2D are the most commonly used river modelling (Anees et al., 2016). HEC- RAS and MIKE11 are suitable for 1D hydraulic modelling in terms of economic and accuracy aspects. One of the advantages of HEC-RAS over MIKE 11 is that the former runs both steady and unsteady flow, whereas the latter runs only unsteady flow Moreover, HEC-RAS is available from an open-source whereas MIKE is commercially available (Pinos et al., 2019) FLO 2D model surpasses 1D HEC-RAS and MIKE11 models but this modelling lacks in making elevation difference and vertical roughness in grids which is necessary for highly terrain regions to understand the dynamic behaviour of flooding in the region (Anees et al., 2016). A numerical model that has enjoyed wide application in floodplain delineation working since the past 35 years is the Hydrologic Engineering Center's HEC-2 model (USACE 1991) (Yang et al., 2006). HEC-Ras can generate stream profile, rating curves, flow depths and velocities, flow areas, widths and volumes, profiling of cross-sectional water surface and flood inundation estimation (Ícaga et al., 2016).

Hasheyman et al. (2015) made the integrated use of HEC-HMS and HEC-RAS models to simulate flood and flood plains of 4 return periods along the Choke Rudan river. The conversion of rainfall data to runoff was performed with the CN (Curve Number) method. The authors computed the hydrograph and generated flood zone mapping of different return periods through HEC-HMS and HEC-RAS models respectively. The model validation was done by Chow's method considering the roughness coefficients. The authors claimed that the HEC-RAS hydraulic model synced with GIS

outperformed the HEC-HMS hydrological model in flood risk management because only the hydrograph could be computed by HEC-HMS but HEC-RAS allows simulation and mapping of flood risk zones with consideration of basin characteristics like geometry, roughness.

Vozinaki et al. (2016) made a comparative analysis of 1D and combined 1D/2D simulation modelling with the case study of the Koiliaris watershed, Greece. The geometric data viz., river cross section and flood plain were extracted from GeoEye-1 stereo-pair imagery, DEM of 1m and 5m resolution prepared by the research team. 1D hydraulic modelling is well accepted and has been effective in many studies and represents only the main channel line and its processes not the flood plains. In 1D model, the considered section of the area is represented through the cross-sections and in 2D modelling in a form of flood plains. However, for running 2D modelling thorough data and sufficient computational time, the fine computational grids are inevitable. DEM was validated through Ground Control Points (GCPs). The model calibration was done considering the channel and its surrounding floodplain frictional value. As per the findings, the author claimed that 1D HEC-RAS model is appropriate to simulate channel processes only but not the flood plains and 1m DEM outperformed the 5m DEM.

Pinos et al. (2019) evaluated the effectiveness of three 1D steady hydraulic models viz., HEC RAS v 4, MIKE and Flood Modeller in the context of estimation of inundation water level for the Santana Barbara Mountain River, Azuay, Southern Ecuador and concluded that the HEC-RAS model outperformed the other two models. For running all three models, the authors extracted geometric data through two means, one from the field survey and another from DEM. In the case of HEC- RAS model, the water surface

elevation was the same in the case of both types of geometric data but the outputs of other two models were highly influenced by geometric data and elicited that these models (MIKE and Flood Modeller) based on the first dataset outperformed those from the latter geometric data in which underestimation of water level seemed to be the problem for which the need of cautiously extracting geometric data from DEM in running these two models was reflected.

#### **1.3.2.f. One Dimensional (1D) v/s Two Dimensional (2D) HEC-RAS Model**

In One-dimensional flood modelling, all water flows are assumed to flow in a longitudinal direction. The 1D models represent the terrain as a sequence of cross-sections and simulate the flow to provide estimates of flow parameters such as flow velocity and water depth. To simplify the computation, HEC-RAS assumed a horizontal water surface at each cross-section normal to the direction of the flow such that the momentum exchange between the channel and the flood plain can be neglected (Dasallas et al., 2019). A 2D flood model allows water to move in both longitudinal and lateral directions, while velocity is assumed to be negligible in the Z-direction. In this model, the terrain is represented as a continuous surface through a mesh or grid. To improve the computational time, HEC-RAS uses a sub-grid approach, which uses a relatively coarse computational grid and finer scale information underlying the topography (Dasallas et al., 2019). Many studies have gone for 2D model but in cases, like in steep topography with straight channel and no sinuosity, 1D gives good result and in area with varying topography and sinuosity also both 1D and 2D gives more or less the same result if there is an appropriate combination of channel and floodplain roughness characterisation (Liu et al., 2018). For the water flowing only in the main channel direction rather than multiple directions, the 1D model works the best (Pinos et al., 2019). For greatly sinuous channel, the 2D model or semi 2D model works best



(Werner, 2001). Içaga et al. (2016) worked on flood inundation mapping of different return periods at Akarkay Sub-basin, Turkey using GIS technique and 1D steady flow HEC-RAS model. In this work, flow data of two return periods viz., 100 and 500 years have been calculated with one of the empirical formulae called Fuller method and this calculated flow data was inputted in HEC-RAS software to simulate inundated area of 100 and 500 years return period and found that mainly the agricultural areas wastewater treatment plant, sugar factory and a small area of settlements, railways and highways got submerged. Pathan and Agnihotri (2020) simulated the 1D steady flow of two major flood events of the year 2002 and 2003 of the river Purna at Navasiri, Gujarat using HEC-RAS version 5.0 and was founded that cross-section lying near to Jalalpore and Viraval area in Navsari more prone to flooding compared to other cross-sections. The result was validated through the comparison of simulated flow data with the observed data.

Beven and Hall (2014) have explicitly discussed in their book the problem of uncertainties in running models both in prediction and calibration in flood risk management because the model is merely an approximate representation of the system, which is calibrated using uncertain observations and generated using uncertain input data. The successful application of the model is based on the successful control of these sources of uncertainties. However, in some cases, these uncertainties might not significantly affect the models e.g., in the case of a bounded floodplain, the extent of inundation may not be significantly affected by uncertainties. According to the authors, uncertainties may be due to knowledge gaps known as epistemic uncertainties due to observation error and small samples of random phenomena (which includes process representation, effective parameter values, input data, or calibration data such as flood discharge estimates) as well as statistical errors also known as aleatory uncertainties.

For instance, in the case of Flood inundation modelling, one of the important components in flood plain risk zonation, the uncertainties arise mainly in the context of input.

#### 1.4. Study area

The study was conducted at some selected reaches along the Teesta River flowing within the state of Sikkim and its three tributaries viz., the Ranikhola, the Rangpo Chu and the Rangit river because as per the pilot survey and Google Earth image analysis, these sites are now highly urbanised and occupied by the built-up areas. Moreover, some distinct built-up areas located along the mentioned rivers are now facing problem due to water level rise. The water level rises mainly during June-July months increasing the risk of inundation of adjoining areas.

The Teesta originates from the Pahuni or (Teesta Kangse) glacier and drains into the Brahmaputra river at Teestamuk Ghat in Rangpur district, Bangladesh. In India, the Teesta basin covers an area of 9,855 km<sup>2</sup> and falls under the state of Sikkim (72.43+%) and West Bengal (27.57%) (ENVIS,2021). Total catchment area of Teesta river in Sikkim is 6930 km<sup>2</sup> (ENVIS, 2021.).

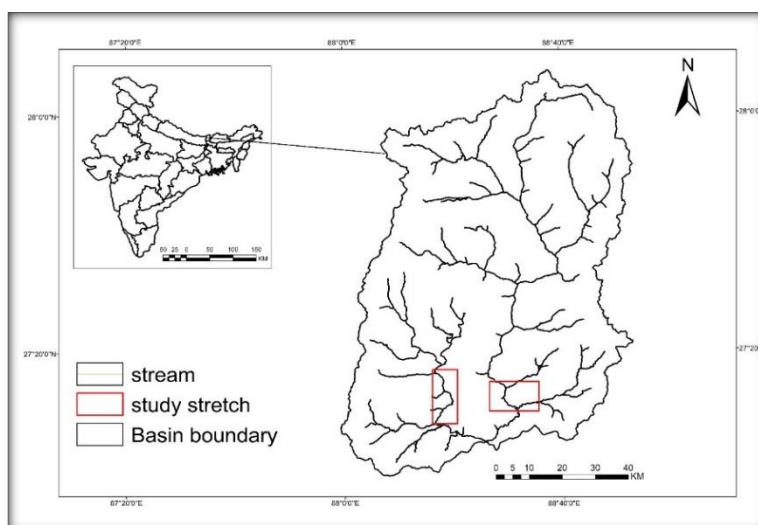


*Figure 1. Location map of the study area*

**Source.** FABDEM, 2022

There are total 8 flood forecasting stations along the Teesta river, Sikkim, 3 water level forecasting Stations at Singtam(East), Rothak (West) and Melli and ( South), and 5 inflow forecast stations viz., Teesta III dam (North), Teesta - IV dam (East), Rangit-3 dam (west), Rangpo and Rangli dam (East) (Ltd, n.d.)The selected stretches of the Teesta, the Ranikhola, the Rangeet and the Rangpochu rivers are taken as study area (Figure.1).

### **1.5. Research Questions**

1. What are the factors influencing the channel morphology in the selected stretches of the Teesta, the Ranikhola, the Rangpochu and the Rangit rivers?
2. Which DEM is appropriate among ASTER (30m), SRTM (30), CARTOSAT-1 (30m), ALOS PALSAR (12m) and FABDEM (30 m) for flood simulation at 25, 50 and 100year return period to demarcate the flood zones?
3. What are the main causes of occupation of built -up areas in flood zones of the 25,50 and 100 year return period at the selected stretches of the Teesta, the Ranikhola, the Rangpochu and the Rangit rivers?

### **1.6. Objectives**

For the selected stretches of the Teesta, Ranikhola, Rangit and Rangpochu rivers, following objectives have been defined:

1. To assess spatio-temporal variation of channel morphology between 2006 and 2021.
2. To demarcate flood zones at 25, 50 and 100-year return period discharges.
3. To assess the areal extent of built-up areas in flood zones defined at 25, 50 and 100- year return period discharges between 2006 and 2021.

## 1.7. Database and Methods

For the fulfilment of the study, both secondary and primary data were taken into consideration detail about which is mentioned below:

### 1.7.1. Database

*Table 1. Primary and secondary data sets*

Data Set	Source	Purpose
Google earth images from 2016 to 2021 (06/02/2006 and 08/03/2021)	Google Earth Pro software.	Change detection of channel morphology and built-up areas
Radiometric corrected ALOS PALSAR DEM (12.5m), 6 December, 2009	Openly available at at( <a href="https://asf.alaska.edu">https://asf.alaska.edu</a> )	Accuracy assessment of DEMs
ASTER GlobalV003 DEM (30m), Nov, 2013	Openly available at ( <a href="https://earthdata.nasa.gov">https://earthdata.nasa.gov</a> )	
SRTM DEM (30m), 2014	Openly available at ( <a href="https://earthexplorer.usgs.gov">https://earthexplorer.usgs.gov</a> )	
CARTOSAT – 1 V-3R1 DEM (30m), April, 2015	Openly available at ( <a href="https://bhuvan.nrsc.gov.in">https://bhuvan.nrsc.gov.in</a> )	
FABDEM (30m), 2022	Openly available ( <a href="https://data.bris.ac.uk/">https://data.bris.ac.uk/</a> )	
Sikkim Himalaya Topographic map, (1: 150000), 2001	Published by the Swiss Foundation for Alpine Research	As a reference point source for accuracy assessment of DEM
Point rainfall data	North Brahmaputra Subzone Isopluvial map prepared by India Meteorological Department (IMD) for 25, 50 and 100-year return period	For computing rainfall at different return period
Geological map	“Carrying Capacity Study of Teesta Basin in Sikkim”, Volume II) “ <i>Carrying Capacity study of the Teesta basin, Volume II</i> ” prepared by the collaborative works of seven pioneer Institutions sponsored by the National Hydroelectric Power Corporation Ltd., Faridabad. The geological map of Sikkim embedded in this report has been modified after Acharya,1989; Ray,1989;Neogi et al,2000;Geological Survey of India(GSI) 2001; Catlos et al,2002,2004.	Comparative analysis of geological settings of the study area

Primary field survey (June-November, 2022)	In-depth interview with senior age group people	To know about extent of flooding and its trend over the period mainly in monsoon season in order to validate the simulated extent of flooding and calculated peak flood flow of 25,50 and 100 year return period.
---	--	--

## 1.7.2. Methods

### 1.7.2.a. Method for Objective 1

The spatio-temporal variation of channel morphology was analyzed with the help of Google Earth (GE) imageries of the period 2006 and 2021 and field survey. River channels were extracted from the imageries and processed in GIS environment.

### 1.7.2.b. Method for Objective 2

The Empirical formulae formulated by four organizations viz., (i) the Central Water Commission of Ministry of Water Resources, (ii) Research Designs and Standards Organisation of Ministry of Railways, (iii) Roads and Bridges wing of Ministry of Surface Transport and iv> Hydromet Directorate of India Meteorological Department, Ministry of Science and Technology were used to estimate return period flood peak for the North-Brahmaputra subzone through simplified approach. These four bodies jointly prepared a report for estimating design flood at ungauged and inadequately ungauged catchment on North Brahmaputra subzone 2 (a) covering the states of Assam (Lower and Upper), West Bengal, Sikkim and Arunachal Pradesh. The Teesta, Torsa, Dhansiri, and Dibang are the major tributaries of the Brahmaputra river falling under this zone. The report has reflected estimation of flood with empirical equation based on two approaches – Detailed SUH approach and Simplified approach. Detailed SUH approach deals with estimation of design flood and the simplified approach deals

simply with estimation of return period peak flood. The current study has used simplified approach which deals merely with estimation of return period flood peaks. covering the states of Assam (Lower and Upper), West Bengal, Sikkim and Arunachal Pradesh. The Teesta, Torsa, Dhansiri, Dibang are the major tributaries of Brahmaputra river falling under this zone. The required data for computing empirical equation were the physiographic parameters (Area, Slope, Length of longest stream,) meteorological parameters (return period point rainfall data) of the catchment. The demarcated design flood zone of 25, 50 and 100 year return period was validated through field data (people's perception and paleoflood marks). This method is applicable for the catchment area ranging from 25 km<sup>2</sup> to 1500 km<sup>2</sup> and can be used for large catchments upto 5000 km<sup>2</sup> but only with proper justification and considering the data of neighbouring catchments only (Central Water Commission, 1991).

#### **1.7.2.c. Method for Objective 3**

Objective 3 was fulfilled by both quantitative and qualitative approach using secondary and primary data. Flood zone-wise areal extent of built-up areas was assessed in GIS environment. Change in built-up areas from 2006 to 2021 along the Teesta and the Rangit rivers was assessed through visual interpretation of GE imageries of the considered period. The result was validated through field survey, to understand reasons behind occupancy of built-up areas along the channel, an in-depth interview was conducted with senior group people of the study area.

### **1.8. Chapterisation Scheme**

Chapter 1 discusses about overall introduction about the study of interest, objectives, research questions. Chapter 2 discusses about spatio-temporal variation of three important aspects of channel morphology that are river terraces, channel margin and

status of aggradation and degradation over the period of 15 years i.e., from 2006 to 2021 conducted with senior group people of the study area. Chapter 3 is based on the demarcation of flood zones of 25, 50 and 100-year return period peak discharge of 4%, 2% and 1% Annual Exceedance Probability (AEP). Chapter 4 underlines change of built-up areas in these three flood zones over the period of 2006 to 2021 and chapter 5 deals with conclusions

### **1.9. Scope of the Study**

This study showed the extent of inundation of built-up areas occupying the flood zones along the Teesta, the Ranikhola, the Rangit and the Rangpochu rivers at flood peak discharge of 25,50 and 100-year return period. The analysis of spatio-temporal variation of channel morphology helps to understand the condition of some of the important aspects of river channel like aggradation, degradation, river detention capacity. Finally, this study is showing occupancy of lower terraces.

### **1.10. Limitations of the study**

The study tries to identify flood zones along the selected reaches of the Teesta, Ranikhola, Rangpochu and Rangit river flowing in Sikkim. All reaches are experiencing increasing occupancy of residential and commercialized activities on the lower terraces. The most vital database for demarcation of flood zone is DEM. After an accuracy assessment of five different freely available DEMs for Sikkim, considering contour crossing elevation and spot heights of toposheet map of Sikkim of year 2001 as referencing elevation, FABDEM appeared to be more accurate than the other DEMs. The RMSE values (in m) of the considered DEMs are 78, 298, 117, 49, and 180 for the SRTM, ALOSPALSAR, CARTOSAT-I, FABDEM, and ASTER Global V003 DEMs, respectively. The spatial resolution of FABDEM is 30 m. Thus, the main limitation of

the study is unavailability of a fine resolution DEM for running the HEC-RAS 1D steady flow model and floodplain mapping. However, the estimated flood zone profile has been validated using inundation of lower terraces and ground truthing based on people's perception but depth and velocity could not be calculated due to the coarse resolution of the FABDEM.

Another limitation of the study is that the flood zones have been demarcated after simulating peak discharge of three return periods from certain geographical points of the study sites without considering the influence of hydraulic structures i.e., dams and embankments on river water flow.

Further works have to be focussed on the application of fine-resolution DEM and incorporation of hydraulic structures in the HEC-RAS model for a detailed flood zonation mapping.



## ***CHAPTER II***

### **Assessment of Spatio-Temporal Variation of Channel Morphology**

#### **2.1. Introduction**

A river is a watercourse flowing within a channel having a well-defined direction and bankline (Garde, 2006) and the term morphology is referred to as a science of structure or form. Thus, river morphology is a science concerned with the form of streams and adjoining areas formed by erosion, transportation, and deposition of sediments by the stream water (Garde, 2006). Channel form and the adjoining areas are subjected to variable change under the influence of erosion and sedimentation (Garde, 2006). A river channel is dynamic and evolves over the period and space and is influenced by the nature of flow and sediment supply in the channel and also the channel boundary conditions like the slope of the valley, channel substrate, riparian vegetation, etc., (Charlton,2008). Thus, it is vital to assess the spatio-temporal variation of channel morphology to understand the status and variation of some of the important aspects of river channels like rate of channel stability, change in channel pattern, change in channel detention capacity through the assessment of nature of aggradation and degradation processes over the period.

As per the Central Water Commission (CWC) report (2009), the channel morphological dynamism is associated with both natural (continuous changes in river course, bank erosion, increment in shoal and bar formation leading to diversion of the main current towards the bank, variation in braided pattern, river instability due to change in bed slope over time and anthropogenic factors (artificial channel constriction, sand and rock mining from the river bed and banks, urbanization along the banks, etc.

However, this chapter aims to analyze and map spatio-temporal variations of channel morphology mainly focused on changes in river terraces, channel margin, aggradation and degradation of the selected stretches (Figure 2.1) of the Teesta, Ranikhola, Rangpochu and Rangit river with the help of geospatial technique. Integration of GIS and remote sensing is a vital contemporary technique that helps in understanding fluvial landscapes (Das et al., 2019). Shift in channel margin, erosion of bank and lower terraces, aggradation and degradation are posing threat to the built-up areas located in the lower terraces. The change of channel margin reflects the status of lateral shifting of channel and erosion of banks and terraces. Status of aggradation and degradation mainly helps to understand channel detention capacity. Aggradation leads to reduction in channel capacity, and as the channel bed rises, flood risk increases (Charlton, 2008). However, degradation is subjected to the removal of river bed loads and erosion of the banks.

### **2.1.1. Demarcation of Valley Floor and Channel Margin**

The Valley floor is composed of active channel, secondary channel, flood plains, terraces, and tributary fans (Grant & Swanson, 1995). The active channel is fed with water even in the summer or dry period and the adjacent unvegetated area (Osterkamp & Hupp, 1984). Edge of the active channel forms the channel margin in many cases corresponding to the bankfull margin. It is a separating line of the zone where water flows regularly and the zone where the water flows occasionally (flood plain) or historically (terraces) (Fryirs et al., 2016; Sear et al., 2021).

River terraces are the out-channel geomorphic unit on the valley floor with an average height exceeding 3m but within 10m (Grant & Swanson, 1995) and are categorized

mainly into two categories viz., alluvium terrace and strath terrace cut into the alluvial deposits and bedrocks respectively (Charlton,2008).

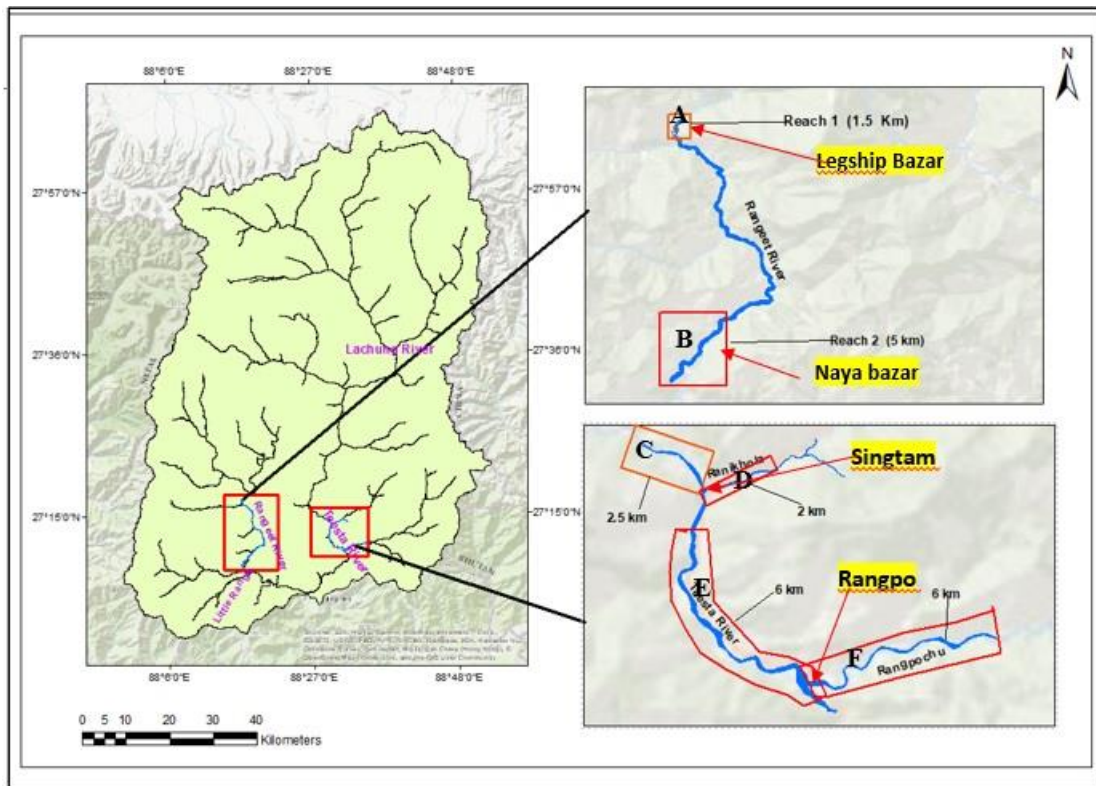


**Figure 2.1.** Selected section of six reaches from the Teesta and the Rangeet river for the analysis of dynamism of the channel morphology

**Table 2.1.** Selected Sampled Reaches

River	Reach	Extent
Rangit 1	A	1.5 km long reach in the upstream section of the Rangit river covering Legship bazar area
Rangit 2	B	5 km long downstream section covering Naya bazar area
Teesta	C	2.5 km long upstream section from the confluence point (Singtam) where it meets the Ranikhola
Ranikhola	D	2km up from the confluence point where it meets the Teesta
Teesta	E	6 km downstream section in between Singtam and Rangpo
Rangpochu	F	6km upstream from the confluence point meeting the Teesta

Main rational behind the selection of these sampled reaches is based on the occupancy of river terraces by built-up areas.

## 2.2. Methods

Analysis of the channel morphological characteristics and its variations over time and geographical points of the sampled reaches have been done through the plan view visual interpretation of the Google Earth (GE) images with 0.5 resolution of the pre-monsoon season considering some important aspects like shape, size, alignments of the reach and the in-channel and out-channel geomorphic units like, tributary fans, terraces. The GE images have been processed and mapped through ArcGIS software version 10.2 (Figure 2.2).

The period for the analysis has been considered as per the availability of images embedded in Google earth pro. The temporal extend for the study is from 2006 to 2021 except in case of two reaches (Ranikhola reach and the 2km long upstream Teesta reach from the confluence point of the Ranikhola and the Teesta reach) where the considered period is from (2010 to 2017) as per the availability of the Google Earth images. Sinuosity Index has been calculated with the help of Equation (1) (Charlton,2008).

$$\text{Sinuosity Index} = \frac{\text{Channel Length (LC)}}{\text{Valley Length (LV)}} \dots\dots\dots (1)$$

The aggradation and degradation processes were analyzed by dividing the total bar area by the channel belt area (equation 2) along the considered six reaches using Equation (2) (Lahiri and Sinha, 2014).

$$\text{Aggradation and degradation} = \frac{\text{Total bar area}}{\text{Channel belt area}} \dots\dots\dots (2)$$

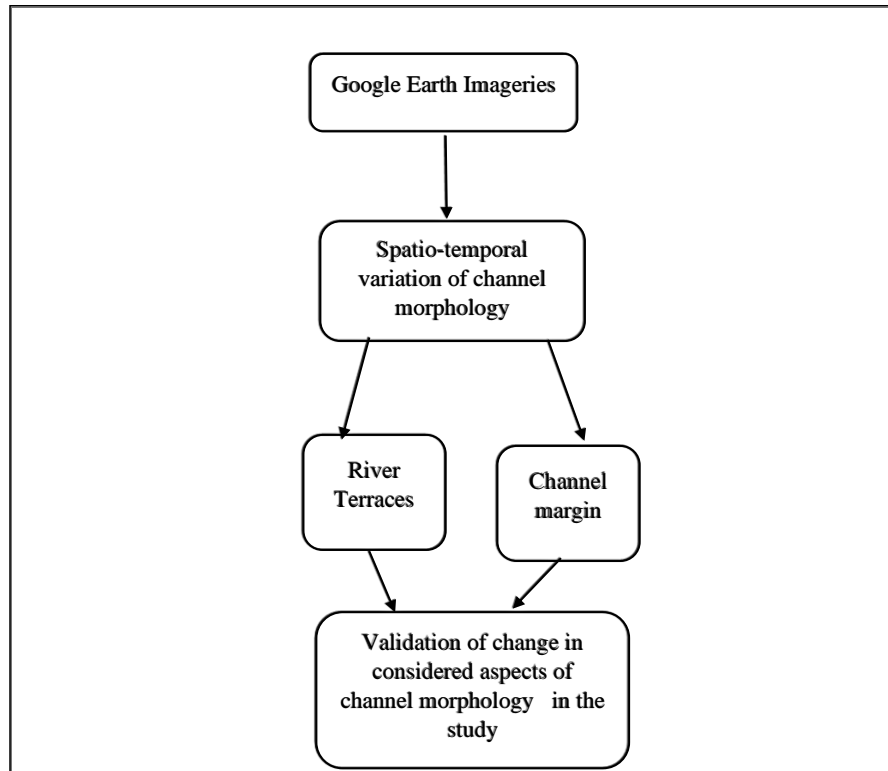


*Figure 2.2. Flow chart of methodology*

### **2.3. Valley and Channel Morphology**

Considering the nature of channel substrates as the criteria, channel reach is generally divided into three categories viz., bedrock reaches, alluvium reaches and colluvium reaches. River channels are of three main types viz., bedrock channel, alluvium channel, and semi-controlled channel (Summerfield, 2014). In the Himalayan region, bedrock type of channel is common. The morphological characteristics of the sampled reaches and their spatial and temporal change have been discussed in the following sub-sections:

#### **2.3.1. Reach 1 and Reach 2 of the Rangit River**

Reach 1 (Figure 2.3) has been sampled from the upstream portion of the Rangit river covering Legship Bazar area and reach 2 has been sampled from the downstream portion covering Nayabazar area (Figures 2.2 and 2.3). Currently, these sampled

reaches are narrow single-channeled, sinuous reaches. with a sinuosity index of 1.28 and 1.16 of reach 1 and reach 2, respectively (Table 2.1). In terms of bed form, the considered reaches are plane bed reach with bars (point, lateral, and, mid-channel). A plane bed is characterized by beds of gravel and cobbles, a featureless bedform pattern (Huggett, 2017). Reach 1 is highly confined by the hillslope and bedrock terraces on either side with a complete absence of floodplain bearing no scope of lateral adjustment during high flow.

However, reach 2 (Figure 2.3) is semi-confined with very less scope for lateral adjustment over the lower terraces. A Channel is considered confined when it is franked either on one or either side by hillslopes, terraces, or artificial structures (embankments, railways, roadways, etc.) hindering the lateral movement of the channel (Nagel et al., 2014; Joyce et al., 2018; Sear et al., 2021).

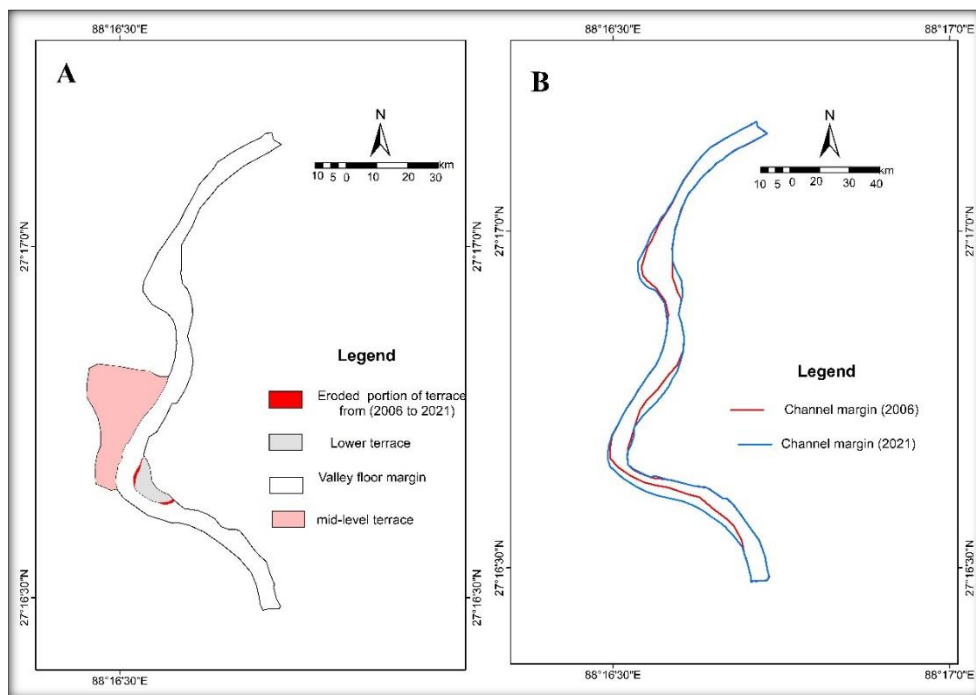


**Figure 2.3.(A):** Change of terrace morphology **(B):** Change of channel margin in reach 1 of the Rangit river between 2006 and 2021

The mapped terraces in reach 1 are the mid-level and lower terraces on the right and left bank, respectively (Figure 2.3). Both the mapped terraces are occupied by built-up areas. The right bank terrace is occupied by roadways, commercial and residential buildings whereas the left bank terrace is occupied by a temple.

It is apparent from Figure 2.3 and also from the field-based evidences that over 15 years (2006 – 2021), the channel margin of the considered reach has shifted laterally on either side at a certain geographical point due to erosion of terraces posing threat to built-up areas (settlement and roadways in this case). The left bank terrace has been eroded more severely compared to the terrace along the right bank. As per field evidences, the flow velocity is very high along the Rangit river due to the narrow and confined channel. Flow depth and stream power are high in a confined channel (Sear et al., 2021). In confined channels, hillslope and confining margins both natural (hillslope, terraces) and artificial (embankments, levees) act as the main source of sediment (Sear et al., 2021).

In the context of reach 2 (Figure 2.4), the channel margin has shifted rightward due to erosion of lower terraces and channel margin between 2006 and 2021. The reach downstream of the dam has undergone intense bank along and lower terraces. The eroded materials have led to an increment of bedload sediments leading to aggradation because riverbank erosion and landslides materials are major sources of sedimentary supply in the river channel (Charlton, 2008).

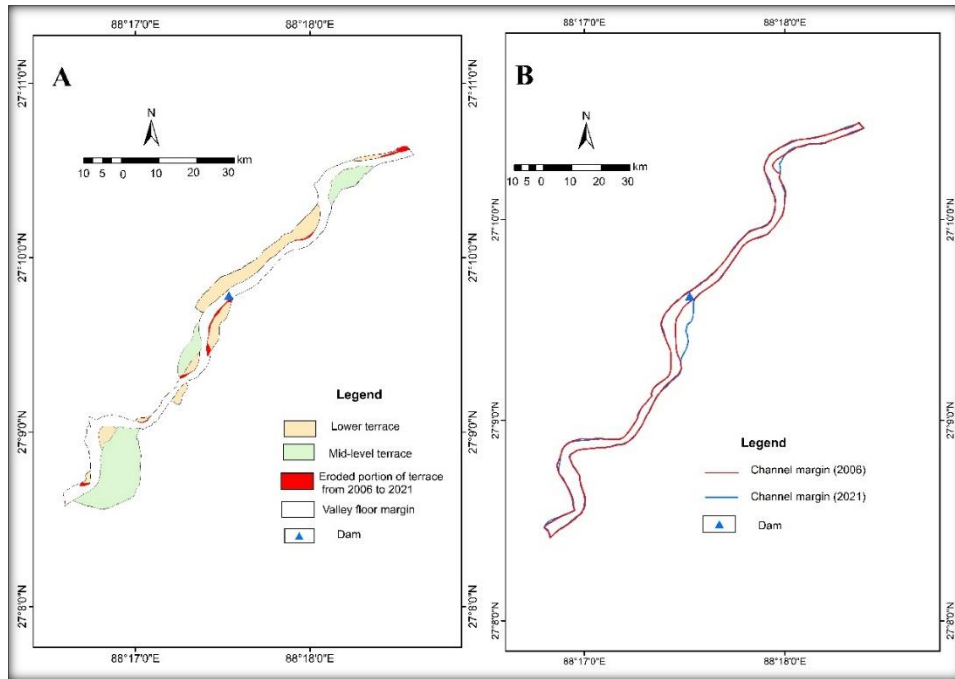


**Figure 2.4. (A): change of terrace morphology (B): change of channel margin in reach 2 of the Rangit river between 2006 and 2021**

As per the field evidences, the main drivers fostering change in channel margin and river terraces in these two reaches are hydraulic structures i.e., dam, bank erosion and landslides. Even within this short period of 15 years, channel diversion and channel confinement have occurred dramatically. For instance, In Rangit river, Jorethang Loop HEP got completed in 2015, Teesta V constructed in 2007, Rangpo dam got completed in 2007. For instance, Jorethang loop hydro-electricity project across the Rangit river was completed in 2015. Teesta V and Rangpodam were constructed in 2007 along the Teesta river and the Rangpochu, respectively.





**Figure 2.5.** Bank failure in the Rangit at Legship area (27.279 N 88.277 E)

*Source.* Field survey, November, 2022



**Figure 2.6.** Erosion of Mid-level terrace in the Rangit at Legship area (22.279 N 88.275E)

*Source.* Field survey, November, 2022

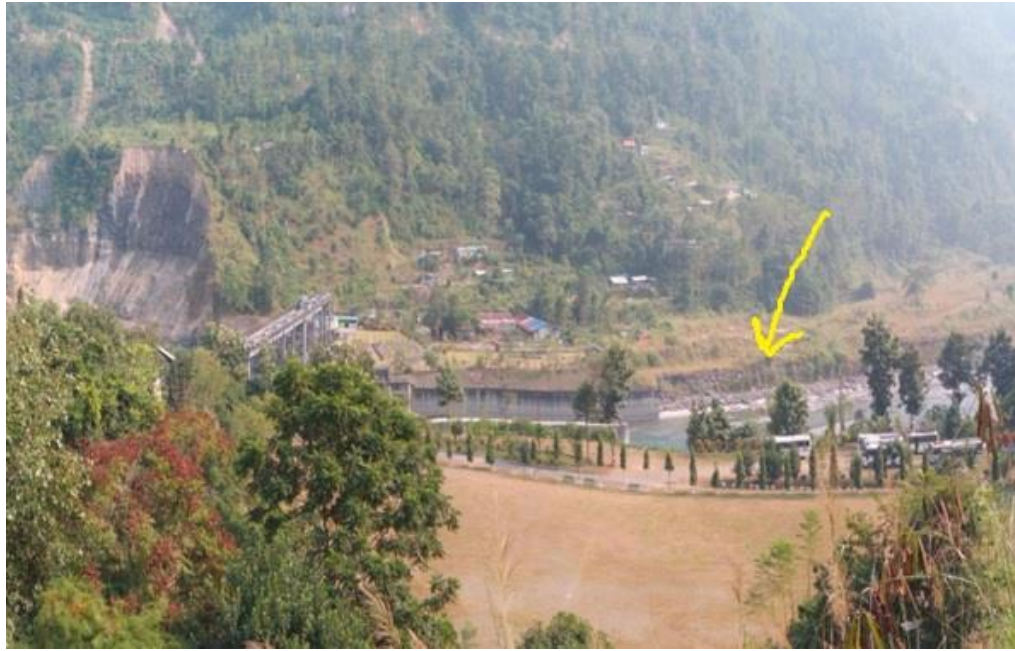


**Figure 2.7.** Erosion of lower terrace downstream of Jorethang Loop HEP in the Rangit at Rothak area (27.164 N 88.296 E)

**Source.** Field survey, November, 2022

### **2.3.2. Selected stretches of the Ranikhola and the Teesta River upstream from the confluence point**

Due to distortion of Google Earth Imageries, change in lower terraces and channel margin of these reaches (reach C and D in Figure 2.1) have been considered for the period of 7 years only (2010 to 2017). As per the findings, the channel margin has undergone diversion due to the construction of a dam in the upper section of the Teesta reach (reach C in Figure 2.1 and Table 2.1). However no significant change was observed in river terraces and tributary fan in both the reaches over the period of 7 years (Figure 2.8). As per the field evidences, the main drivers fostering change in channel margin are hydraulic structures i.e., dam and embankments. Ranikhola is one of the major left bank tributaries of the Teesta River. The reach is confined by terraces. The right bank section of the considered stretch of the Ranikhola reach (reach D in Figure 2.1 and Table 2.1) is subjected to straightening and confinement of the channel. In this

case, channel confinement and straightening are man-made due to the construction of an artificial embankment since 2016

Usually, the channel tends to widen up and deepen down downstream to adjust itself with the accumulated and growing flow volume coming from upstream (Charlton, 2008) but unfortunately, downstream water flows in this reach has no scope to adjust due to channelization. Over 7 years (2010 to 2017), there is no major change in valley floor features and channel margin. Therefore, this reach is in a stable condition.

The Ranikhola (C and D) in Table 1 is confined with very less scope for lateral adjustment.

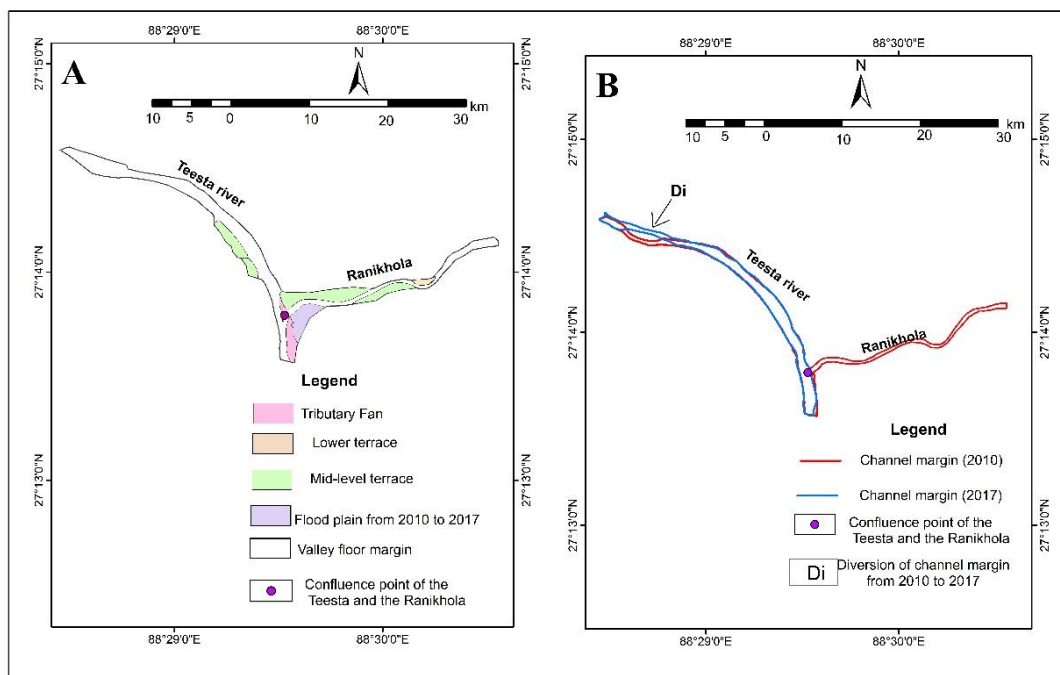


**Figure 2.8.** Change terrace morphology; (B): Change of channel margin of the selected stretches of the Teesta and the Ranikhola between 2010 and 2017

### 2.3.3. Rangpochu Reach

Rangpochu reach (Figure 2.9) is wide, semi-confined, and possesses good scope of lateral adjustment mainly during high flood flow as the major portion of the considered



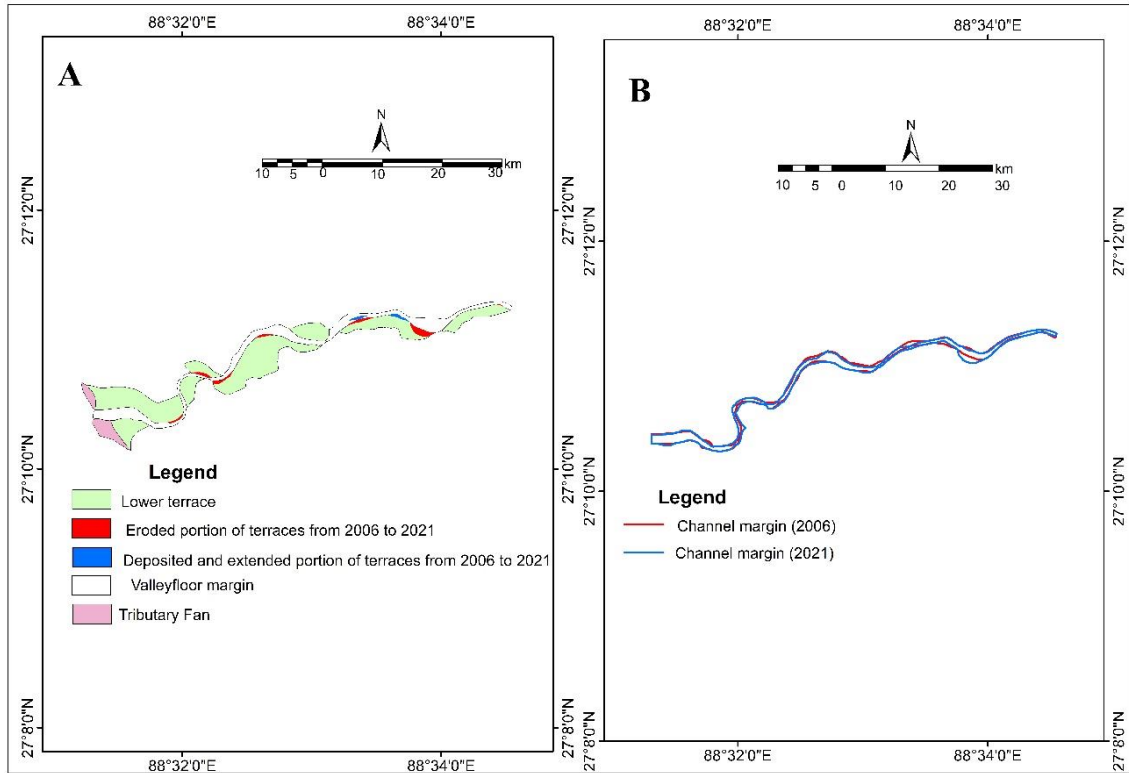


**Figure 2.9.** (A): Change of terrace morphology; (B): Change of channel margin of the selected stretch of the Rangpochu between 2006 to 2021

channel is bounded by the extensive lower terraces that have been eroded due to lateral shift of channel. It is apparent from the analysis of the GE images through visual interpretation that the considered reach has changed considerably over 15 years from 2006 to 2021. In 2006, there is no proper bar formation, the channel bed is covered by the patches of thin bedload sheets. The initial phase for bar formation is the deposition of bedload sheet where the flow becomes incompetent, coarse materials termed as lag deposits get settled and deposited over the bed which obstructs and diversifies the flow direction or pattern further encouraging sediment deposition resulting in bar formation (Charlton, 2008). As per the field evidences, the main drivers fostering change of river channel and lower terraces in this reach seems to be (i) erosion of terraces (ii) landslides washing away river bank and (iii) hydraulic structures.

### 2.3.4. The selected stretch of the Teesta reach flowing in between Singtam and Rangpo

In plan view, the valley floor of this reach between the Singtam bazaar and the Rangpochu (Figure 2.10) is studded with terraces on either side with the total absence of a flood plain. The channel is semi- confined but certain points are open for lateral adjustment where the lower terrace is present whereas in some points the channel is

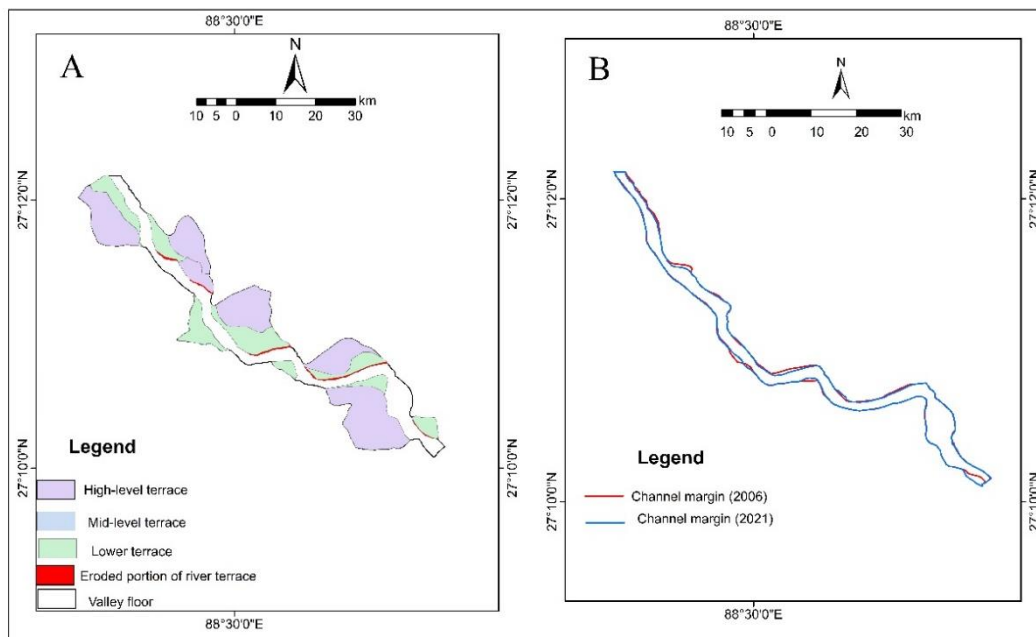


**Figure 2.10.** (A): Change in terrace morphology; (B): Change in channel margin of the Teesta river stretched in between Singtam and Rangpo between 2006 to 2021

confined by a hillslope with no scope of lateral adjustment. From 2006 to 2021, there is no major change in this reach witnessing only a minor erosion of the lower terraces.



**Figure 2.11.** (A): Slope failure at the selected stretch of the Rangpochu due to landslides (27.13 N, 88.533 E) (B): Lateral Shift of lower terrace at the Rangpochu due to erosion ( 27.176 N, 88.532 °E)



**Figure 2.12.** Teesta IV dam upstream of Singtam causing diversion of river channel.

## 2.4. Geological settings of the study area

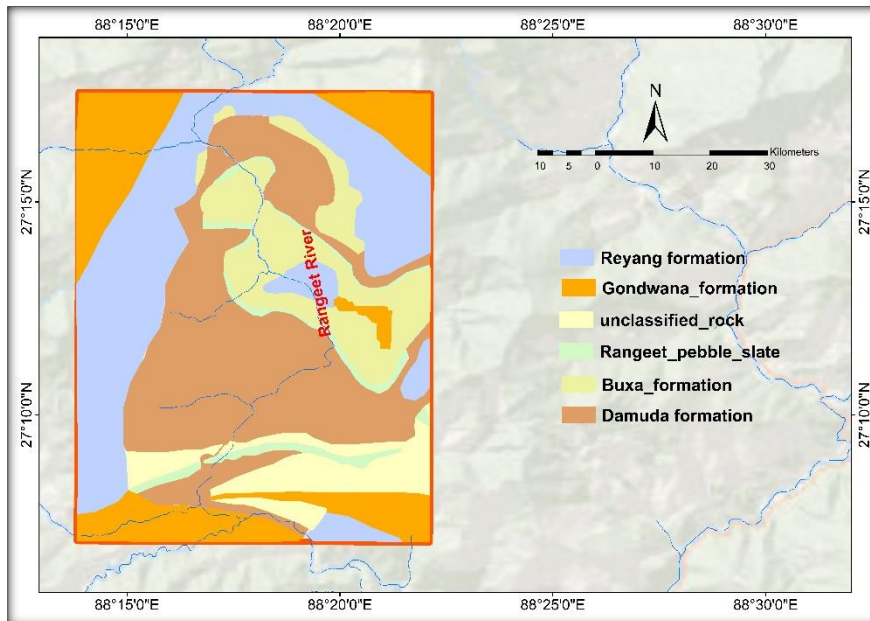


**Figure 2.13.** *Geology of the selected study sites in the Teesta, the Ranikhola , the Rangpochu*

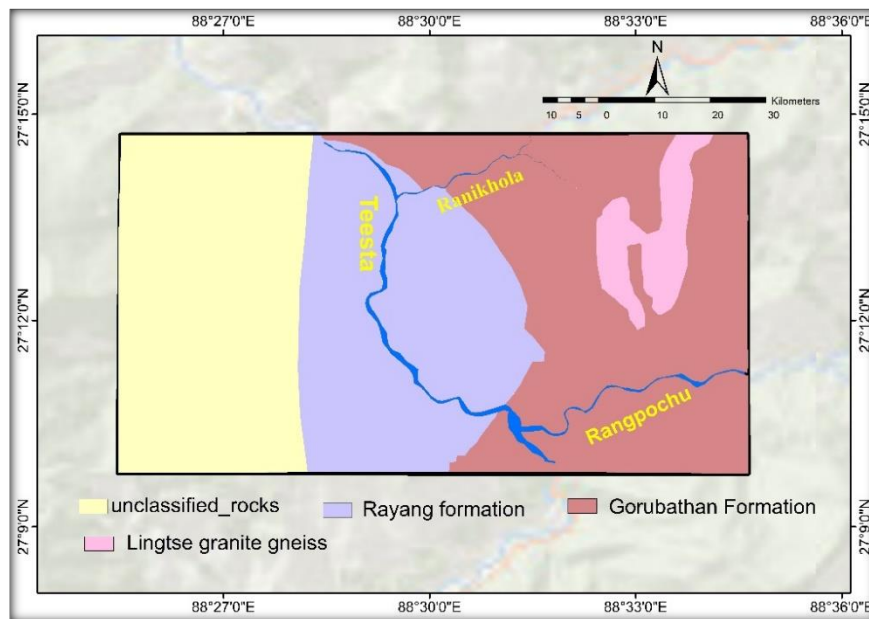


**Figure 2.14.** *Geology of the selected study sites in the Rangit*

The geology of the considered reaches of the Teesta basin (Figure 2.13) is dominated by metamorphic rocks falling under Daling group (Reyang and Gorubathan formation) and Lingtse granite gneiss. The Ranikhola and the Rangpochu are mainly composed of the Gorubathan formation with a minor presence of Lingtse Granite gneiss mainly in

the Ranikhola. The Gorubathan formation is mainly formed by the metamorphic rocks such as quartzite, schist, slate, chlorite phyllite, carbon phyllite, and metagreywacke. There is a proper interbedding of chlorite and quartzite in Rongpo, Duga, Pandem, Singtam, Manka area (Sarkar et al., 2012). The Reyang formation is also marked by the presence of quartzite.

Geology of the Rangit basin (Figure 2.14) is composed of Gondwana formation, Damuda formation, Rangit pebble slate, and Buxa formation. Damuda formation is formed of sedimentary rocks viz., calcareous sandstone, carbonaceous slate with thin coal beds. Buxa formation is an amalgamation of both sedimentary and metamorphic rocks such as dolostone, dolomite and mainly stretched from Naya Bazar to Legship road along the course of the Rangit river (Sarkar et al., 2012).

Thus comparatively, in terms of geology, the selected stretch of the Rangit river is weaker than that of the selected stretch of the Teesta River.

## **2.5. Variation of Sinuosity Index in the Selected Reaches**

A channel exhibits four-channel pattern in plan view namely straight, meandering, braided, and anastomosing (Hugett, 2017). The sinuosity reflects the channel irregularities and can be understood by analyzing two aspects of the channel i.e., channel length and valley length (Table.2.2). The channel length is measured along the center of the channel and the valley length is measured along the valley axis. The sinuosity index for the straight channel is below 1.1, 1.1 to 1.5 for the sinuous channel, and above 1.5 for the meander channel (Charlton, 2008). Both reaches C and D (Figure 2.5) are sinuous with sinuosity index of 1.2 in both time periods (Table 2.2). Overall, in all the selected reaches, the sinuosity index varies from 1.16 to 1.28. Therefore, selected reaches are showing sinuous channel pattern.



*Table 2.2. Variation of Sinuosity Index*

Reach	Channel Length		Valley Length		Sinouosity index	
	2006	2021	2006	2021	2006	2021
Reach 2 (Rangeet river)	5.29	5.3	4.56	4.57	1.16	1.16
Reach 1 (Rangeet river)	1.56	1.56	1.24	1.2	1.26	1.28
Reach in between Singtam and Rangpo	6.38	6.4	5.55	5.55	1.15	1.15
Rangpochu reach	6.77	6.79	5.6	5.55	1.21	1.23
	<b>2010</b>	<b>2017</b>	<b>2010</b>	<b>2017</b>	<b>2010</b>	<b>2017</b>
Ranikhola reach	2	2	1.7	1.7	1.21	1.21
Teesta reach upstream of the confluence point with Ranikhola	2.88	2.87	2.28	2.3	1.20	1.20

*Table 2.3. Channel Belt and Bar Area (2006 to 2021)*

Reach	Channel belt area (sq. km)		Bar area (sq. km)							
	2006	2021	Mid channel		Point bar		Sidebar		Total bar area	
			2006	2021	2006	2021	2006	2021	2006	2021
Reach 1 (Rangit river) (A)	1.57	1.57	No data							
Reach 2 (Rangit river) (B)	0.403	0.472	0.007	0.01	0.048	0.109	0.079	0.035	0.081	0.157
Reach in between Singtam and Rango (C)	0.92	0.88	0.029	0.043	0.076	0.061	0.184	0.215	0.315	0.361
Rangpochu reach (D)	0.483	0.484	0.02	0.056	0.026	0.038	0.112	0.069	0.159	0.163
	<b>2010</b>	<b>2017</b>	<b>2010</b>	<b>2017</b>	<b>2010</b>	<b>2017</b>	<b>2010</b>	<b>2017</b>	2010	2017
Ranikhola (E)	0.062	0.062			0.002		0.009	-----	0.062	----
Teesta reach upstream of the confluence point with Ranikhola (F)	0.236	0.226					0.093	0.074	0.093	0.074

*Table 2.4. Ratio of the Total Bar Area to the Total Channel Belt*

Reach	Total bar area/ channel belt area	
	2006	2021
B	0.27	0.99
E	0.342	0.361
F	0.329	0.337
	<b>2010</b>	<b>2017</b>
D	0.17	---
C	0.40	0.32

## **2.6. Aggradation and Degradation**

Channel aggradation is the river condition dominated by higher sedimentation. It is the process underlined by sediment accumulation downstream supplied from the upstream. Aggraded channels are wide and shallow with abundant numerous bar formations. Aggradation leads to a reduction in channel capacity as the channel bed rises increasing flood risk and also these contrast processes have a great impact on the dynamism of channel slope (Charlton, 2008).

On the other side, channel degradation implies the condition in which the rate of transport of sediments surpasses the accumulation rate due to higher kinetic energy of river water with a high discharge rate or due to low sediment supply in the channel which ultimately results in the removal of river bed loads and erosion of channel bank (Charlton, 2008).

As per the analysis of total bar area from GE imageries for the period 2006 and 2021 in the selected stretches (Table 2.3) and based on the ratio of total bar area and total channel belt area (Table 2.4), Out of six sampled reaches, three reaches viz., the Rangpochu reach (F), reach 2 of the Rangit river (B) and the considered reach in between the Singtam and the Rangpo (E) have undergone the process of aggradation over the period of 15 years (Table 2.3 and 2.4) as per ratio of total bar area and total channel belt area. The status of aggradation and degradation of the Ranikhola reach and the reach 1 of the Rangit river could not be analyzed due to poor resolution hindering the identification of bars and sediments. However, as per field observation and indepth discussion with locals of the study area, reach 1 of the Rangit river has also undergone aggradation. The main reason for aggradation is related to increase in the

supply of sediments due to bank failure, water-carried sediments and boulders and landslides (Figure 2.16).

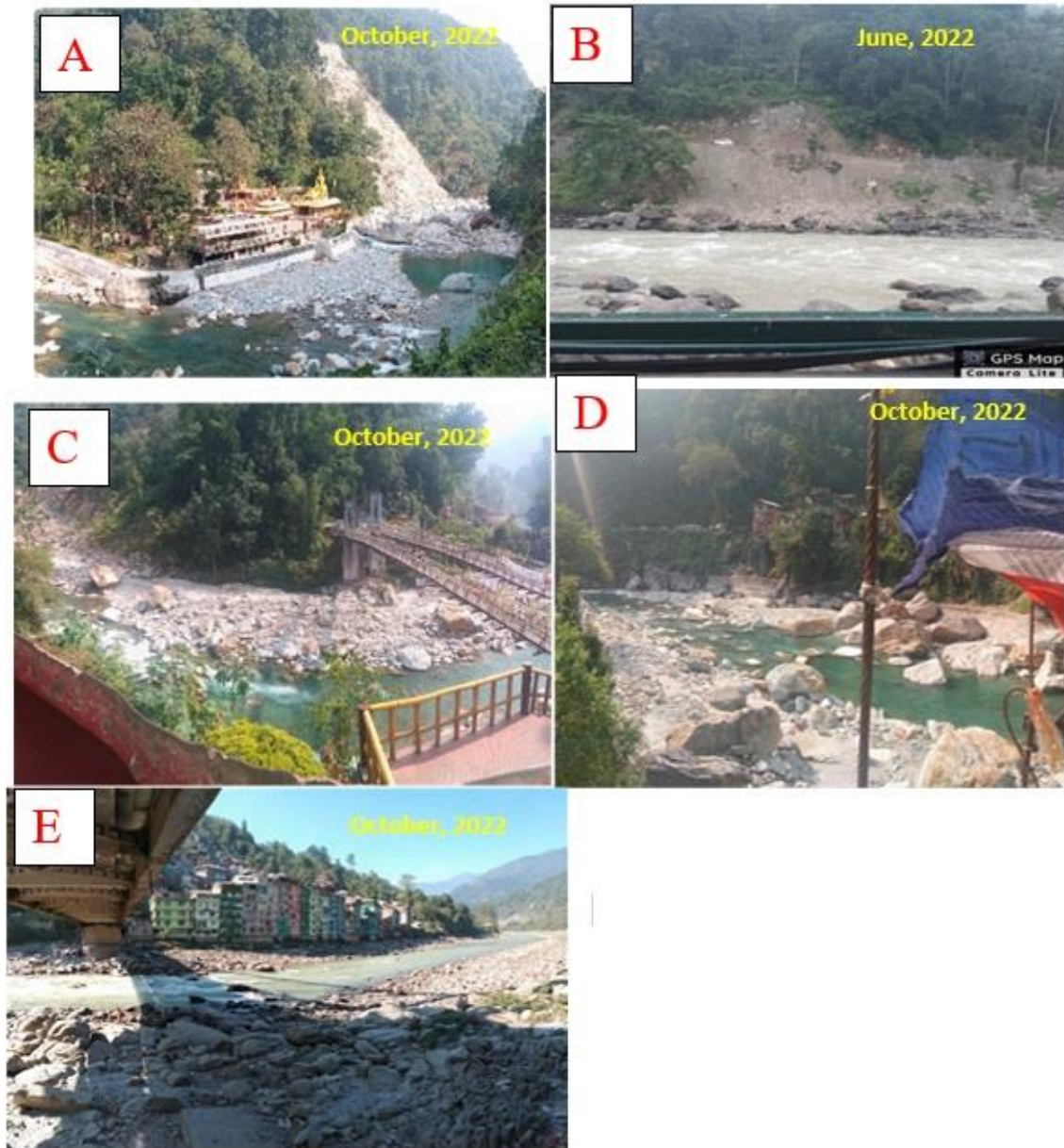


**Figure 2.15.** (A): Landslides as a source of sediments in the Rangit at Legship area (27.278 N 88.277 E). (B): Sediment supply from road construction in the Teesta at Singtam bazar area (27.229 N 88.492 E). (C): Sediment carried down and deposited by October 2021 flood in the Rangit at Legship area (27.278 N 88.276 E). (D): Massive boulders deposited by October 2021 flood in the Rangit at Legship area (27.277 N 88.275 E). (E): Massive accumulation of sediments in the Teesta river at Singtam bazar area over the period (27.231 N, 88.492 E)

**Source:** Field survey, 2022

In the case of the Rangpochu, in 2006, there is no proper bar formation, the channel bed is covered by patches of thin bedload sheet. In 2021, there is distinct view of numerous bar formation which signifies increase in channel bed sedimentation. Thus, the Rangpochu reach is considered to have undergone aggradation. An increase in bar formation implies an addition in sediment supply in the channel. Bars form when there is a huge supply of sediments from the upstream catchment areas fostered more by bank erosions (Charlton, 2008). Bars and Islands are the accumulated sediments in the channel mainly composed of sand, boulders, silt, and gravels (Charlton, 2008) exposed on the channel during the time of low river regime. The stability of bars is lesser than that of Island bars as island bars are covered with vegetation compared to bars which are subject to instability and composed of sands, and gravels (Summerfield, 2014). The initial phase for bar formation is the deposition of bedload sheet where the flow becomes incompetent, coarse materials termed as lag deposits get settled and deposited over the bed which obstructs and diversify the flow direction or pattern further encouraging sediment deposition resulting in bar formation (Charlton, 2008). Thus, the considered Rangochu channel is subjected to an increase in sediment supply and this supply is due to bank and lower terrace erosion and also dredging of lower terraces for the construction of structures as per field observation.

Reach 1 of the Rangit river is subjected to sedimentation and the main reason seem to be the erosion of banks and lower terraces as per field observation.

## **2.7. Conclusions**

Assessment of channel morphology of the considered six reaches has brought the reach-specific analysis of the morphological dynamism of the Teesta and its three major tributaries. From 2006 to 2021, two sampled reaches (Reach 1 and Reach 2) from the Rangit river have experienced erosion of banks and lower terraces causing a shift in the

channel margin posing threat to the settlements and roadways located on the terraces. The replica of man-made channelization is found in the considered reach of the Ranikhola and the Teesta reach located upstream of the confluence point of the Ranikhola. These reaches are greatly influenced by man-made structures causing channel confinement and diversion, For the last 7 years, the Ranikhola reach seemed to be stable in terms of channel characteristics (valley floor features and channel margin) with no major change. The Teesta reach between Singtam and the Rangpo has not witnessed any major change in terms of valley floor features from 2006 to 2021. There is merely a minor erosion of lower terraces. Whereas the considered reach section of the Rangpochu has changed considerably in terms of channel pattern and aggradation from 2006 to 2021. As per the findings, the main drivers of bringing dynamism in channel morphology seems to be bank and terraces erosion, bank failure due to landslides and human disturbance through the construction of hydraulic structures and roadways. The considered stretch of the Rangit river is more dynamic in terms of change in channel morphology from 2006 to 2021 than other considered reaches under study mainly due to weak geology as well as the construction of hydraulic structure i.e., dam.

## ***CHAPTER III***

### **Demarcation of Flood Zones at 25, 50 and 100-Year Return Period**

#### **Discharges**

##### **3.1 Introduction**

Flood zonation mapping at different return periods is one of the vital mitigation measures against flood-induced disaster. Flood zone mapping techniques is mainly based on two techniques, one using remotely sensed data such as optical and SAR while another technique is through 1D and 2D hydraulic modelling using steady and unsteady flow regimes.

Till 2016, 11 major calamitous floods had occurred in the Teesta river in 1950, 1968, 1973, 1975, 1976, 1978, 1993, 1995, 1996, 2000 and 2015. The 1968 flash flooding was the catastrophic one triggered by a cyclonic storm and cloud burst fostering 600 landslides damaging engineering structures like bridges (Tar Khola, Old Anderson Bridge, and Tista Bazar Bridge). Furthermore, the water level at Tista Bazar and Domohani embankment was above 20m above normal level (Pal et al.,2016).

Hazard turns into disaster when there is a realisation of hazard with the actual loss of large number of lives. When the social community encounters great loss and disruptions, it is termed as disaster (Smith & Petley, 2009). However, the outset of disaster can be curbed through various structural and non-structural measures. Assessment of risk or exposure to hazard is one of the non-structural means of disaster management (Smith & Petley, 2009). Risk implies actual exposure of something of human value to a hazard, it is the probability of occurrence of hazard with an involvement of losses (Smith & Petley, 2009).

### **3.1.1 Concept of Floodplain Zoning and Return Period**

Flood zones are the land areas that have the chance of being inundated by floods (Flood Partners, 2022). According to the CWC Model Bill for Flood Plain Zoning (1975), 'Flood plain zoning' means curbing any kind of human activities in the flood plains of the river where the plains are created by overflow of water from the rivers. In India, the CWC Model Bill for Flood Plain Zoning (1975) authorised every Indian state authority to work on curbing human activities along and adjacent to river channel and maintaining certain distance channel thresholds as per the requirements found after proper surveys and no person shall undertake any activity within the prohibited area without the prior permissions of Flood Zoning Authority (International Environmental Law Research Centre, 2021). The Bill was recirculated in 1996 due to a cold response from the State governments. However, till date only three states namely Manipur (1978), Rajasthan and Uttarakhand (December 16, 2012) have enacted or passed these bills through the acts but other states have failed to pay heed to this (International Environmental Law Research Centre, 2021). As per the NITI Aayog report 2021. "Flood plain zoning aim at demarcating zones or areas likely to be affected by floods of different magnitudes or frequencies and probability levels, and specify the types of permissible developments in these zones, so that whenever floods actually occur, the damage can be minimized, if not avoided" (NITI Aayog, 2021). Concept of floodplain zoning in India is based on discharges at 25, 50 and 100-year return period. The term return period ( $T_r$ ) or recurrence interval implies an average time gap in between two events that equal or exceed a particular level or magnitude. N year flood is the flood which is expected to be equal or exceed on an average every N year (Ward, 1978). To understand the concept of the return period, it is vital to understand magnitude and probability. Return period is measured in terms of year (Clarke,2005) and probability



is measured in percentage. Thus, considering this concept, return period discharge refers to the chance of occurrence of discharges of certain magnitude equal to or exceeding to that of a particular return period. Higher the magnitude, lesser is the probability of occurrence and vice-versa (Charlton, 2008; Morisawa, 2017). The term discharge implies the volume flow rate through a river cross section (Dingman & Bjerklie, 2005). Analysis of return period flood is a probabilistic approach of flood prediction that helps to analyse the probability of occurrence of flood during a given time period (Ward, 1978).

### **3.1.2. Significance of Empirical Equation in Discharge Estimation**

Main prerequisite for calculating the discharge at a defined return period is to gather information about the annual peak flow (Charlton, 2008). However, the conventional way of field-based discharge measurement technique is dissipating over the period mainly due to high cost and inaccessible areas in certain cases (Dingman and Bjerklie, 2005). The paucity of data related to major floods events or peak flow due to the lack of well-established observation stations has diverted the trend of flood-related data collection to alternative techniques among which paleo flood analysis (Charlton, 2008), geospatial analysis with the help of remote sensing and GIS techniques (Dingman & Bjerklie, 2005) are grabbing more attention. The paleo flood analysis can be achieved through some vital means like identification of flood marks on bridges and buildings, analysis of historical documents, flood deposits and erosion lines along the channels and valley walls and this branch is termed as paleo flood hydrology. Currently, the remote sensing and GIS techniques have eased the work of discharge estimation (Dingman & Bjerklie, 2005). However, discharge estimation directly through remote means is impossible and this can be accomplished through the calculation and analysis of predictor variables that can be observed remotely (Dingman & Bjerklie, 2005). This

predictor variable can be converted later into discharge through mathematical modelling (Dingman & Bjerklie, 2005). Another means of converting the predictor variables into discharge is the empirical equations. Hence, this chapter deals with estimation of peak floods at 25, 50 and 100-year return periods with the help of empirical equations. Further, this discharge was simulated through HEC-RAS model 1D steady flow model to perform the flood simulation and demarcation of flood zones at 25, 50 and 100-year return periods.

## **3.2. Methods**

This section is devoted to analyse the methods used for the accuracy assessment of the selected DEMs, formulae for estimation of floods at 25, 50 and 100-year return periods and input variables for running the 1D steady flow modelling using HEC-RAS. Methods used for flood zone demarcation have been discussed in the following sections:

### **3.2.1 Accuracy Assessment of DEMs**

Vertical accuracy assessment of SRTM, ALOSPALSAR, CARTOSAT-I, FABDEM, ASTER Global V003 DEMs were done with the help of a reference elevation data obtained from the topographic sheet of Swiss foundation for alpine research. The scale of the topographic map is 1: 1,50,000. Firstly, the topographic map was georeferenced and projected in the UTM zone 45 N projection and WGS 84 datum as in the case of DEM to identify the correct coordinates of which the elevation of the topographic map and DEMs were compared. A sum total of 38 spot heights and 17 contour crossing points on the selected river stretch were identified on topographic map (Figure 3.1) and then the Root Mean Square Error (RMSE) for the considered DEMs have been calculated using the following equation (3) (Schumann et al.,2008).

$$RMSE_{DEM} = \sqrt{\frac{\sum_{i=1}^n (E_{Ri} - E_{DEMi})^2}{n}} \dots\dots\dots (3)$$

Where  $E_R$  implies reference elevation from the topographic map,  $E_{DEM}$  is the elevation of DEMs and  $n$  is the total number of reference data points.

The RMSE values (in m) of the considered DEMs are 78, 298, 117, 49, and 180 for the SRTM, ALOSPALSAR, CARTOSAT-I, FABDEM, and ASTER Global V003 DEMs, respectively. Here, FABDEM appeared to be the most accurate in terms of vertical accuracy among the other DEMs. Further, the FABDEM represents a Digital Terrain Model (DTM) free from the influence of trees and buildings height and this adds more vertical accuracy which is highly favourable for hydrological modelling (Hawker et al., 2022).

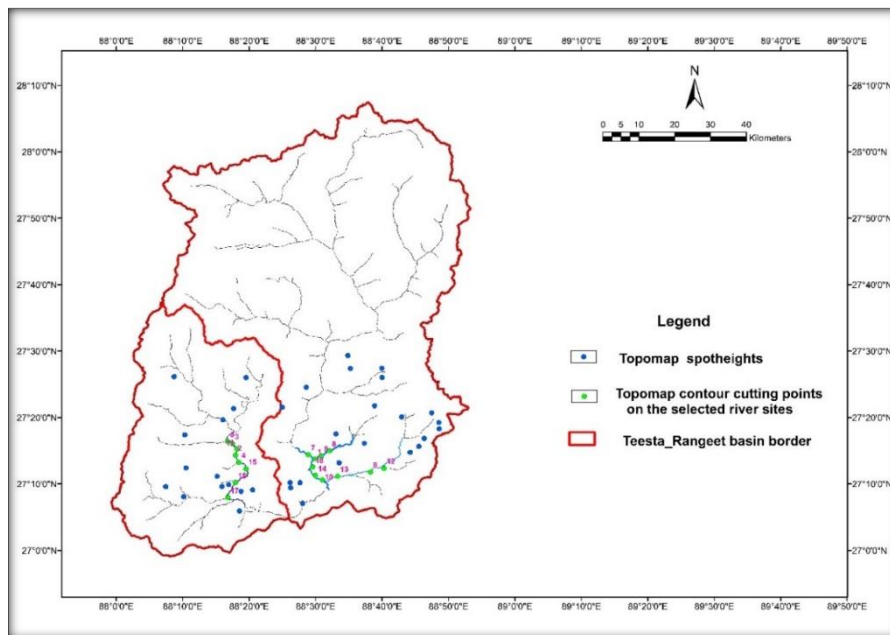


**Figure 3.1.** Planform map of the selected reference points of Topographic sheet for accuracy assessment

**Source:** Sikkim Himalaya Topographic map (1:150000) published by Swiss Foundation for Alpine Research, 2002

### 3.2.2. Empirical Equations for Peak Flood Estimation

This study utilised a simplified approach that deals with the estimation of flood peaks at 25, 50 and 100-year return period. Empirical formulae used under the simplified approach are as follows (CWC, 1991):

$$Q_{25} = 0.6855 (A)^{0.91839} (L)^{-0.39454} (LC)^{-0.19945} (S)^{0.31391} (R_{25})^{1.11481} \dots\dots\dots (4)$$

$$Q_{50} = 0.7262 (A)^{0.90265} (L)^{-0.37461} (LC)^{-0.19224} (S)^{0.31348} (R_{50})^{1.09719} \dots\dots\dots (5)$$

$$Q_{100} = 0.8372 (A)^{0.90662} (L)^{-0.36538} (LC)^{-0.20383} (S)^{0.31038} (R_{100})^{1.05471} \dots\dots\dots (6)$$

Where **A** is the catchment area (km<sup>2</sup>), **L** is the length of the longest stream from the catchment boundary to the site under study (km), **LC** denotes length of the stream from the centroid of the catchment to the discharge estimation site (km) and **R** is the point rainfall at defined return period (cm).

An equivalent channel slope (**S**) in (m/km) was calculated using equation (7).

$$S = \frac{\sum Li(D+Di)}{L} \dots\dots\dots (7)$$

Where **Li** is the length of *i*th segment of the longest stream (km), **D+Di** is a successive height above datum (m) and **L** denotes the total length of the longest stream (km).

Simplified approach considers physiographic as well as meteorological parameters for the computation of peak discharge at 25, 50 and 100-year return period. Catchment area, length of the longest stream, channel slope, and length of the river from the centroid of the catchment to the discharge estimation site. Average rainfall over the basin at 25, 50 and 100-year return period is a meteorological parameter. This approach is applicable to the catchment areas varying from 25 to 1500 km<sup>2</sup> (CWC, 1991). Further, this approach is also applicable to the catchment areas of 5000 km<sup>2</sup> on the basis of proper judgement and data of the neighbouring catchments (CWC, 1991).

### **3.2.3. Site Selection for Computation of Physiographic and Meteorological Parameters**

Selected sites for the computation of physiographic and meteorological parameters are located in the downstream reaches of the Teesta, Ranikhola, Rangpochu and Rangit rivers. Further, the selected site in the downstream section of the mentioned rivers are lying few distance upstream of the built-up areas. The selected sites were shown by P1, P2, P3 and P4 lying along the Rangit Teesta, Ranikhola and Rangpochu rivers, respectively (Figure 3.2). P1 is located upstream of Legship, West Sikkim, P2 is just upstream of Adarsh Gaon, P3 is upstream of Singtam *Bazar*, P 4 is located upstream of Rangpo *Bazar*.

All physiographic parameters at the selected sites (P1-P4) were obtained from the FABDEM. Demarcation of the catchment areas and extraction of the main channels were accomplished using hydrology module of ArcGIS (ver.10.2). For demarcation of the catchment areas, fill, flow direction and accumulation processes were run on the FABDEM. Extraction of the main channels was done using a threshold value of the flow accumulation. Determination of centroid and length of the channels (L and LC) were done using ArcGIS (ver. 10.2). Elevation for the equidistance points (1km) along the channel was computed using ArcGIS for the determination of slope (m/km) (Table 3.1).

Isopluvial maps of the 25, 50 and 100 year return periods were first georeferenced followed by digitization and extraction of isopluvial lines. Further, the isopluvial lines for the mentioned return periods were used to run the topo to raster module of ArcGIS (ver. 10.2).

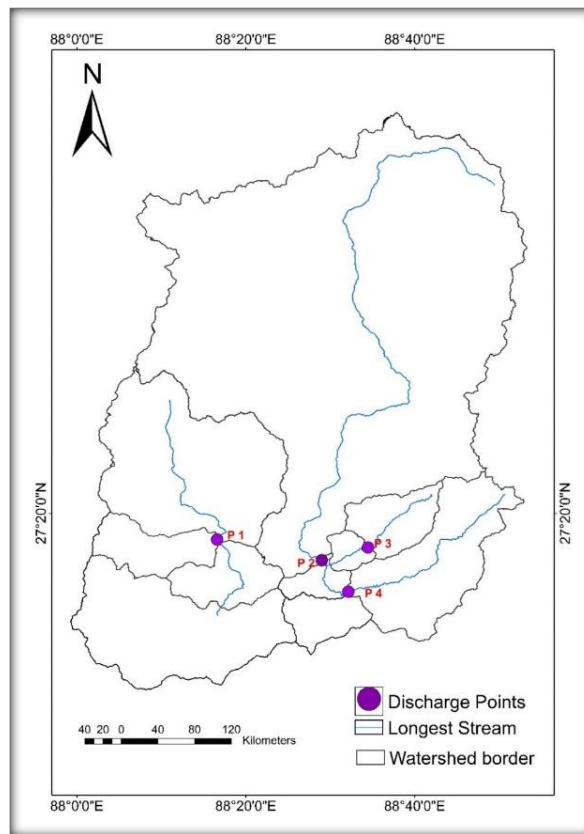


**Figure 3.2.** Location of points where discharge have been calculated using empirical formula

After running the mentioned module, isopluvial raster map for the mentioned return periods was obtained (Table 3.1; Figure 3.3). Further, catchment-wise average rainfall was calculated using an isopluvial raster map in GIS environment for the mentioned period.

**Table 3.1: Catchment-wise computation of physiography and meteorological parameters**

Catchment Name	Catchment area (km <sup>2</sup> )	L (km)	Equivalent stream slope (S) (m/km)	LC (km)	Average rainfall over the basin (cm)		
					25 year	50 year	100 year
Teesta	4553.08	154	24.19	81	17.9	20.1	25.6
Ranikhola	195.37	21	55.6	10	18.5	20.6	29.3
Rangpochu	567.99	47	42.7	26	22.6	24.3	33.6
Rangit	1338.76	61	41	37	19.5	22.4	28.1

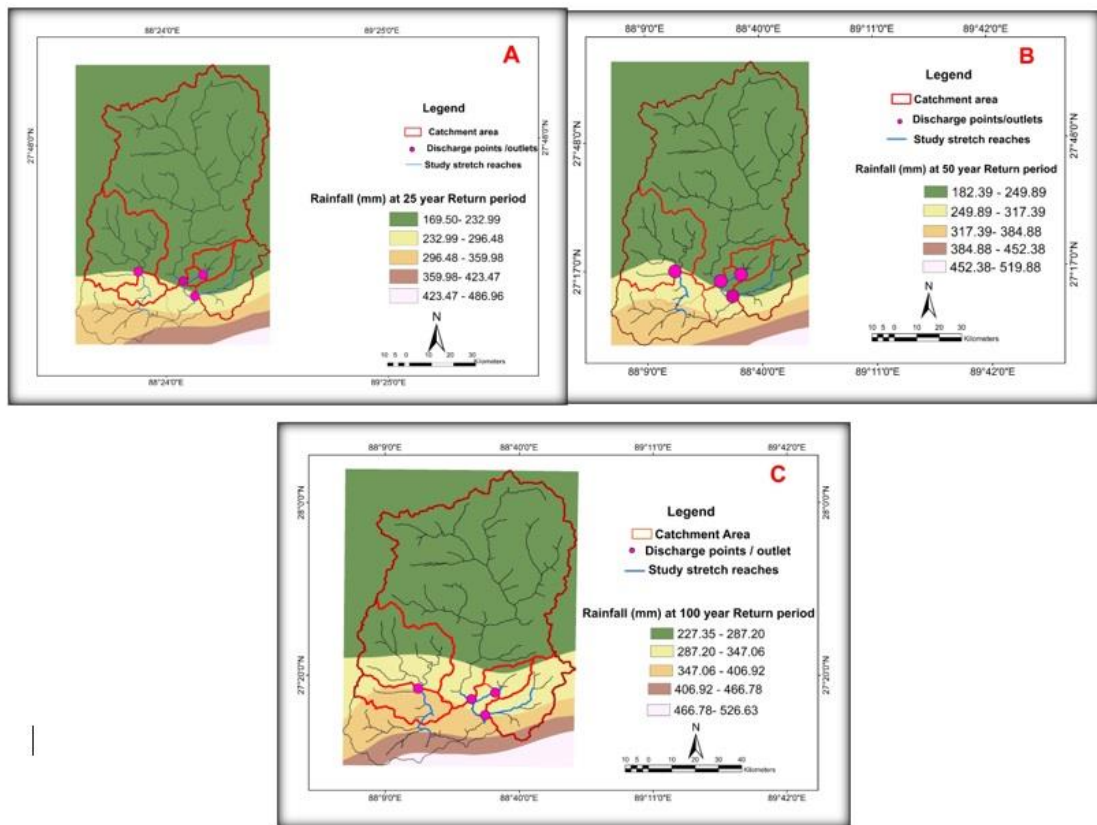


**Figure 3.3.**(A) Rainfall (mm) at 25-year Return period, (B) 50-year Return period and (C)100-year Return period

### 3.2.4. One-Dimensional Steady Flow Modelling

In One-dimensional flood modelling, all water flows are assumed to flow in a longitudinal direction. The 1D model represents the terrain as a sequence of cross-sections and simulates the flow to provide estimates of flow parameters such as flow velocity and water depth. To simplify the computation, HEC-RAS assumed a horizontal water surface at each cross-section normal to the direction of the flow such that the momentum exchange between the channel and the flood plain can be neglected (Dasallas et al., 2019). For 1D steady flow modelling, the input parameters are geometry files, land use and land cover (LULC) based manning's n values, normal depth or channel slope (m/m) and discharges at 25, 50 and 100-year return period (Brunner, 2016).

Required geometric data (river centreline, bank lines, flow paths and cross-sections) were prepared using HEC-geoRas extension of ArcGIS (ver.10.2) (Brunner, 2016) (Appendices I – VI). The geometry data were imported and processed with some other data viz., discharge, LULC-based manning’s n values, downstream boundary condition (normal depth) in HEC-RAS (ver. 6.1) software to run the 1D steady flow model to demarcate flood zones of 25, 50 and 100-year return period. Manning’s n and discharge values used for the 1D steady modelling are given in Table 3.2 and 3.3, respectively. LULC classification was done for the selected reaches of Teesta and Rangit rivers by visual interpretation of Google Earth images of February, 2021 (Figures 3.4 and 3.5). Discharges at 25, 50 and 100-year return period were taken as upstream boundary condition. Further, the HEC-RAS outputs such as water surface profiles were exported to HEC-geoRAS for mapping of flood extent using RAS mapping tool. The entire methods followed in this chapter are summarised in Figure 3.6.

**Table 3.2: LULC-wise Manning’s n values**

LULC	Manning’s n value
Agriculture land	0.035
Bare land and ground	0.045
Built-up	0.04
Forest land	0.1
Playground	0.025
Scrubland	0.03
River channel	0.04
Shrub trees	0.06
Road	0.13

*Source. Agriculture and Food Division of Department of Primary Industries and Regional Development, Government of Australia*



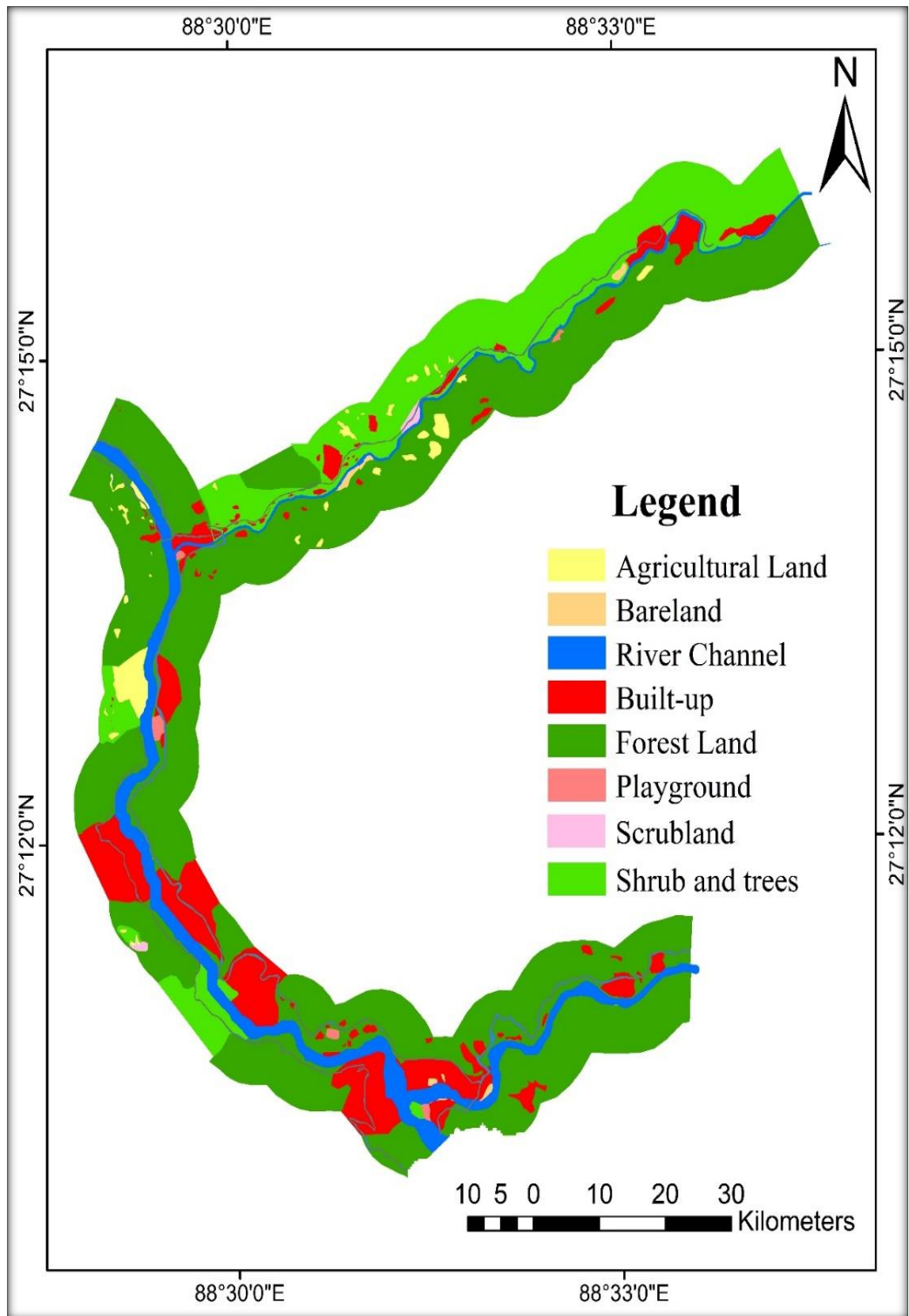


**Figure 3.4.** LULC map of the selected reaches of Teesta, Ranikhola and Rangpochu (2021)

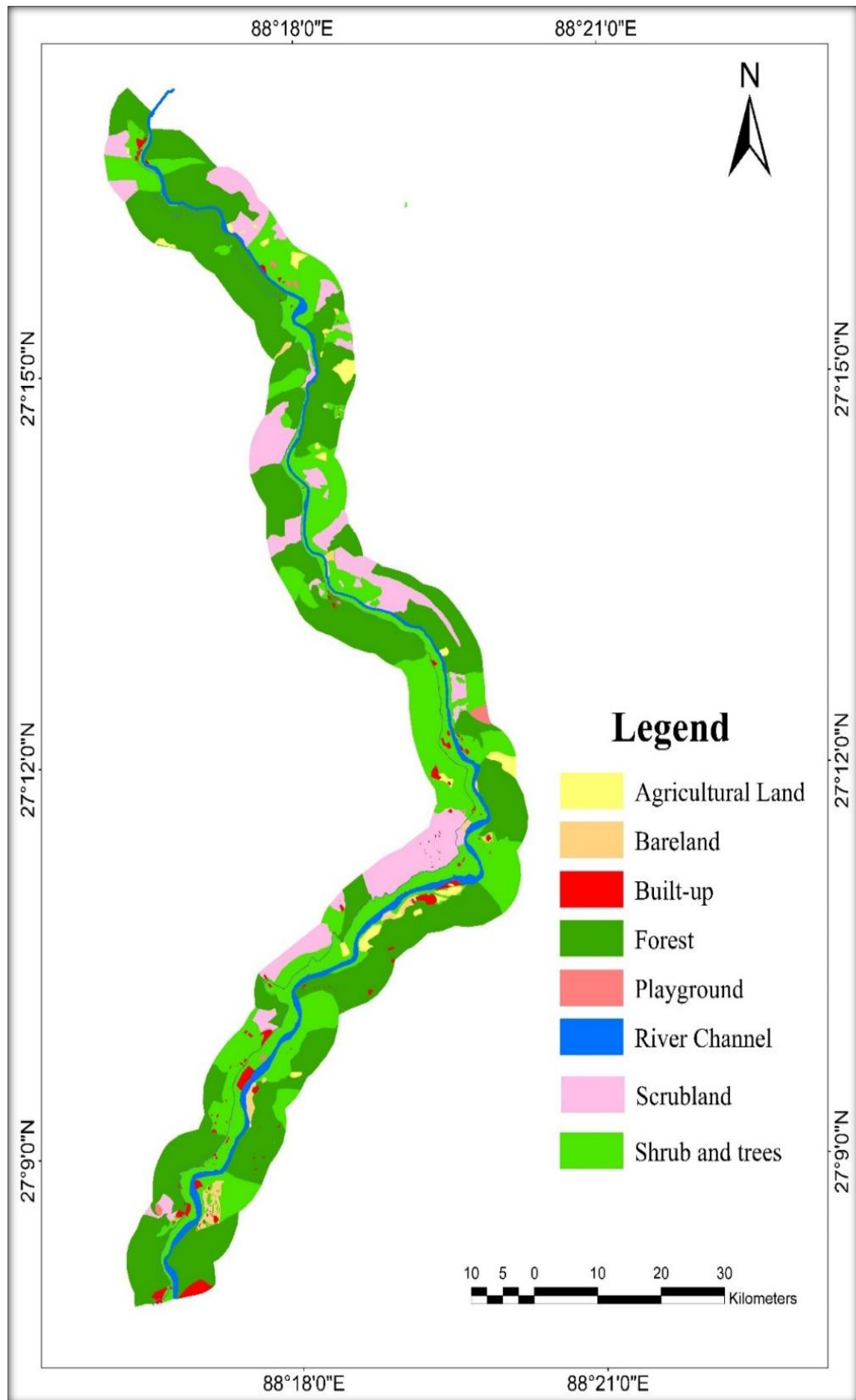


**Figure 3.5.** LULC map of the selected reach of the Rangit river (2021)

**Table 3.3.** Computed discharges at specified sites of the Teesta, Ranikhola and Rangpochu rivers

Catchment/Stretch Name	Discharges in cumec (m <sup>3</sup> /s)		
	<b>25 year</b>	<b>50 year</b>	<b>100 year</b>
Upper Teesta	6068	6926	9244
Ranikhola	1513	1700	2523
Teesta middle course downstream of Teesta-Ranikhola confluence	(6068+1513) =7581	(6926+1700) =8626	(9244+2523) =11767
Rangpochu	2786	3022	4329
Teesta downstream of Teesta-Rangpochu confluence	(7581+2786) =10367	(8626+3022) =11648	(11767+4329) =16096
Rangit	4508	5240	6838

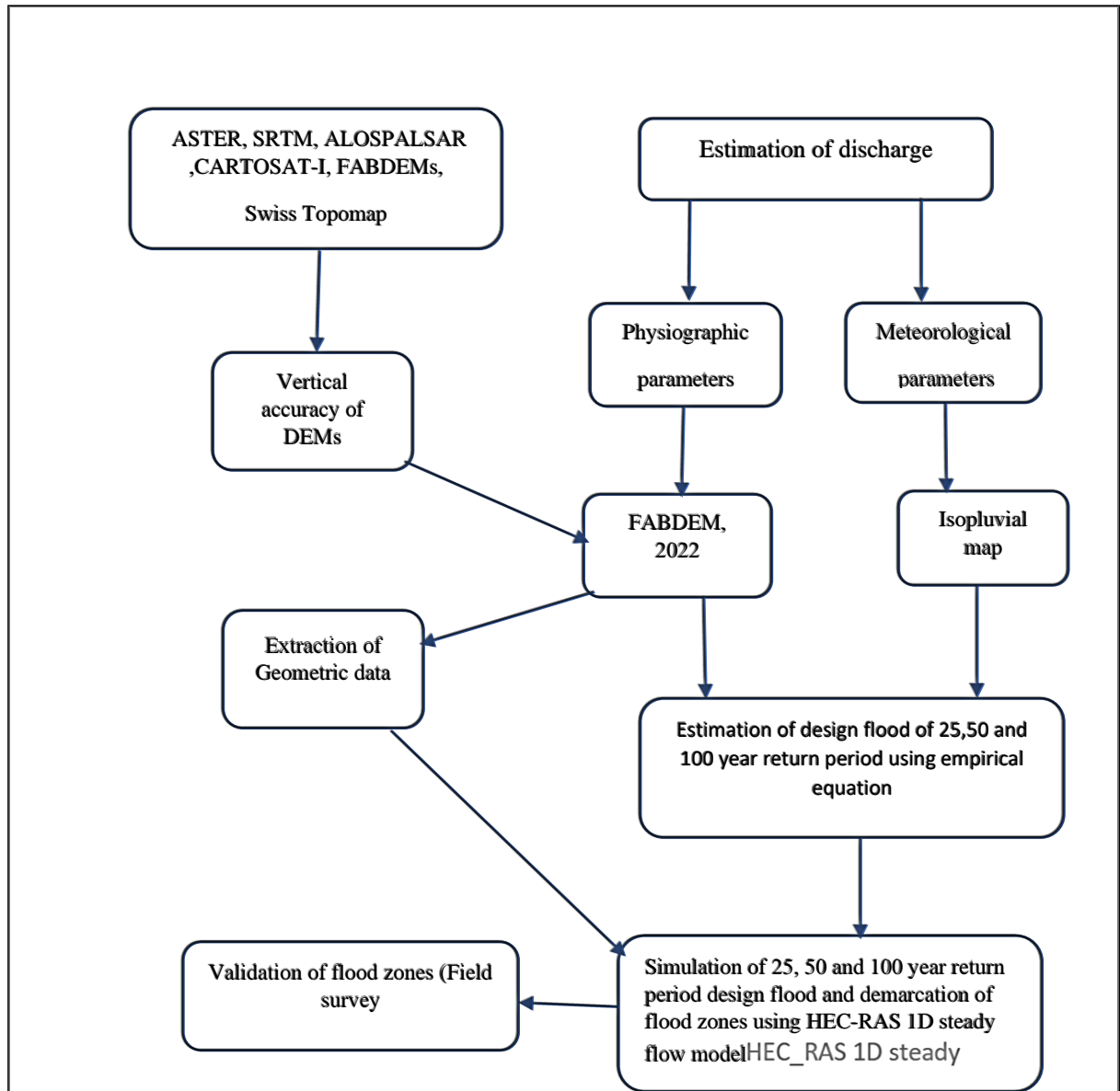


**Figure 3.6:** Flow chart of methods

In the steady flow modelling, hydraulic structures such as dam, embankments and bridges were not taken into consideration because of unavailability of data.

### 3.3. Output of One-Dimensional Steady Flow Modelling

In the case of the Rangit river, discharges at 25, 50 and 100-year return period were simulated for the stretch of 24 km downstream of the discharge point. In the case of Teesta river, discharges at the mentioned return periods were simulated for the stretch of 12 km downstream of the discharge point. For Ranikhola, the stretch of discharge

simulation was 11.38 km. For Rangpochu, discharges were simulated for the stretch of 5 km downstream of the discharge point.

### 3.3.1 Inundated Areas in Flood Zones

Statistics of flooded areas in different flood zones are shown in Table 3.4. The flood zone of 25-year return period is covering a large chunk of total flooded areas along the selected reaches of the Teesta and Rangit rivers because of the low elevation compared to 25-50 and 50-100 years return period zones. Flood zones demarcated along the selected reaches of the Teesta river, Ranikhola, and Rangpochu are shown in Figure 3.7 A-C.

**Table 3.4.** Flood zone-wise flooded area in hectare

Reach	Flooded Area in Flood Zones			Total Flooded Area	Flood Zone-wise Percentage of the Total Flooded Area			
	25 Year	25 - 50 Year	50 – 100 Year		25 Year	25 - 50 Year	50 – 100 Year	Total
Teesta	162.24	9.38	15.23	186.85	87	5	8	100
Ranikhola	64.49	5.16	6.53	76.18	84	7	9	100
Rangpochu	76.92	3.25	6.69	86.86	88	4	8	100
Rangit	365.39	27.79	35.89	429.07	85	7	8	100



**Figure. 3.7 (A):** Flood zone of 25year return period flood in the selected stretches of the Teesta, Ranikhola and Rangpochu

Boundaries of Flood zones in Singtam (confluence of Ranikhola-Teesta rivers), Majitar (Teesta river) and Rangpo (confluence of Rangpochu-Teesta) urban centres are shown in Figure 3.8 A-C. The demarcated flood zones along the Teesta River, Ranikhola and Rangpochu fall within the elevation 210m to 380 m, above mean sea level (amsl). Flood zones along the Rangit river are shown in Figure 3.10 A-C. In Figure 3.11 A-B, flood zones have been zoomed in for Legship area and at the downstream section where Jorethang loop dam is located. Flood zones of the Rangit river are covering the elevation ranging from 210m to 500 m amsl (Figure 3.12).



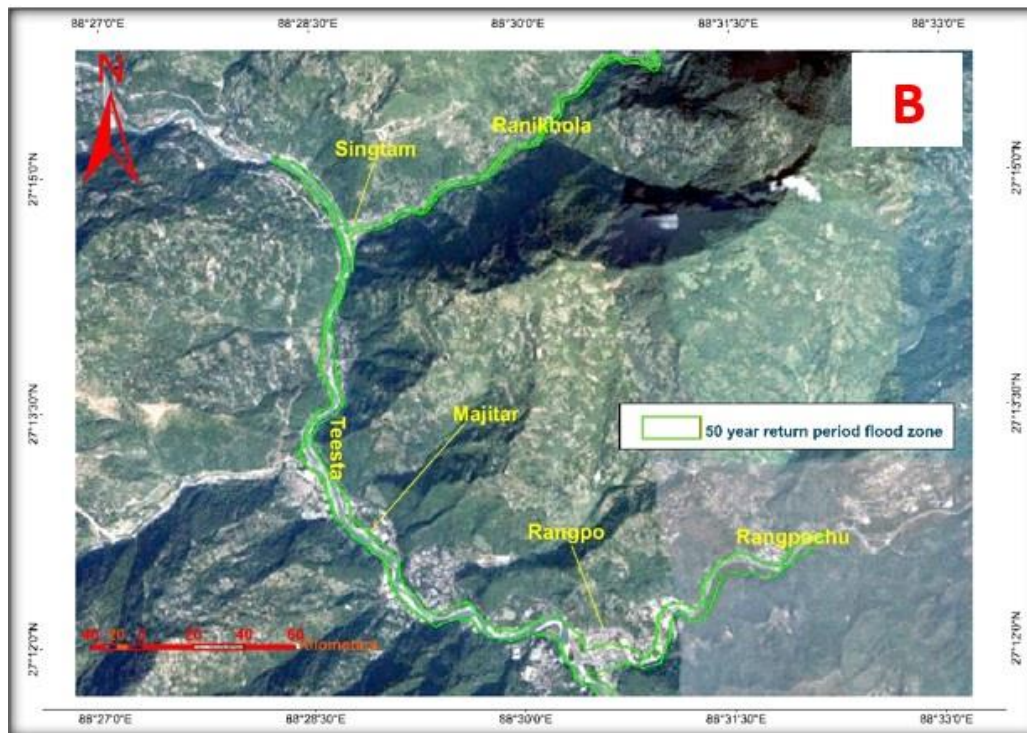


*Figure 3.7.(B): Flood zone of 50-year return period flood in the selected stretches of the Teesta, Ranikhola and Rangpochu.*



*Figure 3.7. (C): Flood zone of 100-year return period flood in the selected stretches of the Teesta, Ranikhola and Rangpochu*

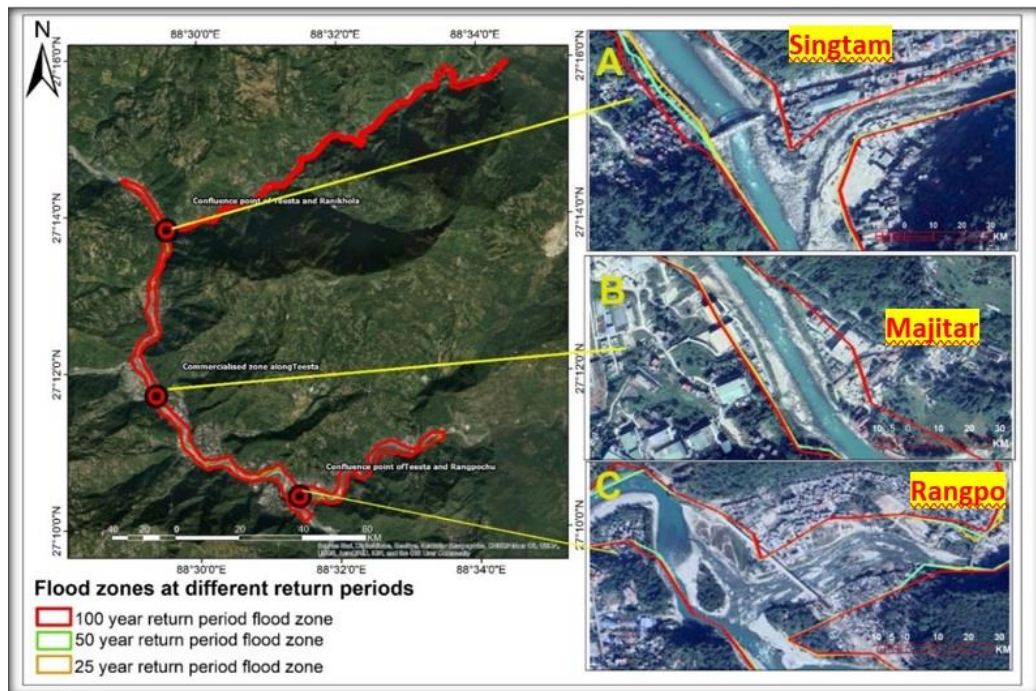


**Figure 3.8.** Flood zones of 25,50 and100 year return period in selected stretches of the Teesta, Ranikhola and Rangpochu. (A): Extent of flood zones at the confluence point of the Teesta and Ranikhola (Signtam) (B): Extent of flood zone in Majitar urban centre (C): Extent of flood zones at the confluence point of the Teesta and Rangpochu (Rangpo)

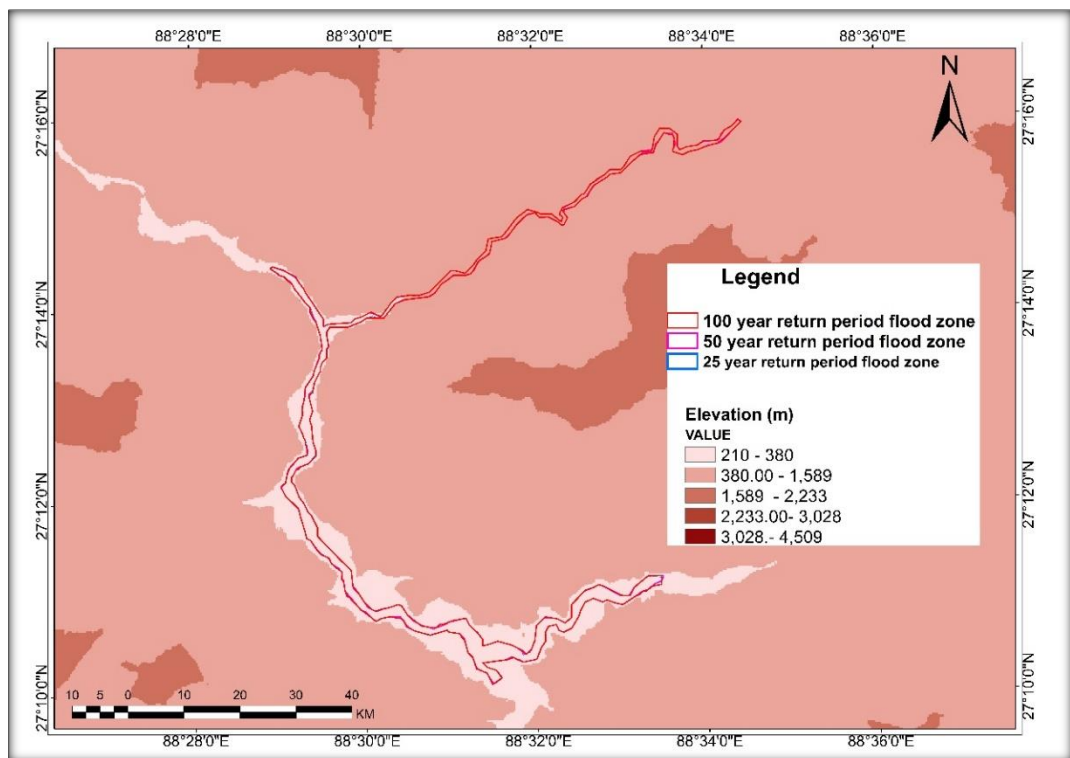


**Figure 3.9.** Elevation range of flood zones of 25, 50 and100 year return period flood in the selected stretches of the Teesta, Ranikhola and Rangpochu



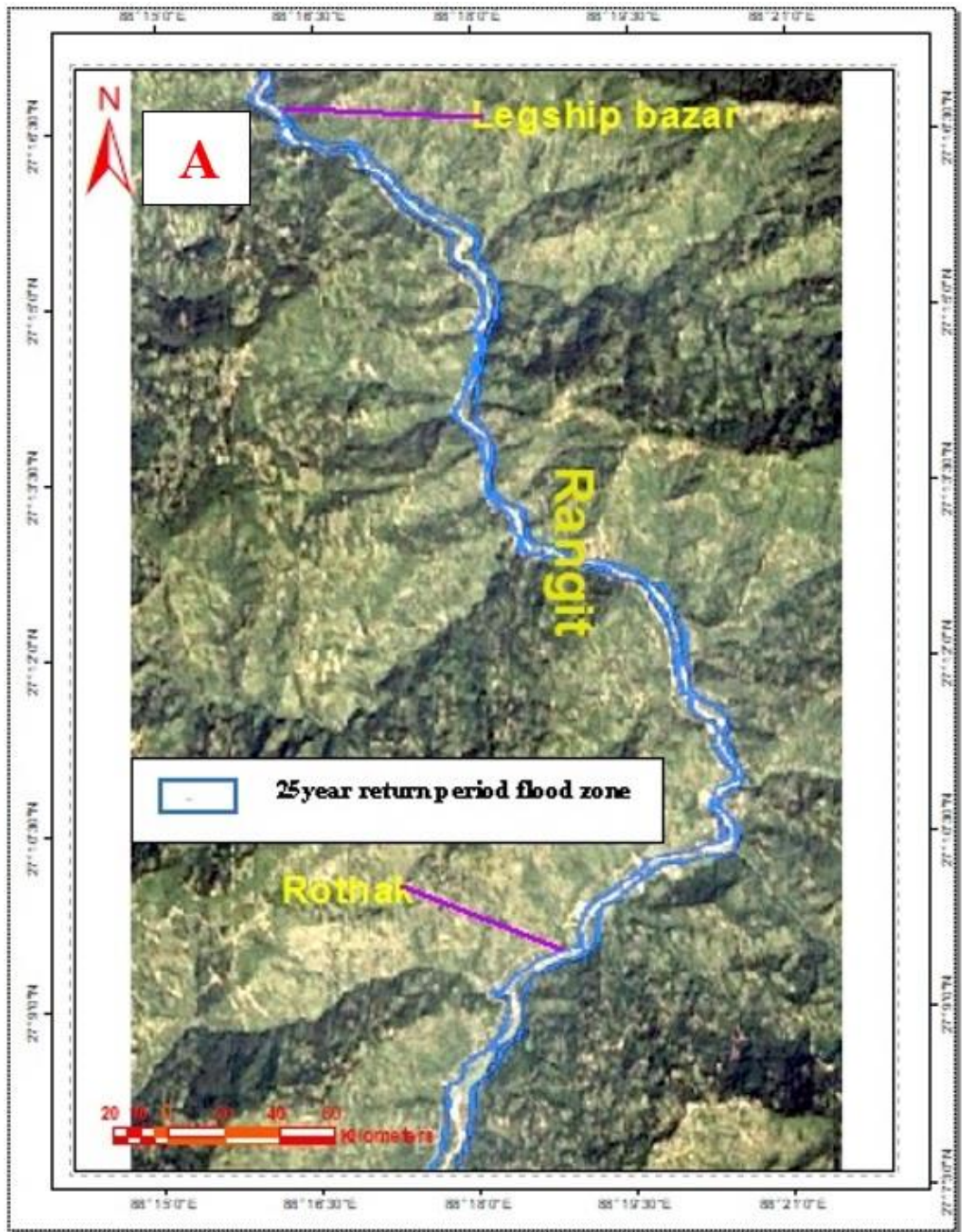


*Figure 3.10. (A): Flood zone of 25-year return period flood along the Rangit river*

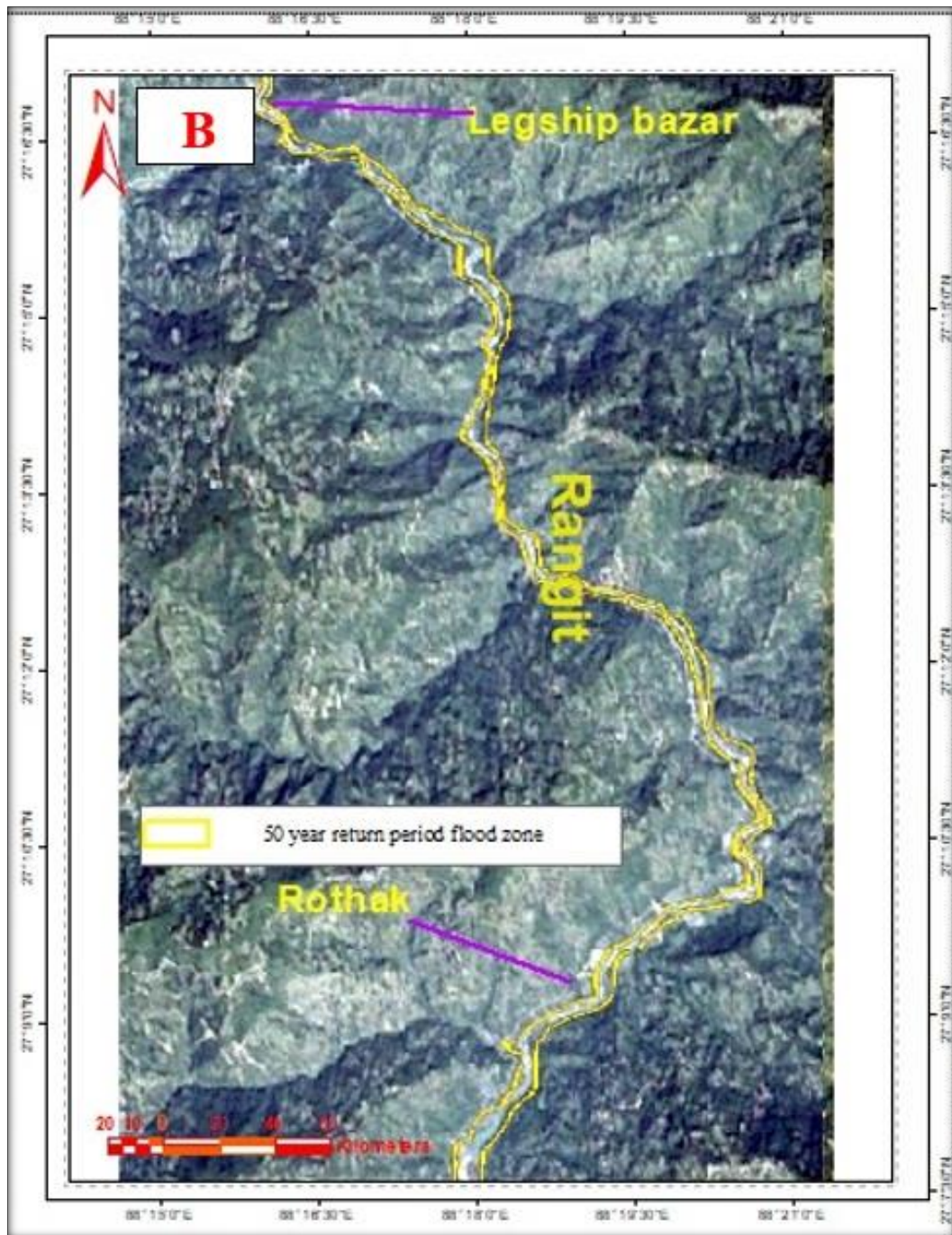


*Figure 3.10. (B): Flood zone of 50-year return period flood along the Rangit river.*



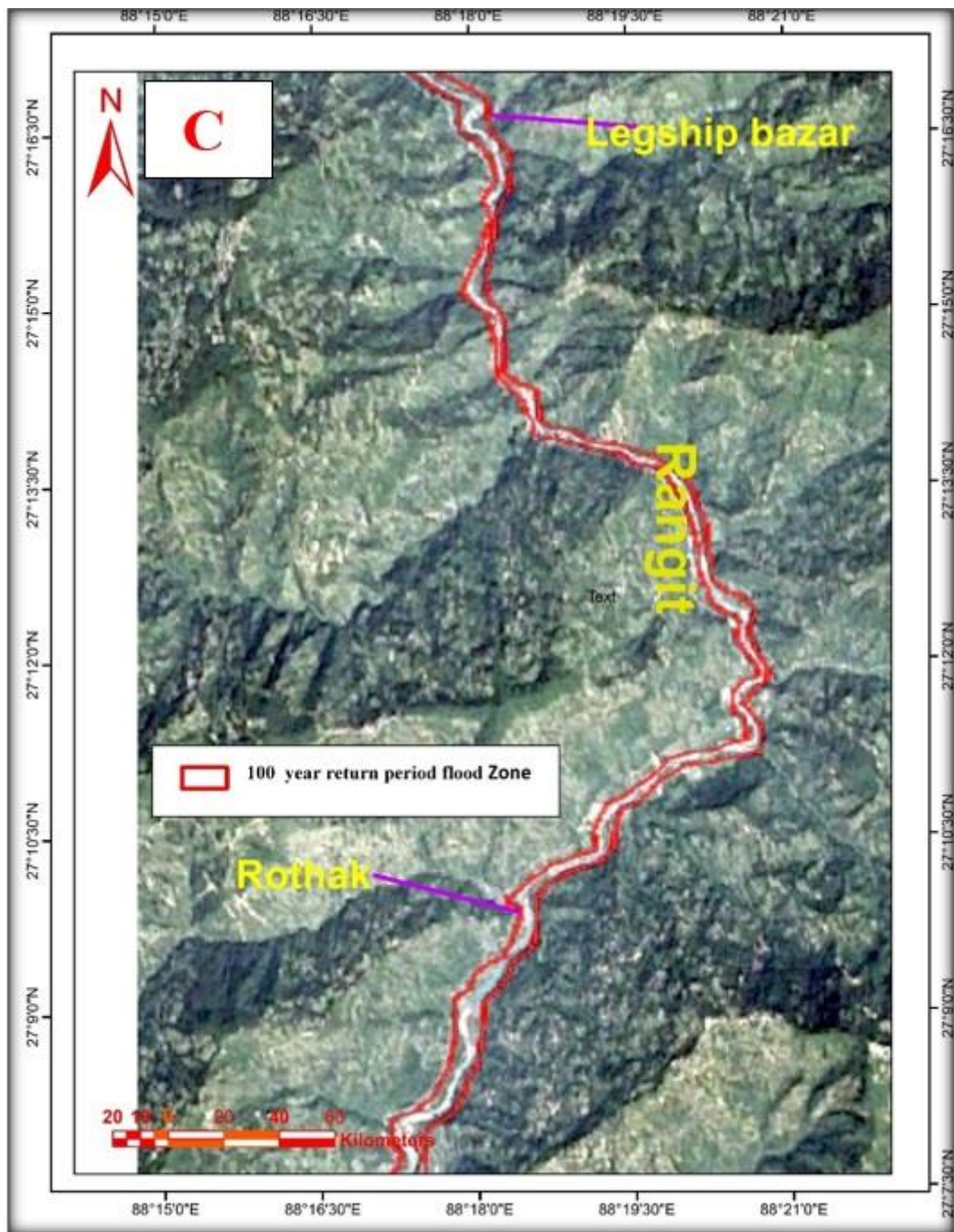


*Figure 3.10.(C): Flood zone of 100-year return period flood along the Rangit river.*

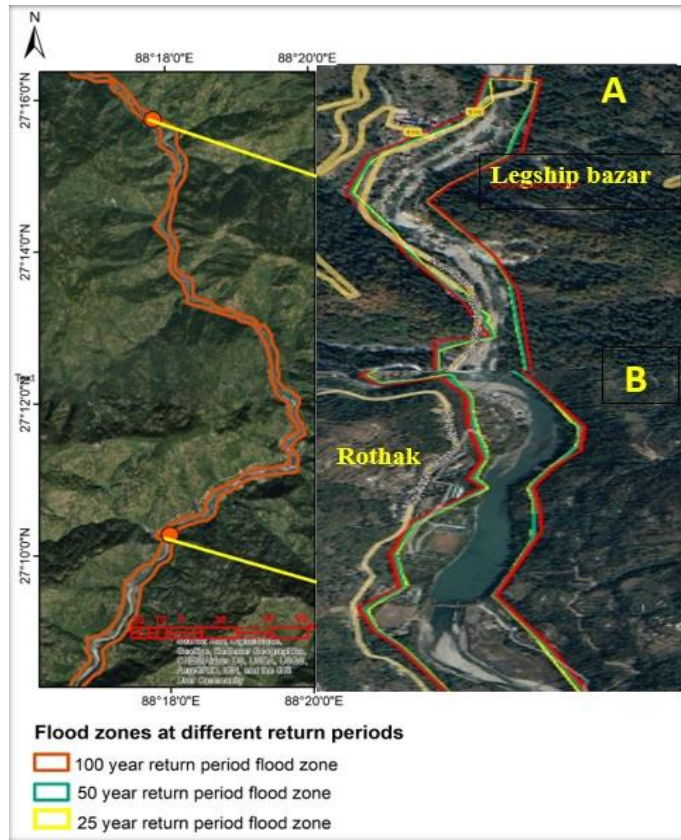


**Figure 3.11.** Flood zones of 25,50 and 100-year return period at selected stretches of the Rangit river. (A): Extent of flood zones at the point near Kirateswar temple (B). Extent of flood zone at the point near Jorethang Legship dam.

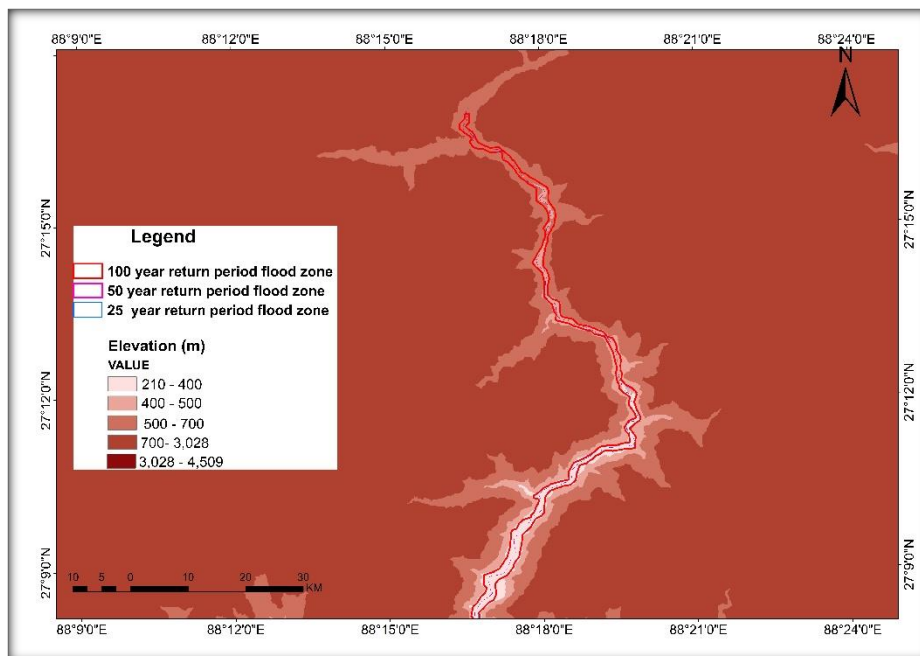


**Figure 3.12.** Elevation range of flood zones of 25, 50 and 100 year return period along the Rangit river.

### **3.4. Validation of One-Dimensional Steady Flow Modelling Output**

Validation of the steady output and estimated discharge was done using maximum discharge of 1968 floods, people's perception and inundation of lower terraces.

Following sub-sections are dealing with validation procedures:

#### **3.4.1 Comparison of Estimated Discharge with Recorded Maximum Discharge**

As per CWC (1991), the percentage variation of flood values of 25,50 and 100 return periods obtained using a simplified approach are within the tolerable limits of  $\pm 15\%$ .

On 4 October, 1968, the maximum discharge of 18,150 cumec was recorded at Teesta Bazar (Wiejackza et al., 2014). On the same date and site, Starkel (1972) estimated a maximum discharge of 27,500 cumec along with mean velocity of 5.5 m/sec and flow depth of 20m. The calculated discharge of the Teesta downstream of Teesta-Rangpochu confluence at 100-year return period is 16096 cumec. By the adding the 100-year discharge of Rangit to Teesta, the obtained discharge is 22,934 cumec which is close to the estimated discharge value (27,500 cumec) by Starkel (1972).

#### **3.4.2 Inundation of Lower Terraces and People's perception**

Complete and partial inundation of lower terrace in the mountainous regions often occurs at 10-100-year return period (Benito and Hudson, 2010). Figures 3.13 and 3.14 show the complete and partial inundation of lower terraces at 25, 50 and 100-year return period discharge along the Rangit and selected reaches of the Teesta and its tributaries.

Recorded perception of the senior age group people at the Teesta -Ranikhola confluence point, extent of flooding extended up to Lal Bazar areas of Singtam and few houses got washed away. The observed extent of flooding in 1968 is matching with simulated flood extent at 100-year return period (Figures 3.15 A-B).

In the upstream reach of the Rangit river, people’s perception at Legship Bazar and Naya Bazar were recorded. As per recorded perception, Flooding in 2021 was the largest at the mentioned places. This flood overflowed embankments and damaged a temple locally termed ‘Kirateswar temple’ located on left bank depositing huge sediments inside it. The observed flood level of 2021 flooding is close to the simulated flood extent at 25-year return period.

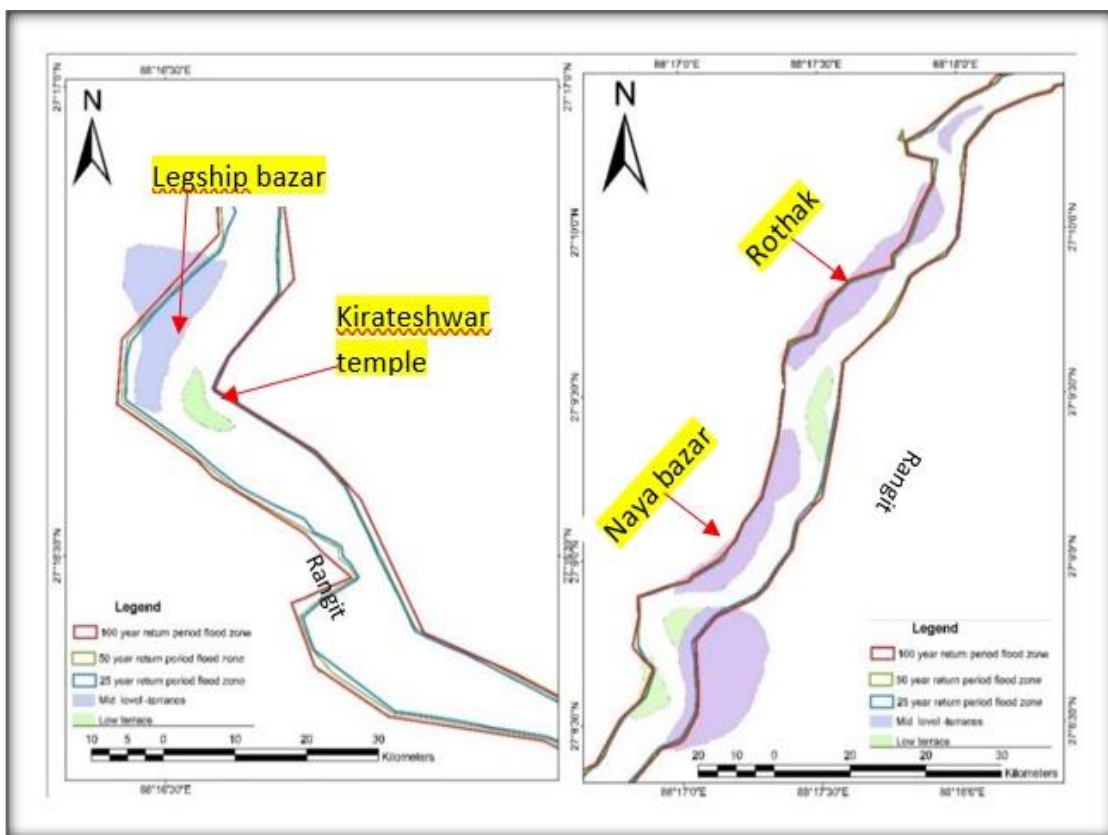


**Figure 3.13.** Portion of mapped lower and mid-level terraces likely to get inundated in case of simulated flood scenarios along the selected stretches of the Rangit river.



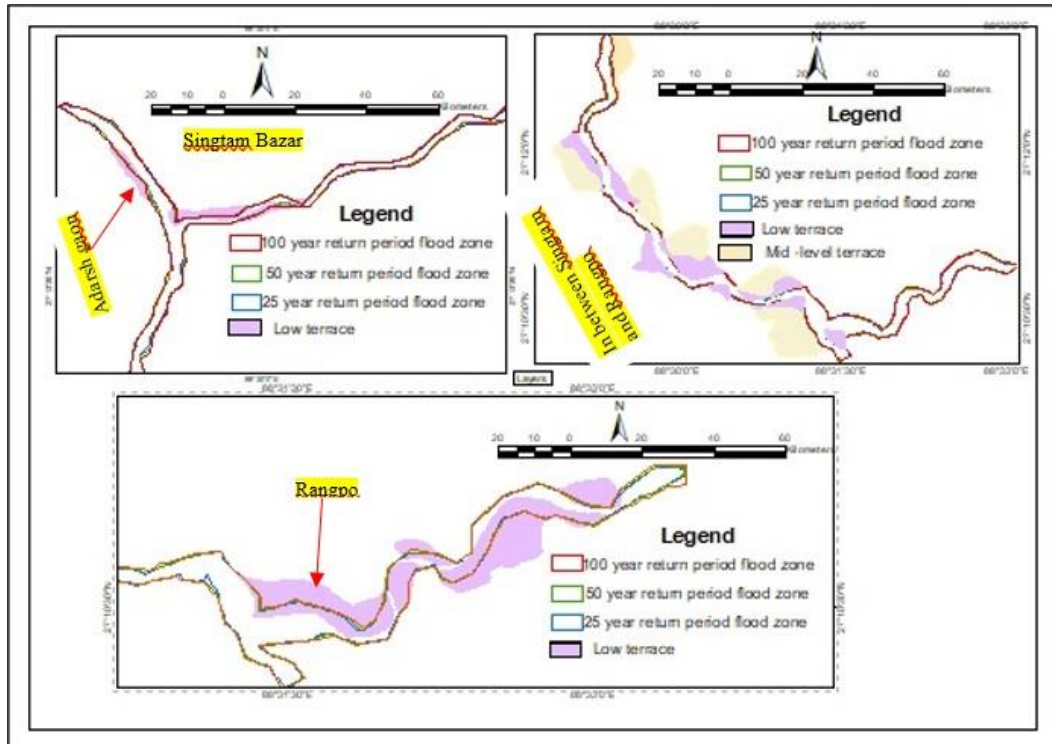


**Figure 3.14.** Portion of mapped lower and mid-level terraces likely to get inundated in case of simulated flood scenarios along the selected stretches of the Teesta, Ranikhola and Rangpochu.



**Figure 3.15.** (A): Simulated flood zone of 25, 50 and 100-year return period flood at Singtam bazar (B): Observed maximum flood zone at Singtam in October, 1968.

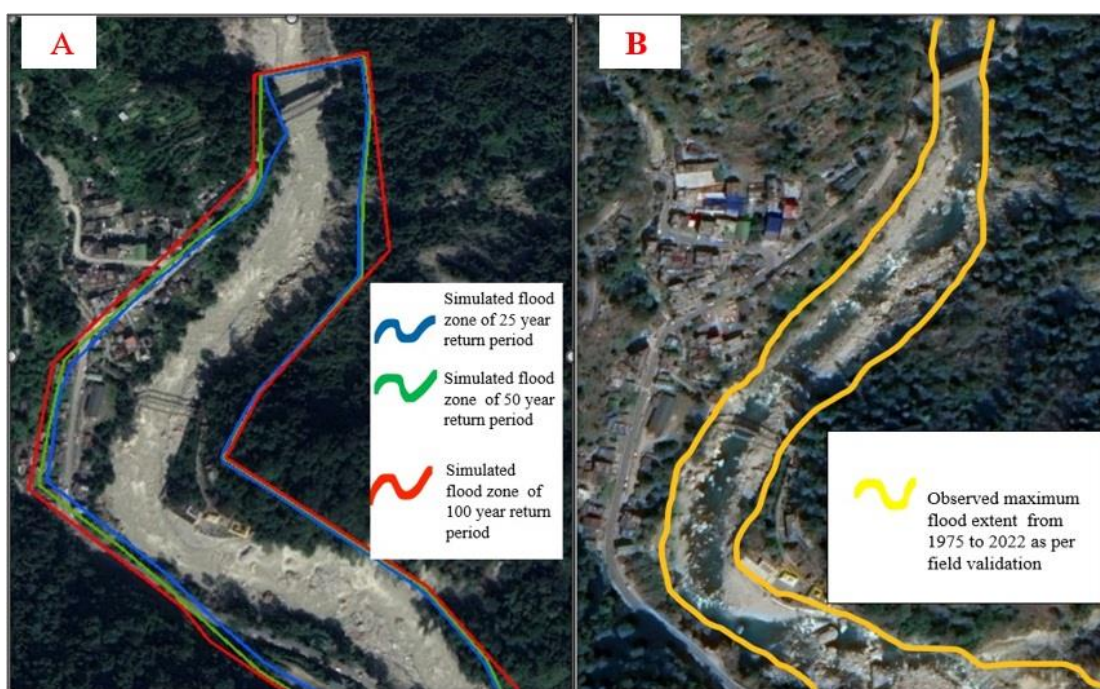


**Figure 3.16.** (A): Simulated flood zone of 25, 50 and 100-year return period flood at Legship Bazar area. (B) and (C): Observed maximum flood zone at Legship bazar area (1975 to 2021).



### **3.5. Conclusions**

FABDEM is considered as an appropriate DEM for hydraulic modelling in the selected reaches of the Teesta basin based on the RMSE value. The modelled extent of flooding is well validated with the help of inundation of lower terraces at 25, 50 and 100-year return period discharges, 1968 flood extent and peak discharge, and people's perception. On the basis of a comparison of the estimated 100-year return period discharges of the Teesta and Rangit rivers, it can be inferred that the return period of the 1968 floods is close to 100-year.

## ***CHAPTER IV***

### **Assessment of Flood Zone-Wise Built-up Areas**

#### **4.1 Introduction**

Hazard is a naturally occurring or human-induced process, or event, with the potential to create loss and hazard turns into a disaster when there is a realisation of the hazard with the actual loss of a large number of lives (Smith & Petley, 2009). However, the outset of disaster can be curbed through various non-structural measures. Assessment of risk or exposure to the hazard is one of the non- structural means of disaster management (Smith & Petley, 2009). Risk implies actual exposure of something of human value to a hazard, it is the probability of occurrence of a hazard with involvement of losses (Smith & Petley, 2009).

As per the analysis of the Central Water Commission report on state-wise flood-induced damage on nine parameters from (1953-2017), there is an increase in flood-induced damage in Sikkim (Central Water Commission, 2019). The highest area affected due to floods was 1.17 million hectares during 1993-2002. Highest number of damaged houses was 14,456 during 1983-1992 and highest loss of public utilities was Rs. 586 crores during 2003-2012. On an average, floods are damaging 756 houses annually in Sikkim (Central Water Commission, 2019).

The woeful 1968 flash flood (2<sup>nd</sup>-6<sup>th</sup> October) that hit Sikkim and West Bengal is still a nightmare. Outset of the 1968 flood is believed to be heavy rain caused by cloud burst and landslides. (Pal et al., 2016). This flood washed away Tar Khola bridge, Old Anderson bridge and Teesta bazaar bridge. Water level went 20m above danger level at Teesta Bazar (Pal et al., 2016). Moreover, Sikkim has become the pivot of landslides due to cloudburst, surface triggering by developmental activities and many other

causes. Landslides along mainly along river valley are the genesis of forming landslide dams adding the risk of flash flooding.

Built-up areas adjacent to river channel have proved to be one of the causes of flood disaster in India. For instance, the main reason for the exacerbation of damages and loss incurred by the 2013 Kedarnath flash floods in Uttarakhand is believed to be mainly due to a higher rate of urbanisation causing encroachment on lower terraces of the river channel and also due to the narrowing of Mandakini River (Uniyal, 2013). Similarly, the flood which hit Srinagar in September 2014 turned into disaster damaging lives and properties mainly due to rapid urbanization and encroachment on Dal, Anchar, Hokrasar, Narkarar inducing shrinkage in wetlands (Ahmad et al., 2019). The Rishiganga flashflood (February 07, 2021) caused the washing away of bridges, roads (Sain et al., 2021) and temple located along the Dhauliganga river (Shugar et al., 2021).

Against the backdrop of the above-mentioned studies, this chapter deals with the assessment of built-up areas in flood zones exposed to floods with 25, 50 and 100-year return period and its spatio-temporal variation over the period of 15 years along the selected reaches of the Teesta and its two major left bank tributaries viz., the Ranikhola, the Rangpochu and its major right bank tributary viz., the Rangit river. The built-up zone is one of the classes of land use type. The term 'built-up' encompasses the areas used intensively and covered mainly by structures. The cities, towns, strip development along the highways, power and communication facilities, areas occupied by mills, industries, institutions and settlements come under the category of built-up area (Lillesand et al., 2015).

## 4.2 Methods

Built-up areas located within the demarcated flood zones of 25,50- and 100-year return period were digitised through the visual interpretation of Google Earth images of dry months i.e., 06/02/2006 and 08/03/2021. The validation of digitised built-up areas has been done through field survey. The flood zones were overlaid on Google Earth images and built-up areas were then extracted and processed in ArcGIS for mapping and calculating areas to assess the variation of areal extent over the considered period. In this study, the percentage change in the areal extent of built-up area (in hectare) over three different return period flood zones from 2006 to 2021 for the selected reaches of the Teesta and its three considered tributaries viz., the Ranikhola, Rangpochu and Rangit river has been calculated using Equation (8) (Pandey et al., 2011).

$$\text{Percentage change} = \left(\frac{T_2 - T_1}{T_1}\right) \times 100 \dots\dots\dots (8)$$

T<sub>1</sub> and T<sub>2</sub> is the built-up area of the year 2006 and 2021, respectively.

## 4.3. Flood Zone-Wise Built-up Area (2006-2021)

The characteristics of built-up area falling within demarcated flood zones and its variation over the period of 15 years (2006-2021) in the selected stretch of the Ranikhola, Teesta, Rangpochu and Rangit rivers have been discussed in the following sections:

### 4.3.1 Built-up Areas in Flood Zones of the Ranikhola (2006-2021)

The built-up areas area falling within flood zones of the selected stretch of the Ranikhola river comprised of residential buildings and small commercial hotels, restaurants and shops (Figures 4.1 C & D). Thus, these areas are less resilient to flood

hazard as they don't own flood insurance too. Resilience refers to the ability of society to deal and recover from the consequence of hazardous events (Smith & Petley, 2009).

All these mapped built-up areas (Figures 4.2 and 4.3) are not older than 25- 30 year and got established after the 1968 floods. According to change detection of built-up areas for the period of 15 years (Figures 4.2 and 4.3), the growth of built-up area within the demarcated flood zone of 25, 50 and 100-year return period flood of magnitude 1513  $m^3/s$ , 1700  $m^3/s$  and 2523  $m^3/s$ , respectively is not much along this stretch and the main cause is the restriction on construction towards river channel due to presence of embankment (approx. 8m) that was constructed in 2016. However, the sign of expansion of built-up area is found along the left bank of the Ranikhola and at upstream section (G5 grid in Figure 4.3) due to the absence of any restricting flood-protecting structures. Prior to the construction of this embankment, people stated that buildings and human lives were at stake and river water would extend inside residential areas but still built-up areas located at the confluence points (G6 and G23 grids in Figures 4.2 and 4.3) are more prone to flood hazard because of back water flow. In 2016, embankments (8m in height) were constructed (Figure 4.1D) along the right bank of the Ranikhola at its downstream section which has played a vital role in safeguarding houses and people's lives. However, people are not sparing even low-lying terraces and tributary fans for developmental activities in this section and the cases of embankment breaching by flood water during monsoon are prominent in this section. As per local people's experience, the flow velocity of the Ranikhola river is higher than that of the Teesta river leading to abrupt and sudden high flow in the Ranikhola because of its narrow, confined channel with no scope of lateral expansion. Mishra et al. (2019) reported that the coverage of built-up area in Ranikhola watershed increased from 1988 to 2017. Percentage change in built-up area is highest in the flood zone of 50–100 year return

period followed by 25-year return period zone (Table 4.1). Overall encroachment of built-up areas on each flood zone is increasing between 2006 and 2021 (Table 4.1).



**Figure 4.1.** Built-up area in (Grid 6) along the Teesta and Ranikhola. (A): Built-up area downstream of Indreni pool part of which currently gets inundated during monsoon season (27.231 N, 88.492 E). (B): Built-up area upstream of Indreni pool (27.233 N, 88.49 E). (C): Built -up area on right bank of the Ranikhola ((27.231 N, 88.499 E). (D): Built – up area at the confluence point of the Ranikhola with Teesta (27.23 N, 88.499 E).

**Table 4.1:** Built-up area (in hectare) and percentage change in the flood zones of the Ranikhola from 2006 to 2021

Flood Zone	Built-up area (2006)	Built-up area (2021)	Percentage change in built-up area (2006-2021)
25	1.43	2.35	64.34
25-50	0.15	0.23	53.33
50-100	0.08	0.43	437.50
Total	1.66	3.01	81.3

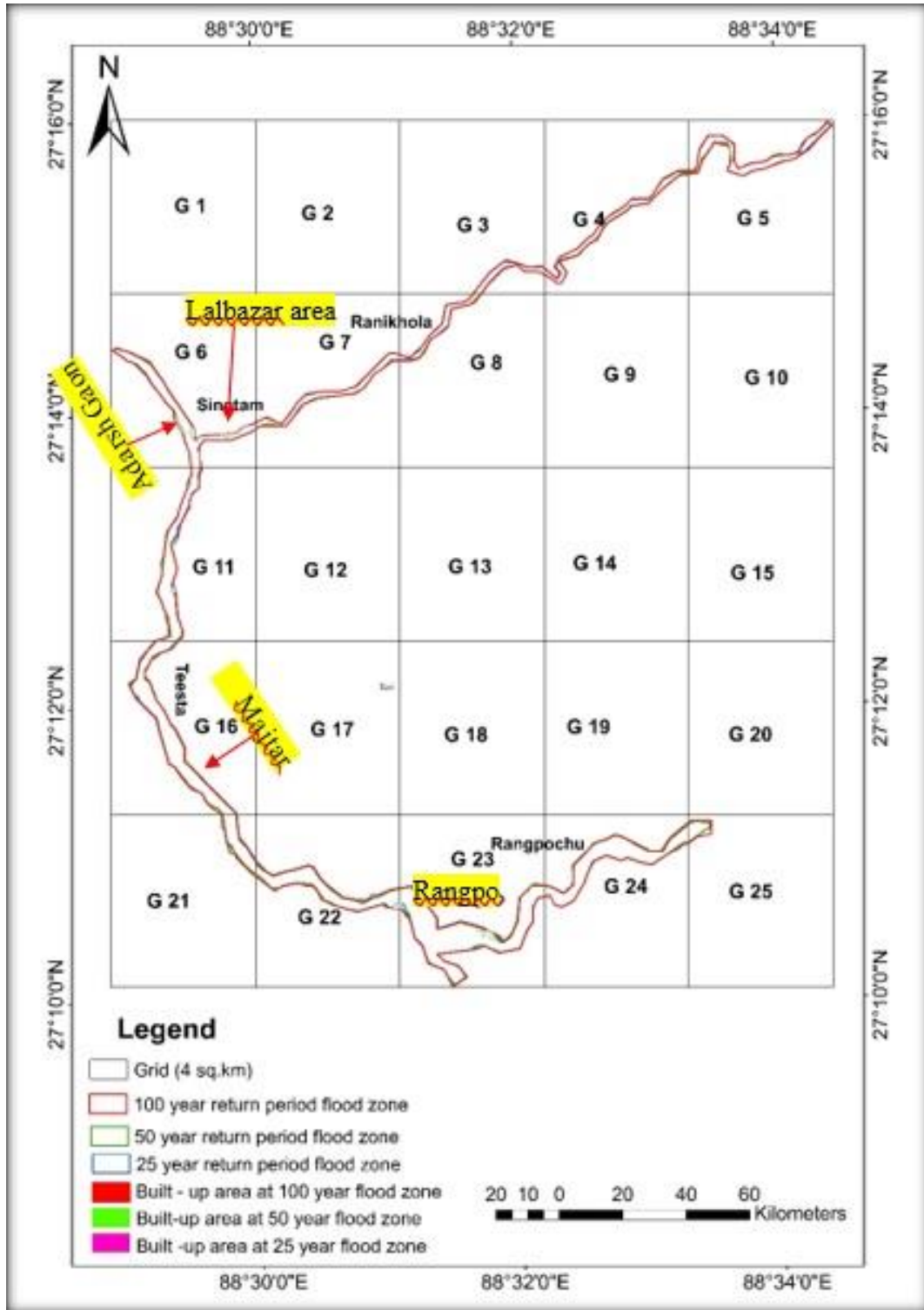


*Figure 4.2. Built-up areas within the flood zones of 25, 50 and 100-year return period in the selected stretches of the Teesta, Ranikhola and Rangpochu in the year 2006*

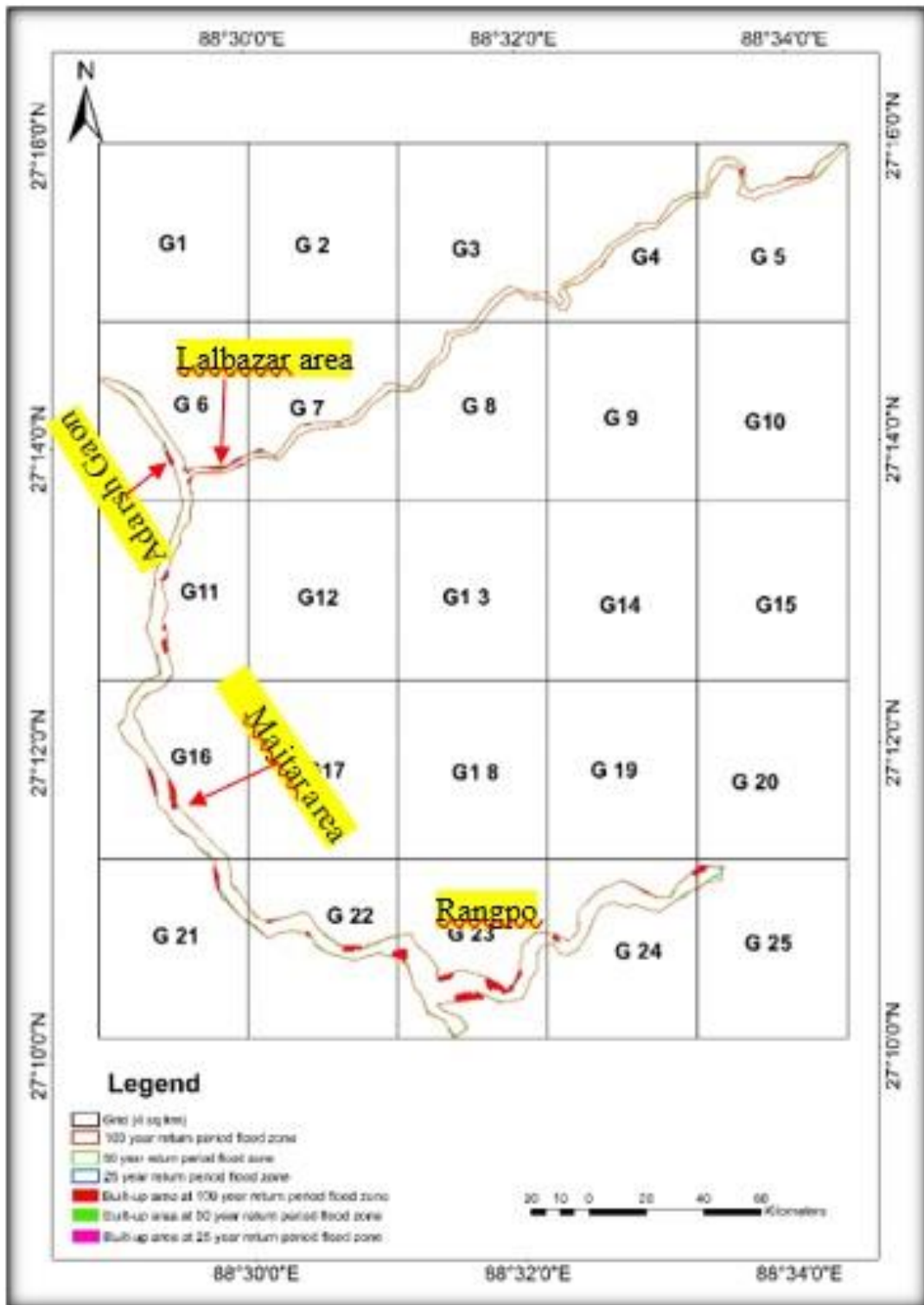


*Figure 4.3. Built -up areas within the flood zones of 25, 50 and 100-year return period in the selected stretches of the Teesta, Ranikhola and Rangpochu in the year 2021*



### **4.3.2 Built-up Areas in Flood Zones of the Teesta (2006-2021)**

In the selected stretch of the Teesta River, extending from Adarsh Gaon area upto the few metres downstream of the confluence point of the Teesta with the Rangpochu, over the period of 15 years (2006-2021), built-up area has expanded drastically in the stretch between the Singtam bazar and the Rangpo bazar (Figures 4.1 and 4.2) Adarsh Gaon is 30 years older whereas Lal bazar is not older than 20-25 years (Figures 4.4A-B). Thus, all built-up areas have been established post-1968 floods. In this stretch, commercialization is the main cause for an increase in built-up areas within the flood zones. The built-up areas between Singtam bazar and Rangpo are more resilient to flood hazard because most of these built-up areas are commercialized well-built buildings engaged for the pharmaceutical industry and educational institutions but the Adarsh Gaon and Lalbazar areas are less resilient. Embankments along Adarsh Gaon and Lal bazar sides get breached during high flood flow.

As per the field survey following in-depth interview with senior citizens in the case of G6, flood water had extended up to Lal bazar during the 1968 floods. However, here structural measures of flood management have played a vital role to control flood-induced disaster. At the current scenario, river water overflows embankments inundating buildings and as discussed in chapter II, the carrying capacity of the Teesta in this stretch is also declining due to aggradation. Figure 4.4 represents the case of embankment breaching at Adarsh Gaon (Figure 4.4A) and Lalbazar side (Figures 4.4B and C). In this figure, the yellow line and arrow show the level upto which water flows during monsoon season. Overall, encroachment of built-up areas is increasing in all flood zones. Flood zone at 25-year return period is showing a higher percentage change in built-up areas than those in 25-50 and 50-100 year return period zones (Table 4.2).



**Figure 4.4.** Water level overflowing embankments at **A:** Adarsh gaon(27.23N 88.49E); **B:** Lalbazar side (27.231 N, 88.492 E); **C:** Lalbazar side (22.23 N 88.49 E); **D:** confluence point of Teesta and the Ranikhola (27.23 N, 88.498 E)

**Table 4.2.** Built-up area (in hectare) and percentage change in the flood zones of the Teesta river from 2006 to 2021

Flood Zone	Built -up area (2006)	Built Up area (2021)	Percentage change in built-up area (2006-2021)
25	1.53	6.84	347.06
25-50	0.38	1.45	281.58
50-100	0.83	1.99	139.76
Total	2.74	10.28	275.18

#### 4.3.3. Built-up Areas in Flood Zones of the Rangpochu (2006-2021)

In the case of the selected stretch of the Rangpochu, within 15 years (2006 to 2021), the lower terraces and tributary fans at the confluence point of the Rangpochu and Teesta are now entirely occupied by built-up areas in the form of residential buildings, garages, car wash at the cost of massive deforestation encouraging concretization

(Figures 4.2-4.3; Figure 4.5). Thus, all built-up areas at the confluence of the Rangpochu and the Teesta are not older than 15 years. There are no proper structural flood management measures such as dykes and embankments.

The confluence point is more prone to flood risk due to back water flow. As discussed in chapter II, this stretch is now subjected to heavy sedimentation with the distinct formation of bars and islands leading to the reduced carrying capacity of the river. The built-up areas in this stretch are at lower elevation (Figure 4.5) with a complete absence of structural flood mitigation measures like embankments.

Percentage change in built-up area is highest in the flood zone of 50–100 year return period followed by 25-50 and 25-year return period zones (Table 4.3). Overall encroachment of built-up areas on each flood zone is increasing between 2006 and 2021 (Table 4.3).



**Figure 4.5.** Built-up area in (Grid 23) along the Rangpochu (A): Rangpo bridge at the borderline of Sikkim and West Bengal which got cracked during heavy discharge flood in Oct 2021 (27.174 N, 88.53 E). (B): Built-up area downstream of Rangpo bridge (27.174 N, 88.529 E). (C & D): Built-up area at the confluence point of the Rangpochu and the Teesta (27.173 N, 88.524 E)

**Table 4.3.** Built-up area (in hectare) and percentage change in the flood zones of the Rangpochu from 2006 to 2021

Flood zone	Built-up area (2006)	Built-up area (2021)	Percentage change in built-up area (2006-2021)
25	1.17	6.44	450.43
25-50	0.06	0.9	1400
50-100	0.08	1.49	1762.50
Total	1.31	8.83	574.05

#### **4.3.4. Built-up Areas in Flood Zones of the Rangit River (2006-2021)**

Over the period of 15 years (2006 to 2021) along the demarcated flood zones in the Rangit river likely, built-up area has sprawled more at downstream section shown in grids (G17, G18, G21 and G22). Despite the fact that along this zone, the built-up area is located at a much higher elevation from the river channel, they are still at risk due to the narrow, confined channel with no scope of lateral adjustment during high water flow.

According to field evidences, floods created chaos among the locals due to the unprecedented rise in water level due to heavy rainfall in October 2021. In this stretch, embankments are of very low height and cases of embankment breaching are common in this case. People have started to occupy lower terraces even river beds in the form of small godowns, residential buildings, small-scale industries and temple (Figure 4.8).

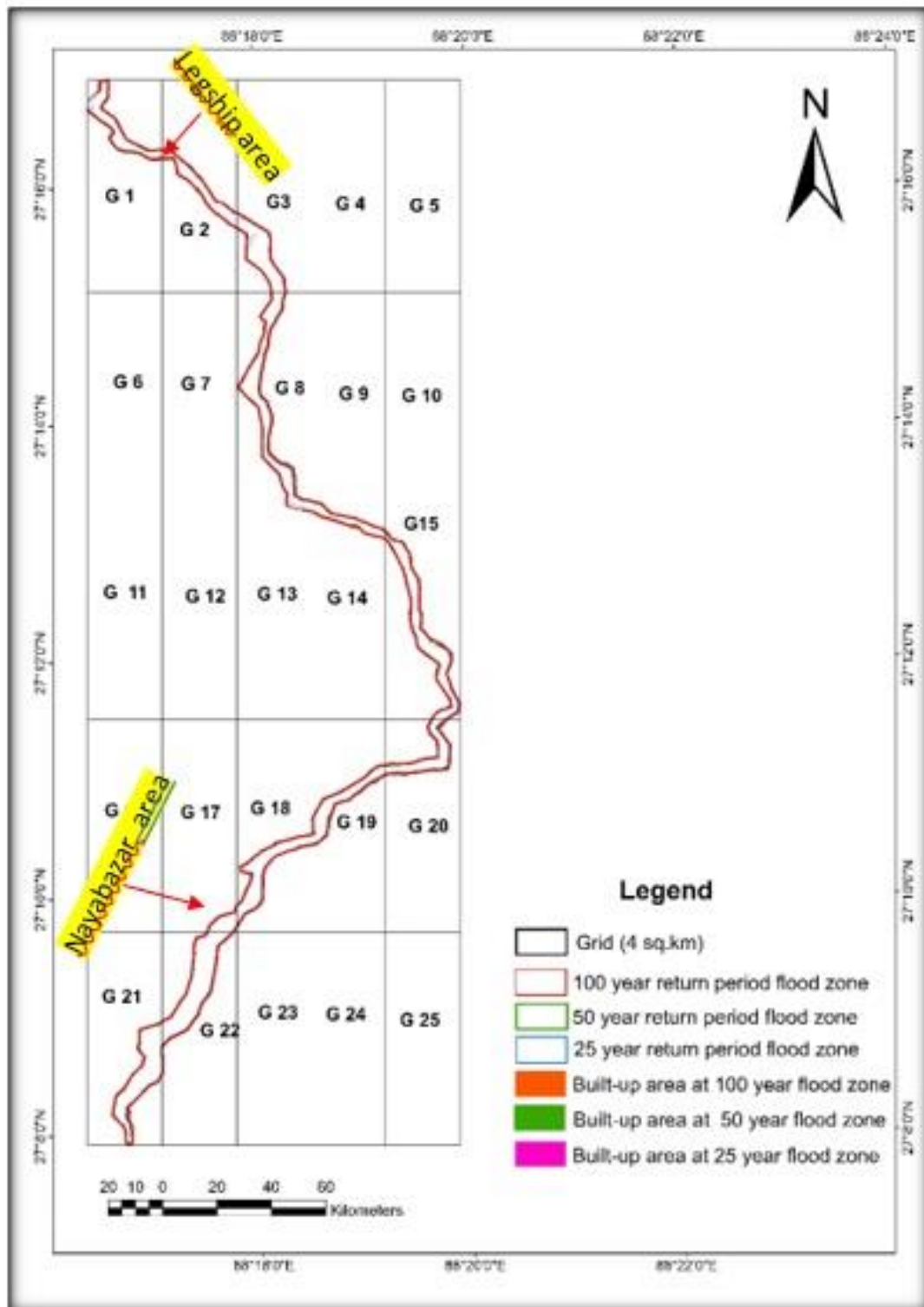


*Figure 4.6. Built -up areas within the flood zones of 25, 50 and 100-year return period in the selected stretches of the Rangit river in the year 2006*



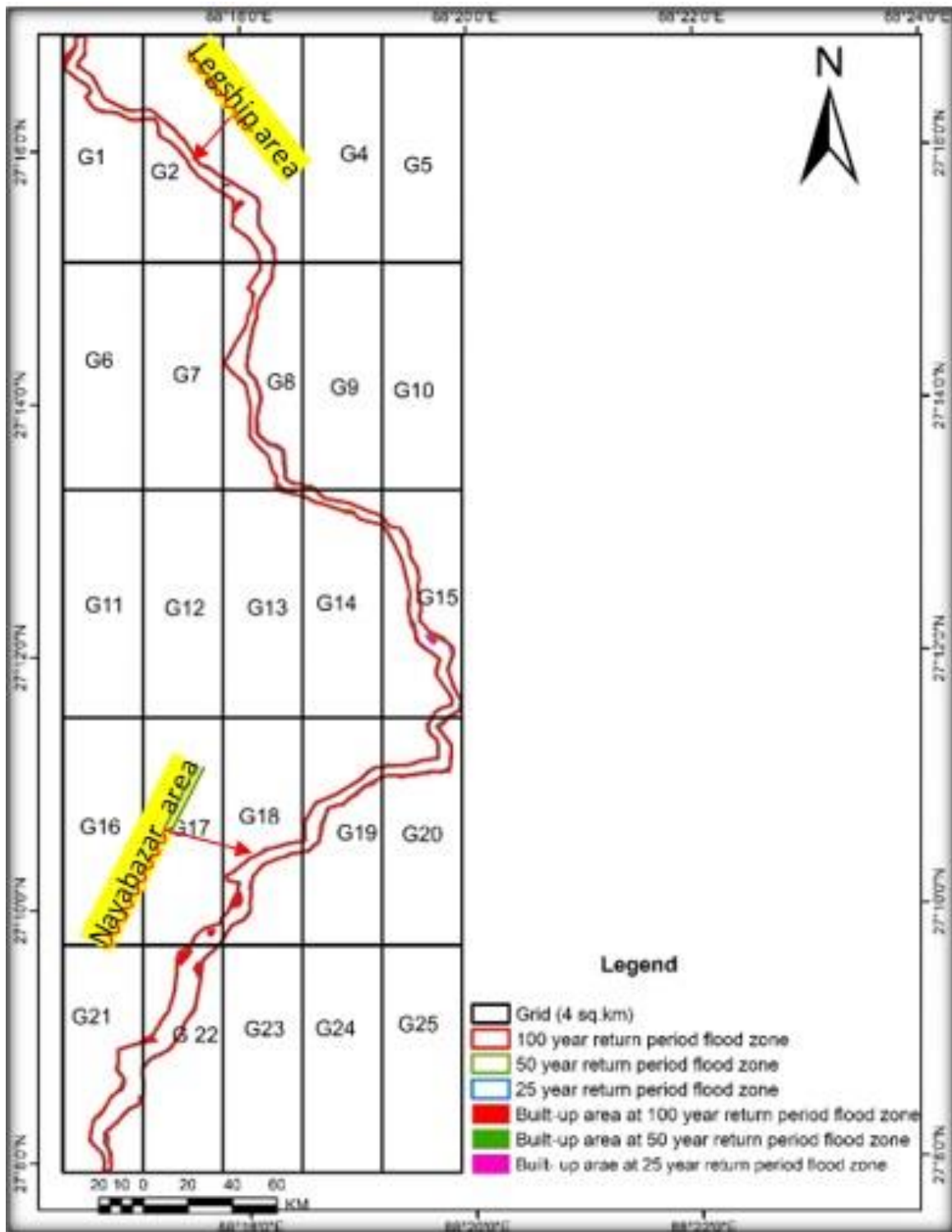


**Figure 4.7.** Built -up areas within the flood zones of 25, 50 and 100-year return period in the selected stretches of the Rangit river in the year 2021

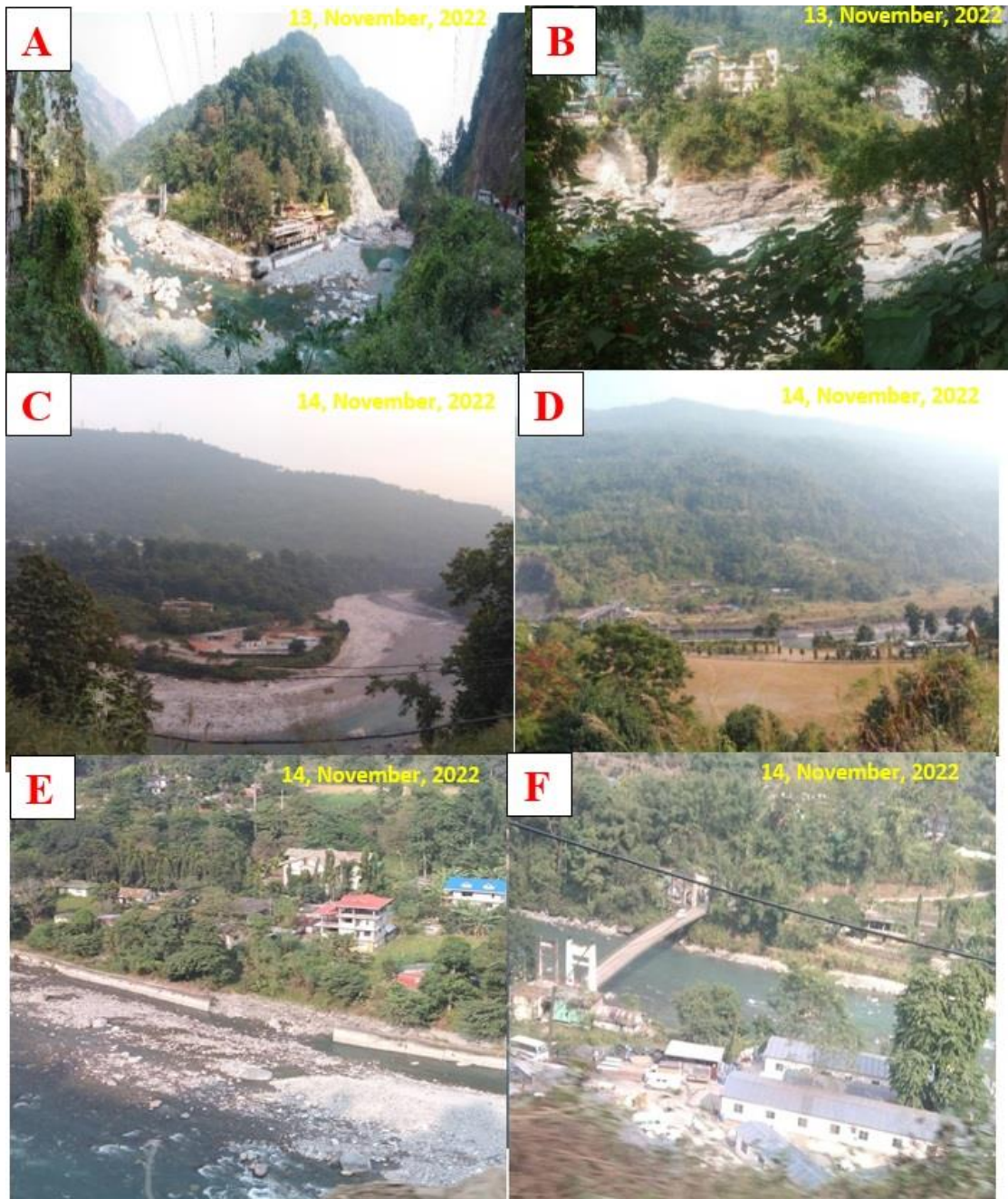


**Figure 4.8.** Built-up area along the Rangit river. (**A and B**): Built-up area, Legship area (27.278 N, 88.273 E, 27.278, 88.276). (**C and D**): Built-up area at Nayabazar and Rothak (27.142 N, 88.284 E, 27.158 N, 88.293 E). (**E and F**) : Built-up area at Nayabazar road (27.202 N, 88.328 E, 27.203 N, 88.325 E)

**Table 4.4.** Built-up area (in hectare) and percentage change in selected stretch of the Rangit river from 2006 to 2021

Flood Zone	Built-up area (2006)	Built-up area (2021)	Percentage change in built-up area (2006-2021)
25	3.84	13.78	258.85
25-50	0.5	1.87	274.00
50-100	0.58	1.95	236.21
Total	4.92	17.6	257.72

Percentage change in built-up area is highest in the flood zone of 25-50 year return period followed by 25 and 50-100 year return period zones (Table 4.3). Overall encroachment of built-up areas on each flood zone is increasing between 2006 and 2021 (Table 4.4) and is characterised by residential and commercial buildings.

As per the recommendation of the Central Water Commission (1996), built-up areas such as public institutions, government offices, universities, public library and residential on stilts or higher level are permitted in 25-year flood zone. The built-up areas such as defence installations, industries, public utilities like hospitals, electricity installations, railway stations, commercial centers, aerodromes etc., should be above 100-year return period flood level or the maximum observed flood level (Central Water Commission, 1996). Only playgrounds and parks are favourable in areas vulnerable to frequent floods.

#### **4.4. Conclusions**

As per the findings, the areal extent of built-up area occupying the demarcated flood zones of 25, 25-50 and 50-100 year return period has increased considerably over the period of 15 years fostering risk of loss by flooding. Built-up area has sprawled dramatically in the Teesta stretch between Singtam and Rangpo the main cause being the growth of pharmaceutical industries and educational institutions. The next point



experiencing drastic growth in built-up along the demarcated flood zones is the confluence point of the Rangpochu and Teesta river and here, the main cause is the occupation of people for residential purpose. In the case of the selected stretch of the Rangit river from Legship bazar upto Nayabazar area, it is seen that there is significant exploitation of lower terraces just within a period of 15 years occupied for certain purposes like residential, small-scale industries, garages, carwash etc. Along this stretch, structural flood mitigation measures are not well because some patches of embankments are of very low height. However, the role of structural flood mitigation measures in the form of embankments is seen only along the downstream section of the Ranikhola river which has restricted expansion of built-up areas at least along its right bank wherever embankments are located. The comparative analysis of the spatio-temporal variation of the selected stretches of the Teesta, the Ranikhola, the Rangpochu and the Rangit underlines that built-up areas along the Rangit river are more prone to flood hazard as most of them are located very close to the river bed. The occupation of built-up areas along and adjacent to living rivers is proved to be one of the causes of flood-based disaster claiming huge lives, public and private properties.

## ***CHAPTER V***

### **Conclusions**

Reaches of the Teesta river and its major tributaries viz., the Ranikhola, Rangpochu and Rangit are selected to analyse (i) change detection in the channel morphology, (ii) demarcation of flood zones at 25, 50 and 100-year return period discharges (iii) status of built-up area expansion within the demarcated flood zones from 2006 to 2021.

Natural and man-made factors are responsible for the change in channel morphology. Analysis of three main aspects of channel morphology viz., change in lower terraces, change in channel margin and change in status of aggradation and degradation reflects that the sampled reaches of the Teesta river and its tributaries have undergone markable change between 2006 and 2021. Overall, the channel pattern in the selected reaches is sinuous. River banks and lower terraces are getting frayed due to erosion and bank failure, channel margins are shifting and aggradation is becoming acute which is imposing threat on expanding built-up in these terraces and banks. The cases of erosion of banks and terraces are more in the selected reaches of the Rangit river compared to that of the Teesta, Ranikhola and Rangpochu due to high flow velocity, weak geology, hydraulic structure, absence of well-built embankments along the Rangit river. Further, the field-based evidences related to channel bed materials and LULC along the channels helped in the selection of an appropriate manning's roughness coefficient which has been considered in running the HEC-RAS model to demarcate flood zones of 25, 50 and 100-year return period.

An accuracy assessment of five freely available DEMs such as ASTER, SRTM, FABDEM, CARTOSAT and FABDEM has been done. FABDEM appeared to be most

appropriate in the context of vertical accuracy for computation of physiographic parameters of the basin (slope, length of the longest stream of the basin, area of the basin, length of the longest stream from the centroid of the catchment to the discharge estimation site) and creation of geometric data (river centerline, bank lines, flow paths and cross-sections). Peak discharge at 25, 50 and 100-year return period have been estimated using two main parameters viz., rainfall at 25, 50 and 100-year return period and physiographic parameters of the basin. Estimated peak discharges at 25, 50 and 100-year return period, LULC-based manning's roughness coefficient and geometric data (river centerline, bank lines, flow paths and cross-sections) required as input for simulating HEC-RAS 1D steady flow model were extracted from FABDEM.

Due to the rapid rate of commercialization and urbanization, people are not sparing even lower terraces and beds of the Teesta and its tributaries. This has been reflected well from this study. As per the findings, just over the period of 15 years (2006-2021), the degree of occupancy of built-up area are increasing dramatically along the demarcated flood zones of 25, 50 and 100-year return period and all these flood zones coincide with lower and mid terraces. Most of the built-up areas are less resilient to flood hazard as most of them are residential and small commercialized buildings with no insurance.

The comparative analysis of the spatio-temporal variation of these four stretches underlines that built-up areas along the Rangit river are more prone to flood hazard as most of them are located very close to river bed and built-up areas are sprawling within 25-year flood zone. The structural flood management measures (dams and embankments) have played a vital role in controlling floods and also restricting developmental activities towards river channel to a certain extent along the study sites of the Teesta, Ranikhola and Rangpochu but this is poor in the Rangit river with some

low-height embankments. However, the case of embankment breaching is common in all four study sites. Moreover, due to the narrow, confined channel, flood water in Rangit does not possess scope for lateral adjustment leading to aggressive flow with high velocity and depth that foster erosion of banks and terraces.

This study elicited how the increasing thirst of people for developmental activities not sparing even river terraces, banks and beds is posing a future threat to lives and properties. People are not concerned about the natural mechanism of the river and give more importance to their need and unlimited desire causing the change in channel morphology, occupying terraces that ultimately opens the door for catastrophic disaster and one such example could be seen in the case of the Teesta basin of the Sikkim Himalaya through this study.

In Sikkim, 756 houses are damaged by floods every year. Therefore, the state of Sikkim should come forward for flood zonation mapping as a non-structural measures of flood management for restricting high-value built-up areas in different flood zones. This study can be useful for the policymakers of Sikkim to implement the guidelines on floodplain zoning provided by the Central Water Commission (1996).

## References

- Abrams, M., Crippen, R., & Fujisada, H. (2020). ASTER Global Digital Elevation Model (GDEM) and ASTER Global Water Body Dataset (ASTWBD). *Remote Sensing*, 12(7), 1156. <https://doi.org/10.3390/rs12071156>
- Aggarwal, S., Rai, S. C., Thakur, P. K., & Emmer, A. (2017). Inventory and recently increasing GLOF susceptibility of glacial lakes in Sikkim, Eastern Himalaya. *Geomorphology*, 295, 39–54. <https://doi.org/10.1016/j.geomorph.2017.06.014>
- Ahmad, T., Pandey, A. C., & Kumar, A. (2019). Evaluating urban growth and its implication on flood hazard and vulnerability in Srinagar city, Kashmir Valley, using geoinformatics, *Arabian Journal of Geosciences*,12(9).
- Anees, M. T., Abdullah, K., Nawawi, M., & Norulaini, N. (2016). Numerical Modeling techniques for flood analysis. *Journal of African Earth Sciences*, 124, 478–486. <https://doi.org/10.1016/j.jafrearsci.2016.10.001>
- Apeh, O. I., Uzodinma, V. N., Ebinne, E. S., Moka, E. C., & Onah, E. U. (2019). Accuracy Assessment of Alos W3d30, Aster Gdem and Srtm30 Dem: A Case Study of Nigeria, West Africa. *Journal of Geographic Information System*, 11(02), 111–123. <https://doi.org/10.4236/jgis.2019.112009>.
- Barnes, B., Dunn, S., & Wilkinson, S. (2019). Natural hazards, disaster management and simulation: a bibliometric analysis of keyword searches. *Natural Hazards*, 97(2), 813–840. <https://doi.org/10.1007/s11069-019-03677-2>.
- Benito, G. and Hudson, P.F (2011). Flood hazards: The context of fluvial geomorphology. In Irasema Alcantara-Ayala & Andrew S. Goudie (Eds.), *Geomorphological Hazards and Disaster Prevention* (pp. 111-128). Cambridge University Press.
- Beven, K. J., & Hall, J. (2014). *Applied uncertainty analysis for flood risk management*. Imperial College Press.
- Bhatta, B. (2020). *Remote Sensing and GIS*. Oxford University Press.

- Brunner, G.W. (2016). HEC -RAS River Analysis System User's Manual Version 5.6. *US Army Corps of Engineers*.
- Buckingham, S. E., & Whitney, J. W. (2007). GIS Methodology for Quantifying Channel Change in Las Vegas, Nevada. *Journal of the American Water Resources Association*, 43(4), 888–898. <https://doi.org/10.1111/j.1752-1688.2007.00073.x>
- Bull, W. B. (1977a). The alluvial-fan environment. *Progress in Physical Geography: Earth and Environment*, 1(2), 222–270. <https://doi.org/10.1177/030913337700100202>
- Central Water Commission. (1991). *Flood Estimation Report For North Brahmaputra Basin (SUBZONE-2a)* (p. 94). [wc.gov.in/sites/default/files/north-brahmaputra-subzone-2-a.pdf](http://wc.gov.in/sites/default/files/north-brahmaputra-subzone-2-a.pdf)
- Central Water Commission. (1996). *Flood Plain Zoning*. CWC, New Delhi.
- Charlton, R.(2008). *Fundamentals of Fluvial Geomorphology*.Routledge.
- Clarke, R. T. (2005b). Rainfall Trend Analysis: Return Period. In M. G. Anderson & J. J. McDonnell (Eds.), *Encyclopedia of Hydrological Science* (pp. 1–3243). John Wiley & Sons Ltd.
- Clarke, R. T. (2005). Rainfall Trend Analysis: Return Period. In M. G. Anderson & J. J. McDonnell (Eds.), *Encyclopedia of Hydrological Science* (pp. 547–557). John Wiley & Sons Ltd.
- Cook, A., & Merwade, V. (2009). Effect of topographic data, geometric configuration and modeling approach on flood inundation mapping. *Journal of Hydrology*, 377(1), 131–142. <https://doi.org/10.1016/j.jhydrol.2009.08.015>
- Dar, R. A., Mir, S. A., & Romshoo, S. A. (2019). Influence of geomorphic and anthropogenic activities on channel morphology of River Jhelum in Kashmir Valley, NW Himalayas. *Quaternary International*, 507, 333–341. <https://doi.org/10.1016/j.quaint.2018.12.014>

- Demeritt, D., & Wainwright, J. (2005). Models, Modelling, and Geography. In N. Castree, A. Rogers, & D. Sherman (Eds.), *Questioning Geography: Fundamental Debates* (pp. 1–330). Wiley-Blackwell.
- Dasallas, L., Kim, Y., & An, H. (2019). Case Study of HEC-RAS 1D–2D Coupling Simulation: 2002 Baeksan Flood Event in Korea. *Water*, *11*(10), 1-14. <https://doi.org/10.3390/w11102048>
- Das, B. C., Ghosh, S., & Islam, A. (2019). Quaternary Geomorphology in India: Concepts, Advances and Applications. In B. C. Das, S. Ghosh, & A. Islam (Eds.), *Quaternary Geomorphology in India* (pp. 1–224). Springer International Publishing
- Dingman, S. L., & Bjerklie, D. M. (2005). Estimation of River Discharge. In M. G. Anderson & J. J. McDonnell (Eds.), *Encyclopedia of Hydrological sciences* (pp. 920–937). John Wiley & Sons Ltd.
- Du, J., Cheng, L., Zhang, Q., Yang, Y., & Xu, W. (2018). Different Flooding Behaviors Due to Varied Urbanization Levels within River Basin: A Case Study from the Xiang River Basin, China. *International Journal of Disaster Risk Science*, *10*(1), 89–102. <https://doi.org/10.1007/s13753-018-0195-4>
- ENVIS. (2021). *River*. Retrieved November 6, 2021, from <https://sikervis.nic/database/rivers781.aprx>
- Elkhrachy, I. (2018). Vertical accuracy assessment for SRTM and ASTER Digital Elevation Models: A case study of Najran City, Saudi Arabia. *Ain Shams Engineering Journal*, *9* (4), 1807-1817.
- Felder, G., Zischg, A., & Weingartner, R. (2017). The effect of coupling hydrologic and hydrodynamic models on probable maximum flood estimation. *Journal of Hydrology*, *550*, 157–165. <https://doi.org/10.1016/j.jhydrol.2017.04.052>
- Flood Partners. (2022). *Flood Zones*. Retrieved December 24, 2022. from <https://floodpartners.com/flood-zones>.

- Fryis, K.A., Wheaton, J.M., & Brierley. (2015). An approach for measuring confinement and assessing the influence of valley setting on river forms and processes. *Earth Surf. Process. Landforms*, 41,701-710. <https://doi.org/10.1002/esp.3893>.
- Gazi, Md. Y., Hossain, F., Sadeak, S., & Uddin, Md. M. (2020). Spatiotemporal variability of channel and bar morphodynamics in the Gorai-Madhumati River, Bangladesh using remote sensing and GIS techniques. *Frontiers of Earth Science*, 14(4), 828–841. <https://doi.org/10.1007/s11707-020-0827-z>.
- Garde, R. J. (2006). *River Morphology*. New Age International Publisher.
- Grant, G. E., Swanson, F. J. (1995). Morphology and processes of valley floors in mountain streams, western Cascades, Oregon. In: Costa. In John E., Miller, Andrew J., Potter, Kenneth W., Wilcock, Peter. (Eds). *Natural and anthropogenic influences in fluvial geomorphology*. pp. 83-101. American Geophysical Union.
- Gesch, D., Oimoen, M., Danielson, J., & Meyer, D. (2016). Validation of the Aster Global Digital Elevation Model Version 3 over the Conterminous United States. *ISPRS - International Archives of the Photogrammetry, Remote Sensing and Spatial Information Sciences*, XLI-B4, 143–148. <https://doi.org/10.5194/isprsarchives-xli-b4-143-2016>
- Goudie, A. (2004). *Encyclopedia of geomorphology*. Routledge.
- Grabs, W., Tyagi, A. C., & Hyodo, M. (2007). Integrated flood management. *Water Science and Technology*, 56(4), 97–103. <https://doi.org/10.2166/wst.2007.541>
- Huggett, R.J. (2017). *Fundamentals of Geomorphology*. Routledge, New Delhi
- Hassan, Md. S., & Mahmud-ul-islam, S. (2016). Quantification of River Bank Erosion and Bar Deposition in Chowhali Upazila, Sirajganj District of Bangladesh: A Remote Sensing Study. *Journal of Geoscience and Environment Protection*, 04(01), 50–57. <https://doi.org/10.4236/gep.2016.41006>



- Hashemyan,F., Khalegi,M.R., M,Kamyar.(2015). Combination of HEC-HMS and HEC-RAS models in GIS in order to simulate Flood, Case Study: Khoshke Rudan river in Fars Province, Iran. *Research Journal of Recent Studies*, 4(8),122-127
- Hawker, L., Uhe, P., Paulo, L., Sosa, J., Savage, J., Sampson, C., & Neal, J. (2022). A 30 m global map of elevation with forests and buildings removed. *Environmental Research Letters*, 17(2), 024016. <https://doi.org/10.1088/1748-9326/ac4d4f>
- Hawwa, M. S., Knudsen, T., Kokkendorff, S. L., & Oisen, B. P. (2011). Horizontal Accuracy of Digital Elevation Models. In *Research Gate* (p. 21). file:///C:/Users/win/Downloads/KMS\_Technical\_Report\_10.pdf
- İcaga, Y., Tas, E., & Kilit, M. (2016). Flood inundation mapping by GIS and a hydraulic model (hec ras): a case study of Akarcay Bolvadin subbasin, in Turkey. *Acta Geobalcanica*, 2(2), 111–118. <https://doi.org/10.18509/agb.2016.12>.
- International Environmental Law Research Centre (2021). *Model Bill for Flood Plain Zoning, 1975*. Retrieved December 1,2021, from <https://www.ielrc.org/content/e7503.pdf>.
- Islam, N., & Patel, P. P. (2021). Inventory and GLOF hazard assessment of glacial Lakes in the Sikkim Himalayas, India. *Geocarto International*, 37(13), 1–28. <https://doi.org/10.1080/10106049.2020.1869332>
- Joyce,H.M.,Hardy,R.J.,Warburton,J.,&Large,A.R.G.(2018). Sediment continuity through the upland sediment cascade: geomorphic response of an upland river to an extreme flood event. *Geomorphology*, 317, 45-61. <https://doi.org/10.1016/j.geomorph.2018.05.002>
- Kim, S. J., Kim, G. T., Jeong, J. H., & Han, S. O. (2013). Flood Inundation Scenario Development and Analysis Using HEC-HMS/RAS and HEC-GeoRAS Models. *Journal of Korean Society of Hazard Mitigation*, 13(4), 199–205. <https://doi.org/10.9798/kosham.2013.13.4.199>

- Knight, D., Knight, D. W., & Asaad Shamseldin. (2006). *River Basin Modelling for Flood Risk Mitigation*. CRC Press.
- Konadu, D. D., & Fosu, C. (2009). Digital Elevation Models and GIS for Watershed Modelling and Flood Prediction – A Case Study of Accra Ghana. In E. k Yanful (Ed.), *Appropriate Technologies for Environmental Protection in the Developing World* (pp.325-332). Springer.
- Kourgialas, N. N., & Karatzas, G. P. (2011). Flood management and a GIS modelling method to assess flood-hazard areas—a case study. *Hydrological Sciences Journal*, 56(2), 212–225. <https://doi.org/10.1080/02626667.2011.555836>
- Kumar, R., Sharma, R. K., Pradhan, P., Sharma, N., & Shrestha, D. G. (2020). Melt Runoff Characteristics and Hydro-Meteorological Assessment of East Rathong Glacier in Sikkim Himalaya, India. *Earth Systems and Environment*, 4(3), 567–582. <https://doi.org/10.1007/s41748-020-00168-4>
- Lahiri, S. K., & Sinha, R. (2014). Morphotectonic evolution of the Majuli Island in the Brahmaputra valley of Assam, India inferred from geomorphic and geophysical analysis. *Geomorphology*, 227, 101–111. <https://doi.org/10.1016/j.geomorph.2014.04.032>
- Lauer, J. W., Echterling, C., Lenhart, C., Belmont, P., & Rausch, R. (2017). Air-photo based change in channel width in the Minnesota River basin: Modes of adjustment and implications for sediment budget. *Geomorphology*, 297, 170–184. <https://doi.org/10.1016/j.geomorph.2017.09.005>
- Lillesand, T. M., Kiefer, R. W., & Chipman, J. W. (2015). *Remote sensing and image interpretation*. John Wiley & Sons, Inc.
- Liu, Z., Merwade, V., & Jafarzaghan, K. (2018). Investigating the role of model structure and surface roughness in generating flood inundation extents using one- and two-dimensional hydraulic models. *Journal of Flood Risk Management*, 12(1), e12347. <https://doi.org/10.1111/jfr3.12347>
- Lo, C.P and Yeung, A.K.W. (2007). *Concepts and Techniques of Geographic Information System*. Printice Hall.

- Ltd, E. (India) P. (n.d.). *Flood Forecast - Central Water Commision, Govt. Of India.*  
Flood Forecast - Central Water Commision, Govt. Of India. <https://ffs.india-water.gov.in/>
- Mandal, S. P., & Chakrabarty, A. (2016). Flash flood risk assessment for upper Teesta river basin: using the hydrological modeling system (HEC-HMS) software. *Modeling Earth Systems and Environment*, 2(2). <https://doi.org/10.1007/s40808-016-0110-1>
- Manglesdorf, J., Scheurmann, K., WeiB, F.H. (1990). *River Morphology: A Guide for Geoscientists and Engineers*. Springer -Verlag Berlin Heidelberg.
- Ministry of Housing and Urban affairs, GOI. (2021). *River Centric Urban Planning Guidelines* (pp. 1–36).
- Mishra P.K., Rai, A., Rai, S.C. (2019). Landuse and Land cover change detection using Geospatial techniques in the Sikkim Himalaya, India. *The Egyptian Journal of Remote Sensing and Space Science*, 1-12.
- Mitra, S., Roy, A. K., & Tamang, L. (2020). Assessing the Status of Changing Channel Regimes of Balason and Mahananda River in the Sub-Himalayan West Bengal, India. *Earth Systems and Environment*, 4(2), 409–425. <https://doi.org/10.1007/s41748-020-00160-y>.
- Moglen, G. E., & Maidment, D. R. (2005). Digital Elevation Model Analysis and Geographic Information Systems. In M. G. Anderson & J. J. McDonnell (Eds.), *Encyclopedia of Hydrological sciences* (pp. 1–3243). John Wiley & Sons Ltd.
- Mohapatra, P.K Singh, R.D., 2003. Flood Management in India. *Natural Hazards*, 28, 131-143.
- Morisawa, M. (2017). *Streams; Their Dynamics and Morphology*. Academic Publishers.
- NITI Aayog. (2021). *Report of the Committee Constituted for Formulation of Strategy for Flood Management Works in Entire Country and River Management Activities and Works Related to Border Areas (2021-26)* (pp. 1–98).

- Opolot, E. (2013). Application of Remote Sensing and Geographical Information Systems in Flood Management: A Review. *Research Journal of Applied Sciences, Engineering and Technology*, 6(10), 1884–1894. <https://doi.org/10.19026/rjaset.6.3920>
- Osterkamp, W.R., Hupp, C.R. (1984). Geomorphic and vegetative characteristics along three northern Virginia streams. *Geological Society of America Bulletin*, 95(9), 1093. [https://doi.org/10.1130/0016-2093\(1984\)95<1093:GVC>2.0.CO;2](https://doi.org/10.1130/0016-2093(1984)95<1093:GVC>2.0.CO;2)
- Pal, R., Biswas, S. S., Mondal, B., & Pramanik, M. K. (2016). Landslides and Floods in the Tista Basin (Darjeeling and Jalpaiguri Districts): Historical Evidence, Causes and Consequences. *Journal of Indian Geophysical Union*, 20(2), 209–215.
- Pathan, A. I., & Agnihotri, P. G. (2020). Application of new HEC-RAS version 5 for 1D hydrodynamic flood modeling with special reference through geospatial techniques: a case of River Purna at Navsari, Gujarat, India. *Modeling Earth Systems and Environment*, 7(2), 1133–1144. <https://doi.org/10.1007/s40808-020-00961-0>
- Pinos, J., Timbe, L., & Timbe, E. (2019). Evaluation of 1D hydraulic models for the simulation of mountain fluvial floods: a case study of the Santa Bárbara River in Ecuador. *Water Practice and Technology*, 14(2), 341–354. <https://doi.org/10.2166/wpt.2019.018>
- Qiu, L., Du, Z., Zhu, Q., & Fan, Y. (2017). An integrated flood management system based on linking environmental models and disaster-related data. *Environmental Modelling & Software*, 91, 111–126. <https://doi.org/10.1016/j.envsoft.2017.01.025>
- Rao, D., Rao, V., Dadhwal, V. K., Diwakar, P. G. (2014). Kedarnath flash floods: a hydrological and hydraulic simulation study. *Current Science*, 106, 598–603
- Ray, K., Pandey, P., Pandey, C., Dimri, A. P., & Kishore, K. (2019). On the Recent Floods in India. *Current Science*, 117(2), 204. <https://doi.org/10.18520/cs/v117/i2/204-218>

- Rhoads, B. L. (2020). *River dynamics: geomorphology to support management*. Cambridge University Press.
- Sain, K., Kumar, A., Mehta, M., Verma, A., Tiwari, S. K., Garg, P. K., Kumar, V., Rai, S. K., Srivastava, P., & Sen, K. (2021). A Perspective on Rishiganga-Dhauliganga Flash Flood in the Nanda Devi Biosphere Reserve, Garhwal Himalaya, India. *Journal of the Geological Society of India*, 97(4), 335–338. <https://doi.org/10.1007/s12594-021-1691-5>
- Sandrp. (2016, August 14). Landslide Dam Blocks Teesta Tributary in North Sikkim: Major Risk to Teesta River Bank Communities. <https://sandrp.in/2016/08/14/landslide-dam-blocks-teesta-tributary-in-north-sikkim-major-risk-to-teesta-river-bank-communities/>
- Santillan, J. R., & Makinano-Santillan, M. (2016). Vertical Accuracy Assessment of 30-m Resolution Alos, Aster, and SRTM Global Dems over Northeastern Mindanao, Philippines. *ISPRS - International Archives of the Photogrammetry, Remote Sensing and Spatial Information Sciences*, XLI-B4, 149–156. <https://doi.org/10.5194/isprs-archives-xli-b4-149-2016>
- Sanyal, J., & Lu, X. X. (2004). Application of Remote Sensing in Flood Management with Special Reference to Monsoon Asia: A Review. *Natural Hazards*, 33(2), 283–301. <https://doi.org/10.1023/b:nhaz.0000037035.65105.95>
- Sarkar, S. S., Ali, A., & Bhattacharya, G. (Eds.). (2012). *Geology and Mineral Resources Sikkim* (pp. 1–48). Geological Survey of India.
- Sayers, P., Yuanyuan, L., Galloway, G., Wen Kang, S. F., Yiwei, C., & Quesne, T. L. (2013). *Flood Risk management: A Strategic Approach*. UNESCO.
- Sear, D., Hornby, D., Wheaton, J., & Hill, C. (2021). *Understanding river channel sensitivity to geomorphological changes*. Environment Agency. <https://assets.publishing.service.gov.uk/>. Retrieved on 07/02/2022.

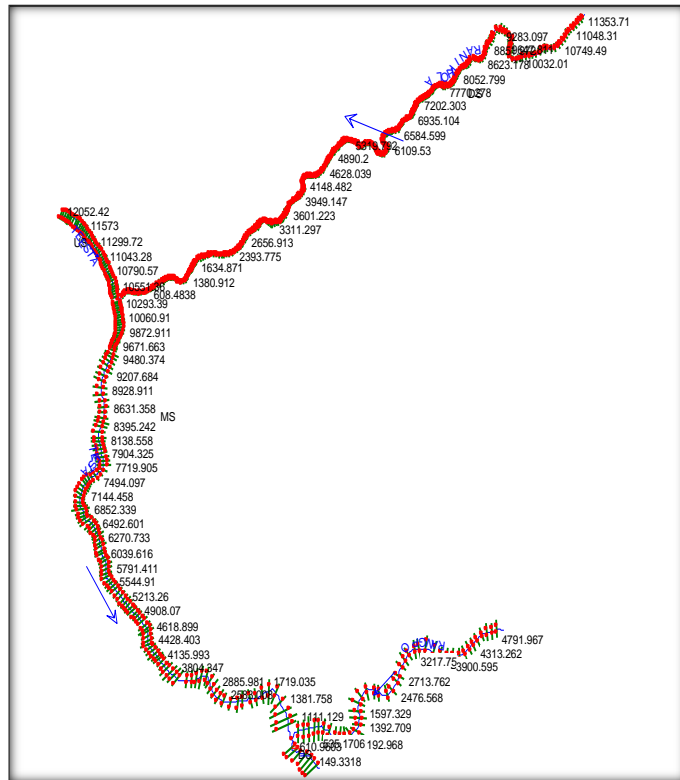
- Schumann, G., Matgen, P., Cutler, M. E. J., Black, A., Hoffmann, L., & Pfister, L. (2008). Comparison of remotely sensed water stages from LiDAR, topographic contours and SRTM. *ISPRS Journal of Photogrammetry and Remote Sensing*, 63(3), 283–296. <https://doi.org/10.1016/j.isprsjprs.2007.09.004>
- Shah, M. (2013). Water: Towards a Paradigm Shift in the Twelfth Plan. *Economic and Political Weekly*, 48(3), 40–52.
- Shawky, M., Moussa, A., Hassan, Q. K., & El-Sheimy, N. (2019). Pixel-Based Geometric Assessment of Channel Networks/Orders Derived from Global Spaceborne Digital Elevation Models. *Remote Sensing*, 11(3), 235. <https://doi.org/10.3390/rs11030235>
- Sharma, A., & Goyal, M. K. (2020). Assessment of the changes in Precipitation and temperature in Teesta River basin in Indian Himalayan Region under climate change. *Atmospheric Research*, 231, 1–16. <https://doi.org/doi.org/10.1016/j.atmosres.2019.104670>
- Shugar, et al. (2021). A massive rock and ice avalanche caused the 2021 disaster at Chamoli, Indian Himalaya. *Science*, 373(6552), 300-306.
- Smith, Keith. Petley, David. N. (2009). *Environmental Hazards: Assessing Risk and Reducing Disaster*. Routledge
- Summerfield, M.A. (2013). *Global Geomorphology*. Routledge.
- Suriya, S., & Mudgal, B. V. (2012). Impact of urbanization on flooding: The Thirusoolam sub watershed – A case study. *Journal of Hydrology*, 412-413, 210–219. <https://doi.org/10.1016/j.jhydrol.2011.05.008>
- Smith, Keith. Petley, David. N. (2009). *Environmental Hazards: Assessing Risk and Reducing Disaster*. Routledge
- Srivastava, P., Kumar, A., Chaudhary, S., Meena, N., Sundriyal, Y. P., Rawat, S., Rana, N., Perumal, R. J., Bisht, P., Sharma, D., Agnihotri, R., Bagri, D. S., Juyal, N., Wasson, R. J., & Ziegler, A. D. (2017). Paleofloods records in Himalaya. *Geomorphology*, 284, 17–30. <https://doi.org/10.1016/j.geomorph.2016.12.01>

- Starkel, L. (1972). The Role of Catastrophic Rainfall in the Shaping of the Relief of the Lower Himalaya (Darjeeling Hills). In L. S, J. Kondracki, & J. Kostrowicki (Eds.), *Geographica Polonica* (103-147). Polish Scientific Publisher.
- Tripathi, Prakash., 2015. Flood Disaster in India: An Analysis of trend and preparedness. *Interdisciplinary Journal of Contemporary Research*.2(4),91-98.
- Uniyal, Aniruddha. (2013). Lessons from Kedarnath Tragedy of Uttarakhand Himalaya, India. *Current Science*,105(11), 1472-1474.
- Uuemaa, E., Ahi, S., Montibeller, B., Muru, M., & Knoch, A. (2020). Vertical Accuracy of Freely Available Global Digital Elevation Models (ASTER, AW3D30, MERIT, TanDEM-X, SRTM, and NASADEM). *Remote Sensing*, 12(21), 3482. <https://doi.org/10.3390/rs12213482>
- Vozinaki, A.E. K., Morianou, G. G., Alexakis, D. D., & Tsanis, I. K. (2016). Comparing 1D and combined 1D/2D hydraulic simulations using high-resolution topographic data: a case study of the Koiliaris basin, Greece. *Hydrological Sciences Journal*, 62(4), 642–656. <https://doi.org/10.1080/02626667.2016.1255746>
- Werner, M. G. F. (2001). Impact of grid size in GIS based flood extent mapping using a 1D flow model. *Physics and Chemistry of the Earth, Part B: Hydrology, Oceans and Atmosphere*, 26(7-8), 517–522. [https://doi.org/10.1016/s1464-1909\(01\)00043-0](https://doi.org/10.1016/s1464-1909(01)00043-0)
- Wesley Lauer, J., Echterling, C., Lenhart, C., Belmont, P., & Rausch, R. (2017). Air-photo based change in channel width in the Minnesota River basin: Modes of adjustment and implications for sediment budget. *Geomorphology*, 297(297), 170–184. <https://doi.org/10.1016/j.geomorph.2017.09.005>
- Wiejaczka, L., Bucala, A., & Sarkat, S. (2014). Human role in shaping the hydromorphology of Himalayan rivers: study of the Tista River in Darjeeling Himalaya. *Current Science*, 106(5), 717–724.
- Ward, Roy. (1978). *Floods. A Geographical Perspective*.The Macmillan Press Ltd.

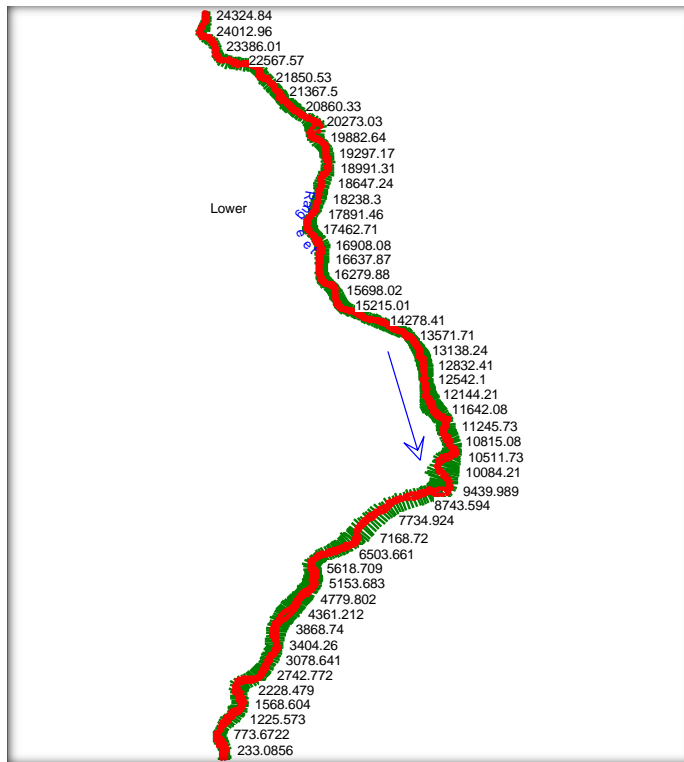
- Yang, J., Townsend, R. D., & Daneshfar, B. (2006). Applying the HEC-RAS model and GIS techniques in river network floodplain delineation. *Canadian Journal of Civil Engineering*, 33(1), 19–28. <https://doi.org/10.1139/105-102>
- Yin, H., & Li, C. (2001). Human impact on floods and flood disasters on the Yangtze River. *Geomorphology*, 41(2-3), 105–109. [https://doi.org/10.1016/s0169-555x\(01\)00108-8](https://doi.org/10.1016/s0169-555x(01)00108-8)



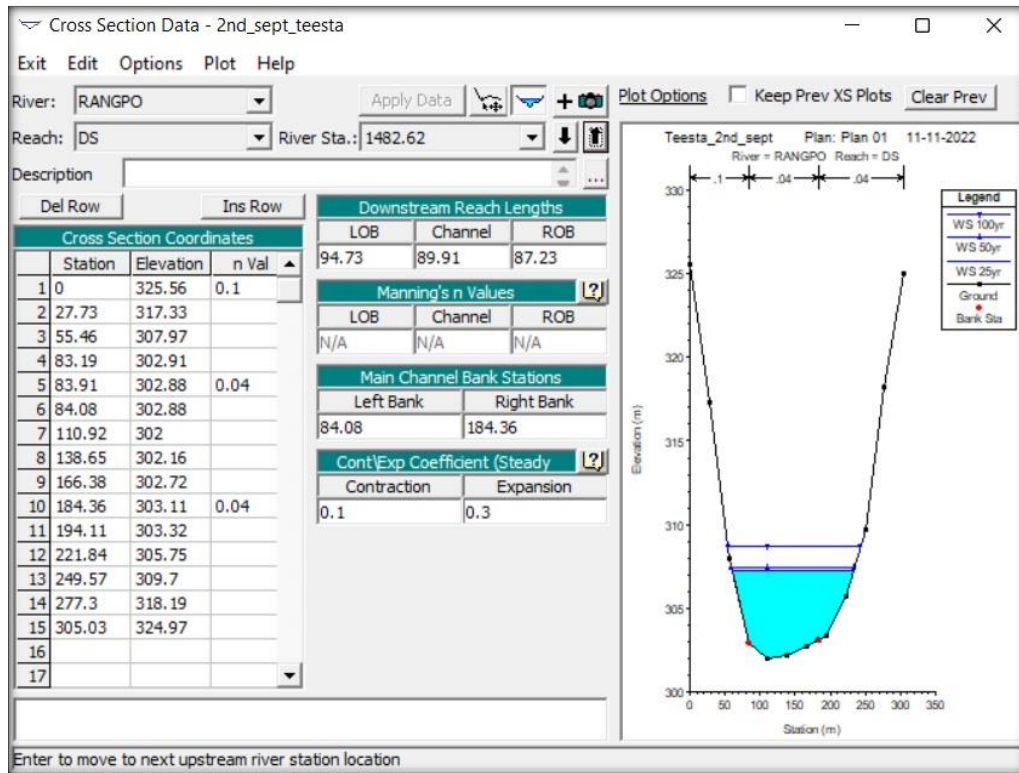
## Appendices



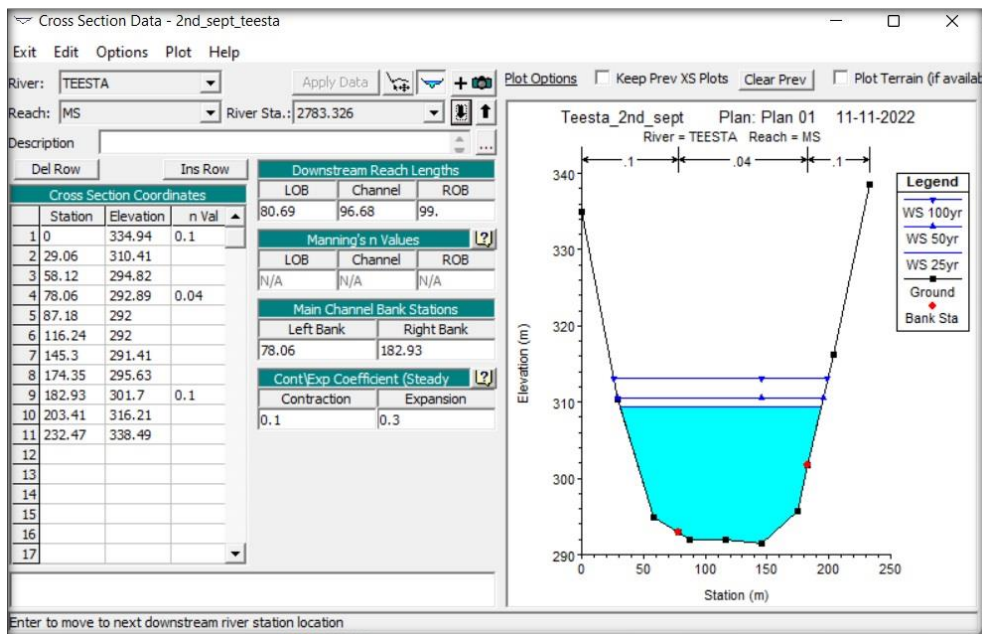
**Appendix I. Geometry file of the selected stretches of Teesta, Ranikhola and Rangpochu for running HEC-RAS 1 d steady flow**



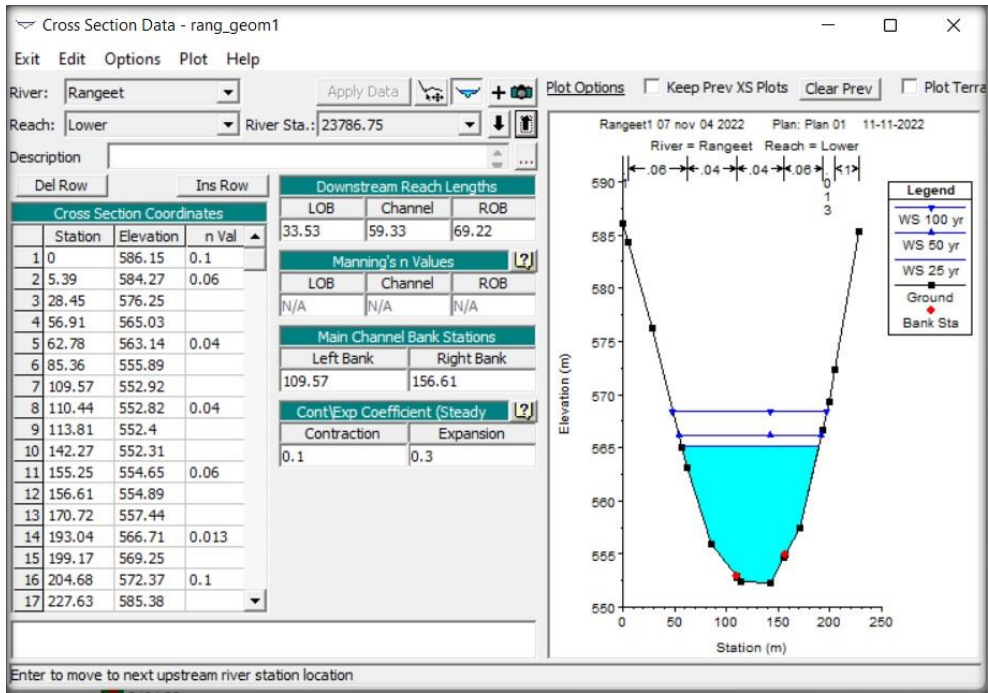
**Appendix II. Geometry file of the selected stretches of Teesta, Ranikhola and Rangpochu for running HEC-RAS 1 d steady**



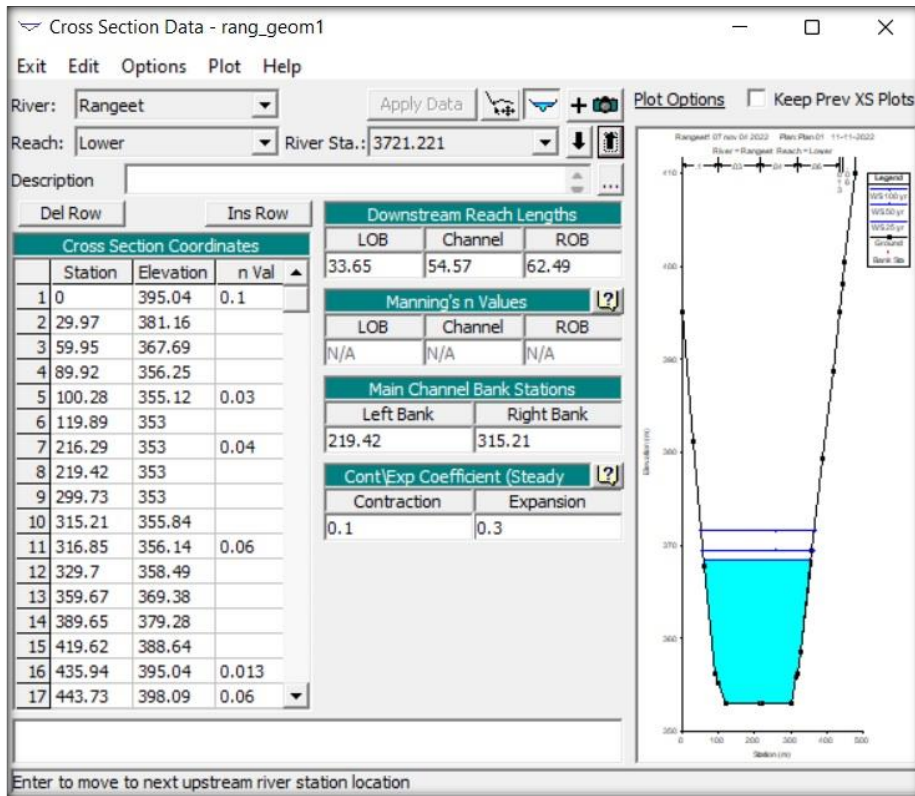
*Appendix III. Cross section at Rangpo area along the Rangit*



*Appendix IV. Cross section at Khanitar area along the Rangit*



*Appendix V. Cross section at Khanitar area along the Rangit*



*Appendix VI. Cross section at Rothak area along the Rangit*